



City Research Online

City St George's, University of London

Citation: Aziz, T., Osabel, D. M., Kim, Y., Kim, S., Bae, J. & Tsavdaridis, K. (2025). State-of-the-Art Artificial Intelligence Techniques in Structural Engineering: A Review of Applications and Prospects. *Results in Engineering*, 28, 107882. doi: 10.1016/j.rineng.2025.107882

This is the accepted version of the paper.

This version of the publication may differ from the final published version. To cite this item please consult the publisher's version.

Permanent repository link: <https://openaccess.city.ac.uk/id/eprint/36095/>

Link to published version: <https://doi.org/10.1016/j.rineng.2025.107882>

Copyright and Reuse: Copyright and Moral Rights remain with the author(s) and/or copyright holders. Copies of full items can be used for personal research or study, educational, or not-for-profit purposes without prior permission or charge, unless otherwise indicated, provided that the authors, title and full bibliographic details are credited, a hyperlink and/or URL is given for the original metadata page and the content is not changed in any way. For full details of reuse please refer to [City Research Online policy](#).

1
2
3
4
5
6
7
8
9
10
11
12
13
14
15
16
17
18
19
20
21
22
23

State-of-the-Art Artificial Intelligence Techniques in Structural Engineering: A Review of Applications and Prospects

Md. Tarif Aziz^a, Dave Montellano Osabel^b, Youngju Kim^c, Sanghoon Kim^{d*}, Jaehoon Bae^{b*},
Konstantinos Daniel Tsavdaridis^{e*}

^aDepartment of Sustainable Architecture ICT Convergence, Chonnam National University, 50 Daehak-ro Yeosu-si, Jeonnam 59626, Republic of Korea

^bDepartment of Architectural Design, Chonnam National University, 50 Daehak-ro Yeosu-si, Jeonnam 59626, Republic of Korea

^cKorea Institute of Structural Engineering & Consulting Busan, Republic of Korea

^dDepartment of Mechanical Design Engineering, Chonnam National University, 50 Daehak-ro Yeosu-si, Jeonnam 59626, Republic of Korea

^eDepartment of Engineering, School of Science & Technology, City St George’s, University of London, Northampton Square, London EC1V 0HB, UK

*Corresponding authors’ e-mail addresses: shkim83@chonnam.ac.kr,
konstantinos.tsavdaridis@city.ac.uk, skycity-bjh@jnu.ac.kr

Abstract: Artificial intelligence (AI) has emerged as a key driver of modern technological development, with widespread applications across various domains, including civil engineering. Structural engineering, a subdiscipline of civil engineering, requires the evaluation of the suitability of different structural components before the final construction phase and during recycling processes. Traditionally, this evaluation relies on laboratory experiments and highly complex numerical simulations, which are often impractical due to space and time constraints, equipment complexity, and high costs. To address these challenges, researchers worldwide have

24 developed AI-based solutions for applications such as structural damage detection and the
25 prediction of failure loads and patterns. These solutions offer predictive accuracy comparable to
26 that of experimental and numerical analyses. This review presents a detailed analysis of 100 AI-
27 integrated studies in structural engineering conducted between 2020 and 2024, with a focus on
28 concrete, steel, and composite structures, particularly building frames. The study summarizes the
29 performance benchmarking of commonly used AI algorithms, such as neural networks, genetic
30 algorithms, tree-based algorithms, and boosting methods, reporting accuracy scores above 0.80
31 (out of 1.00), and highlights average accuracy values of 0.90 for optimized and hybrid AI
32 approaches. Additionally, the review explores emerging AI applications, including retrofitting
33 technologies, buckling-restrained braces, dampers, column-beam connections, and life-cycle
34 assessment. Critical analysis identifies key limitations of recent AI-based research, especially
35 those implemented regionally, and proposes novel solutions to overcome existing challenges.

36 **Keywords:** *Artificial Intelligence, Structural Engineering, Reinforced Concrete Structures, Steel*
37 *Structures, Structural Safety*

38 **1 Introduction**

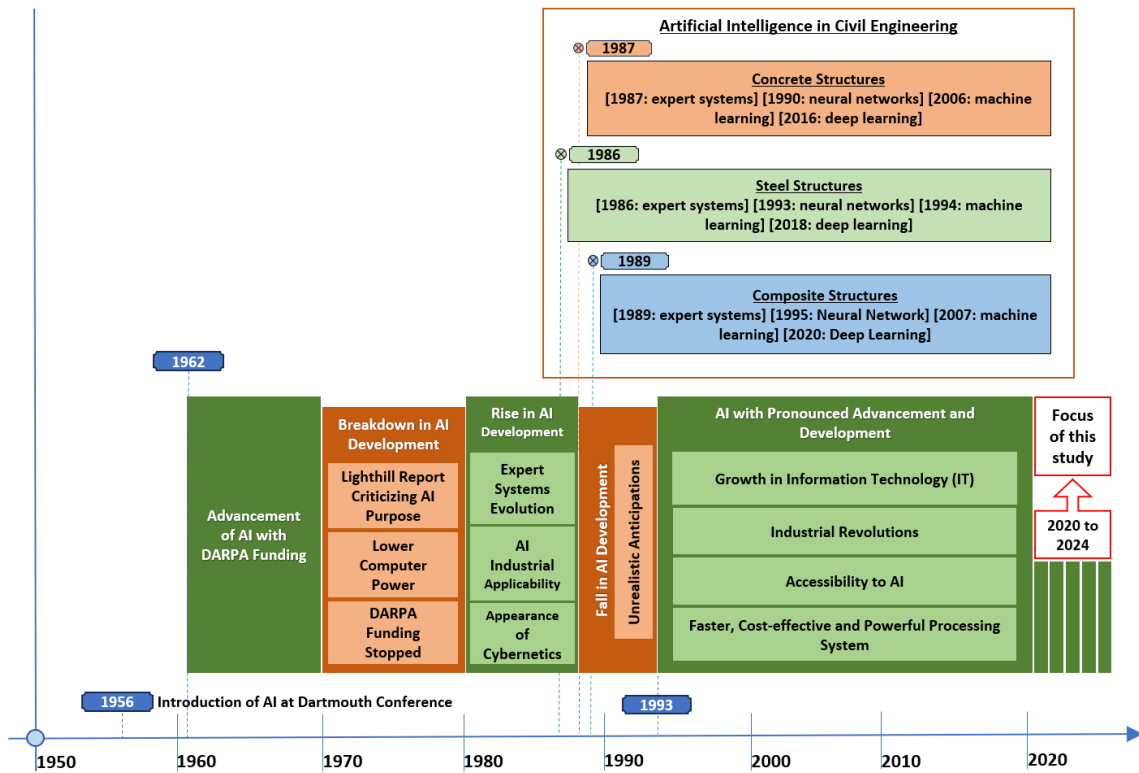
39 Artificial Intelligence (AI) was first conceptualized by a group of scientists at a conference at
40 Dartmouth College in 1956 [1] to develop intelligent systems capable of reasoning and exhibiting
41 human-like intelligence [2]. Significant interest and growth in AI emerged through U.S. Defense
42 Advanced Research Projects Agency (DARPA) funding from 1962 [3] (Figure 1). However,
43 between 1970 and 1980, AI research stagnated due to limited high-performance computing
44 resources, and DARPA funding was discontinued following the critical “Lighthill Report”, which
45 reported AI to have failed to achieve its purpose [4]. From the 1980s, AI experienced a resurgence
46 driven by the evolution of some early methods (e.g., expert systems and cybernetics) and practical

47 industrial applications [2]. Nevertheless, between 1987 and 1993, AI faced another decline caused
48 by unrealistic expectations and limited computational power [5]. Later, subsequent advances in
49 Information Technology (IT) and the industrial revolution enabled significant progress in AI [6].
50 Today, the availability of faster, cost-effective, and more powerful processing systems has
51 facilitated the widespread adoption of AI [7].

52 AI encompasses a broad range of methods, including—but not limited to—machine learning (ML),
53 neural networks (NN), deep learning (DL), data mining, knowledge discovery and advanced
54 analytics, rule-based modeling and decision making, fuzzy logic, knowledge representation,
55 reasoning under uncertainty, expert systems, case-based reasoning, text mining and natural
56 language processing, visual analytics, computer vision and pattern recognition, hybrid approaches,
57 and optimization techniques [8]. These techniques are closely associated with disciplines such as
58 computer science, information theory, cybernetics, linguistics, and neurophysiology [9]. By
59 integrating the capabilities of these methods, AI can mimic human intelligence and apply human-
60 inspired reasoning and algorithms to solve complex engineering problems [10]. Researchers
61 worldwide are actively developing innovative AI approaches that are cost-effective, rapid, robust,
62 and highly accurate [11]. Sarker [8] provided a comprehensive review of AI-based modeling in
63 real-world applications.

64 In recent years, ML, DL, and NN have been extensively applied in civil engineering subfields,
65 including structural, geotechnical, transportation, water supply, and hydraulic engineering. Recent
66 studies have reviewed AI developments and applications in these areas. Pan and Zhang [12]
67 conducted a scientometric analysis of AI-related publications from 1997 to 2020, highlighting AI's
68 potential in automation and construction engineering and management. Manzoor et al. [13]
69 reviewed 105 studies from 1995 to 2021, focusing on AI's role in sustainable development. Xu et

70 al. [11] presented a systematic review on intelligent architectural design, structural health
 71 monitoring, and disaster prevention, emphasizing computer-vision-based advancements. Vadyala
 72 et al. [14] investigated the integration of ML methods with physics-based models to address data
 73 shift problems in supervised learning and proposed a physics-informed ML approach. Rezania et
 74 al. [15] discussed pioneering software, AI-related terminology, and parameters affecting
 75 progressive structural collapse. More recently, Harle [16] provided an overview of AI applications
 76 across some areas of civil engineering, including analysis and design, construction management,
 77 geotechnical engineering, and transportation planning, with a focus on ML and genetic algorithms.



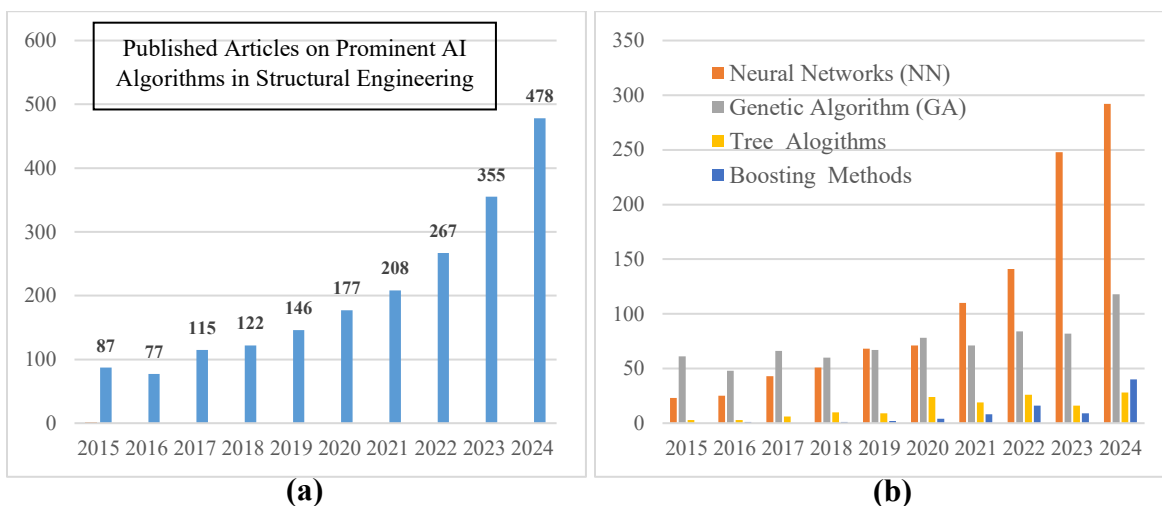
78 **Figure 1.** Historical timeline and evolution of artificial intelligence (AI) in structural
 79 engineering.

80 AI has been applied in structural engineering for decades, particularly in the design of structural
 81 systems that account for critical factors such as load application characteristics, service life

82 expectancy, durability against environmental effects, and fire-induced issues [17-20]. It serves as
83 a powerful tool for generating efficient and accurate preliminary structural design predictions,
84 reducing the reliance on cumbersome experimental setups, and enhancing safety measures during
85 laboratory testing. Moreover, AI reduces the demand for high-precision instruments, which are
86 often unavailable in many institutions and industries. For example, large-scale fire tests on
87 structural frames cannot typically be conducted in laboratory settings, forcing researchers to rely
88 on small-scale experiments and assumptions. AI can overcome such limitations by processing
89 large-scale variable inputs and producing highly accurate predictions. However, as emphasized in
90 this review, AI-based results must be validated against experimental and code-based outcomes,
91 particularly in light of challenges such as data shift, domain shift, and extrapolation risk [18,21].
92 As illustrated in Figure 1, AI was first applied to structural engineering in the early 1990s through
93 expert systems, particularly for concrete, steel, and composite structures. In subsequent years,
94 advanced methods such as ML, DL with NN were increasingly adopted in structural engineering.
95 Following the first major AI revolution in 2012, DL has become increasingly prevalent in
96 structural health monitoring (SHM) and structural damage detection.

97 In terms of AI's development and application within structural engineering, a review study
98 examined four novel ML algorithms in structural system identification, SHM, structural vibration
99 control, and structural design and prediction between 2017 and 2020 [22]. Another review [23] on
100 fundamental ML techniques addressed a wide range of applications, including structural analysis
101 and design, SHM, damage detection, fire resistance assessment, evaluation of mechanical
102 properties, and concrete mix design. A more recent review [24] focused exclusively on ML
103 applications in SHM. A comprehensive literature review [25] covering AI, ML, and DL discussed
104 commonly used algorithms in structural engineering across more than 200 sources. Although the

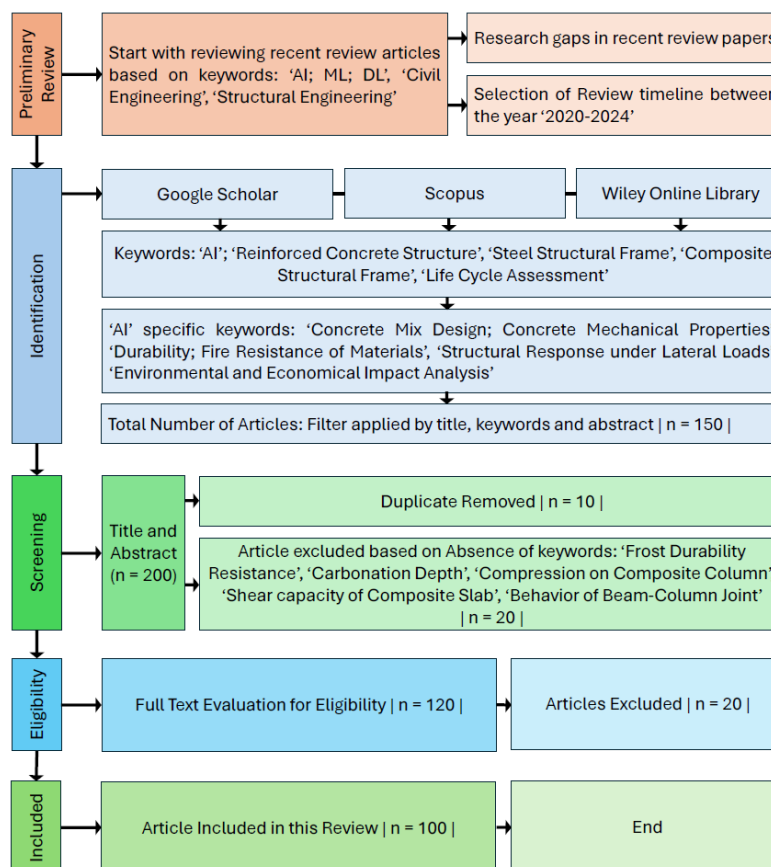
105 study conducted a scientometric analysis to map the best practices from several scholarly works,
 106 its primary focus was on supervised learning methods up to the year 2021. However, these reviews
 107 only partially addressed recent trends of AI in structural engineering for material- and component-
 108 level analysis. They did not provide an in-depth discussion of structural components such as
 109 reinforced concrete, steel, and composite frames exposed to fire or seismic effects for the published
 110 studies during 2020-2024. Similarly, they did not explicitly consider innovative approaches such
 111 as AI integration with buckling-restrained braces (BRBs), viscoelastic dampers, retrofitting
 112 technologies (e.g., fiber-reinforced jacketing), beam-column joints, or life-cycle assessment
 113 (LCA) of buildings.



114
 115 **Figure 2.** Published article trends in Structural Engineering (Scopus-sourced, 2015–2024): (a)
 116 overall use of prominent AI algorithms, (b) categorized by specific methods (NN, GA, tree-
 117 based, and boosting algorithms).

118 As presented in [Figure 2a](#), based on Scopus search results, published articles on prominent AI
 119 algorithms (NN, GA, tree-based algorithms, and boosting algorithms) in structural engineering
 120 have increased significantly from 2015 to 2024. The number of published articles in the last five
 121 years (2020–2024) has increased by 2.72 times in comparison to 2015–2019. [Figure 2b](#) illustrates

122 a similar upward trend for each prominent group of algorithms. Research on NN has grown most
 123 dramatically, increasing by approximately 4.8 times during 2020–2024 compared with 2015–2019.
 124 Tree-based algorithms also expanded substantially, with a 3.2-fold increase, while GA showed
 125 only modest growth of about 1.3 times. Boosting methods, which were rarely applied before 2019,
 126 experienced the strongest relative growth, rising nearly 11-fold over the last five years. These
 127 findings highlight a clear trend: NN and boosting methods are being adopted at accelerating rates,
 128 GA continues to attract steady interest, and tree-based approaches are strengthening as
 129 complementary techniques. Since previous review articles only covered trends up to 2020 [22],
 130 with partial updates through 2021 [25], this present study focuses specifically on 2020–2024, when
 131 the number of AI-related publications in structural engineering increased most sharply (Figure 2).



132
 133 **Figure 3.** PRISMA flow diagram for the reviewed articles.

134 Following the PRISMA flow diagram (Figure 3), five steps are followed as the formal review
135 protocol of this study (i.e., preliminary, identification, screening, eligibility and inclusion). Firstly,
136 the preliminary stage involved analyzing recent review articles on AI in civil and structural
137 engineering to identify research gaps. The review timeline was set to 2020–2024, given the sharp
138 rise in AI applications during this period (Figure 2) and the absence of prior reviews covering this
139 interval. Identification of relevant studies was carried out using keywords such as AI in *reinforced*
140 *concrete structures*, *steel structural frames*, *composite structural frames*, and *LCA*. Additional
141 topic-specific keywords—such as *concrete mix design*, *concrete mechanical properties*,
142 *durability*, *fire resistance of materials*, *structural response under lateral loads*, and *life cycle*
143 *impact analysis*—were also employed, yielding 150 candidate papers. The screening process
144 involved removing duplicates (n = 10) and excluding irrelevant topics (n = 20), including works
145 focusing on *frost durability resistance*, *carbonation depth*, *compression on composite columns*,
146 *shear capacity of composite slabs*, and *behavior of beam–column joints*. Next, eligibility was
147 confirmed through full-text evaluation, resulting in the exclusion of an additional 20 articles.
148 Ultimately, this review selected 100 papers, prioritizing studies that compared AI predictive results
149 against laboratory-scale experimental and numerical datasets.

150 The application of AI in structural engineering is diversifying through innovative approaches such
151 as its integration with BRBs, viscoelastic dampers, retrofitting technologies (e.g., fiber-reinforced
152 jacketing), beam–column joints, and LCA of buildings. For example, AI has been applied in
153 seismic protection systems to enhance energy dissipation and resilience using dampers and BRBs.
154 In retrofitting, AI-driven models assist in identifying structural weaknesses and recommending
155 cost-effective strengthening strategies. For beam–column connections, AI improves the prediction
156 of joint behavior under cyclic loading. AI has also been introduced in small-scale LCA studies to

157 evaluate sustainability and long-term structural performance. In this context, the present review
158 highlights the limitations, challenges, and potential solutions for such emerging applications. It
159 also addresses practical implications of AI, barriers to its adoption, and prospects for industry
160 implementation. Specifically, the study evaluates prediction accuracy in terms of the coefficient
161 of determination (R^2), the number of databases used, and key input parameters or governing factors
162 across various applications (e.g., mechanical and durability properties of concrete members, fire-
163 induced effects on structural components, seismic impact-based design, and LCA of structures).
164 In addition, it examines accuracy levels achieved by optimized versions of traditional AI models.
165 This review does not cover AI research trends for 2025, nor does it address structural health
166 monitoring, remote sensing, or construction automation. Although R^2 is adopted as the primary
167 performance benchmark, other evaluation metrics inconsistently applied across the literature (e.g.,
168 RMSE, MAPE) are not considered. Likewise, variations in dataset size and characteristics among
169 studies (e.g., for durability assessment of concrete or fire-induced effects) are not discussed in
170 detail, as the focus remains on comparative evaluation of prominent algorithms with key input
171 parameters.

172 In view of these considerations, this paper provides a comprehensive analysis of effective AI
173 methodologies in structural engineering, emphasizing advancements between 2020 and 2024.
174 **Section 2** presents a critical overview of widely adopted AI techniques. **Section 3** evaluates the
175 predictive accuracy of these models relative to traditional numerical simulations, experimental
176 data, and design codes, with applications in concrete, reinforced and composite concretes, and
177 steel structures, as well as in structural response to lateral loads and LCA. A summary of
178 comparative structural analyses using AI methods is also included. **Section 4** discusses limitations
179 of current AI-driven research and the potential implications for industry. For the first time, it

180 highlights future research directions such as AI applications in retrofitting technologies, BRBs,
181 dampers, easy-to-dismantle beam–column connections, and LCA-driven sustainability
182 assessments. By bridging the gap between AI advancements and structural engineering challenges,
183 this review aims to serve as a practical guide for researchers and engineers seeking to integrate AI
184 into structural analysis, design, and sustainability practices.

185 **2 Overview of Basic AI Techniques Relevant to Structural Engineering**

186 This section introduces the AI techniques most commonly applied in structural engineering and
187 discusses their applications in detail. It begins with the general process of AI model development
188 (Section 2.1), followed by brief introductions to the widely used AI techniques in structural
189 engineering (Sections 2.2–2.8). Finally, the evaluation of model accuracy and precision is
190 addressed (Section 2.9).

191 **2.1 Model Development**

192 A well-structured model development process ([Figure 4](#)) is essential for generating reliable
193 predictions. The process begins with data retrieval and preprocessing, which are critical because
194 model performance largely depends on data quality. Typical preprocessing tasks include outlier
195 detection and treatment, data encoding, feature scaling, feature engineering, and partitioning the
196 dataset into training and testing subsets to ensure suitability for modeling. The next stages involve
197 algorithm selection and model training using the training data. Training is usually performed
198 iteratively, with hyperparameter tuning to optimize performance until satisfactory cross-validation
199 (CV) results are achieved. Finally, the model’s performance is evaluated using a separate test
200 dataset, and predictions are generated for comparison with the observed outcomes [[26](#)]. This
201 development framework is common to all AI models and serves as the foundation for the
202 evaluation methods described in subsequent sections.

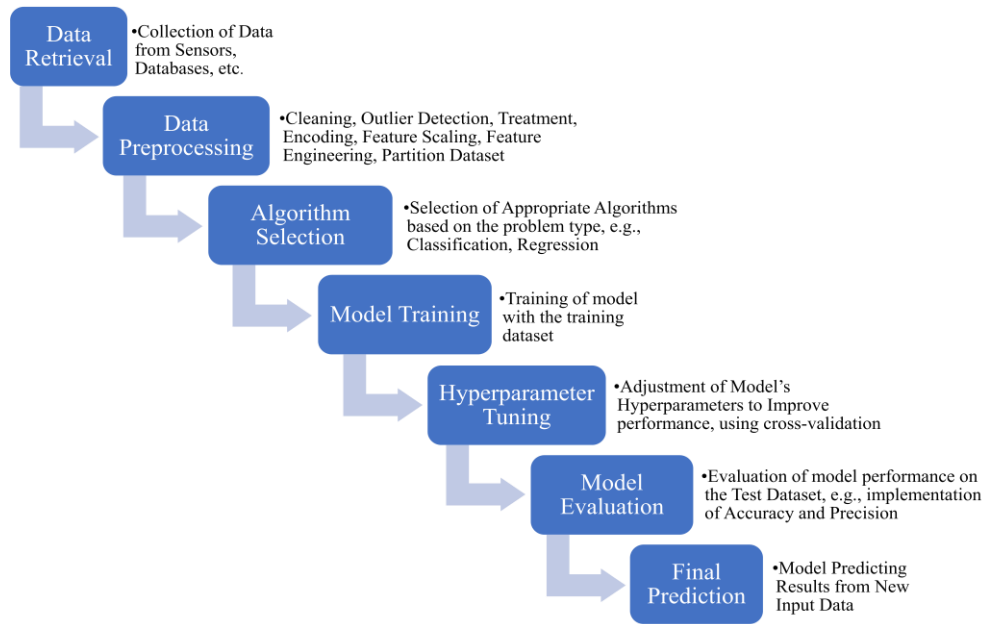


Figure 4. Artificial intelligence (AI) model development in structural engineering.

203 **2.2 Neural Networks (NN) Architecture**

204 To handle complex data relationships, NN consist of artificial neurons interconnected in a specific
 205 topology, designed to mimic the behavior of the human nervous system and adopting a structure
 206 analogous to the human brain. Artificial neural networks (ANNs), a basic form of NN, leverage
 207 their self-learning capability to produce highly accurate results as the amount of experimental data
 208 increases. By managing high dimensional data, ANN can solve highly nonlinear classification and
 209 regression problems, as well as complex relationships. Essentially, an ANN can be considered an
 210 information-processing system with specialized neurons for receiving external input and
 211 generating output [27].

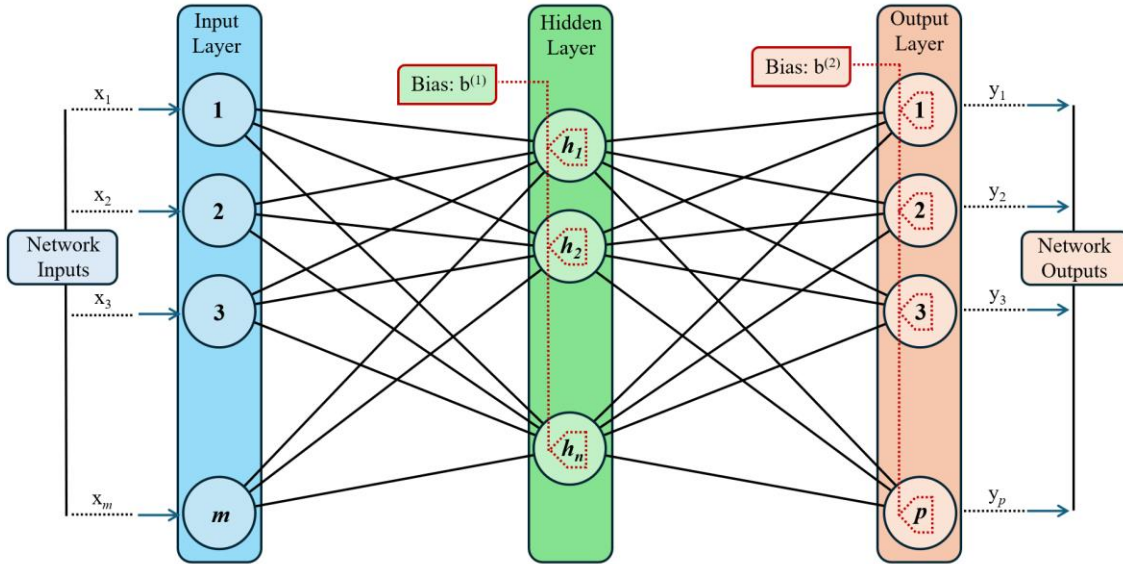


Figure 5. Artificial neural networks (ANN) structure (adapted from [28]).

212 As illustrated in Figure 5, an ANN model consists of an input layer, one or more hidden layers,
 213 and an output layer, interconnected with randomly assigned weights and biases. For the input layer,
 214 the number of neurons (nodes) are equal to the number of variables of the specific problem to be
 215 solved. The product of the inputs and their respective weights is added to the deviation (bias). For
 216 the hidden layer that lies between the input and output layers, a predefined activation function is
 217 applied to the nodes to process the inputs. The optimal weights and biases are determined through
 218 training to minimize the error between the outputs and targets. The training is considered complete
 219 when the model achieves the desired performance with the smallest errors. The output layer
 220 produces the final response from the network when the model is considered suitable for generating
 221 predictions from unknown data [19].

222 ANNs can be classified based on the number of hidden layers, i.e., single layer perceptron for one
 223 hidden layer or multilayered perceptron (MLP) for two or more hidden layers [29]. Since an MLP
 224 is a deep ANN that has excellent ability of function approximation, it can be used in diverse

225 engineering applications. It implements nonlinear transformations to convert input variables to an
 226 expected output. As shown in Figure 6, similar to ANN, each layer of an MLP network contains
 227 several nodes (neurons) or processing elements that may be partially or fully connected. A
 228 feedforward process is executed between nodes of different layers, with each neuron processing
 229 an input and generating an output, which is then used as the input for the next neuron. The
 230 connection strength or weight between nodes includes independent values that are modified
 231 throughout the training stage in a process known as backpropagation. This combined process of
 232 forward signal propagation and backward error correction is referred to as feedforward
 233 backpropagation (FFBP). The optimum set of weights, yielding the smallest errors, is subsequently
 234 used to perform predictions with new data [30].

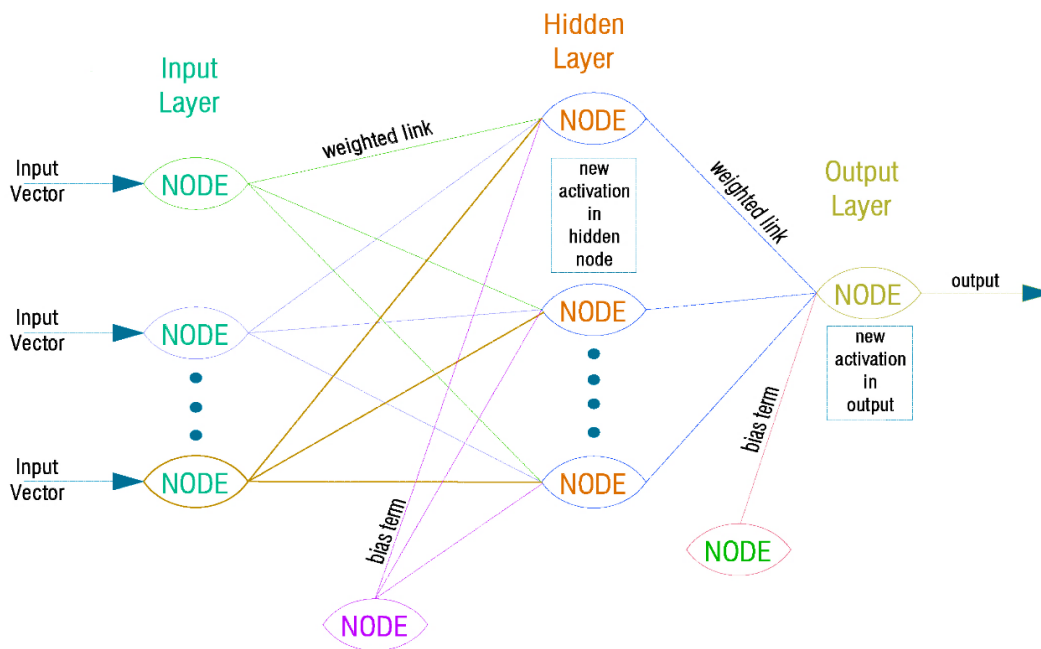


Figure 6. Representative multilayered perceptron–artificial neural networks (MLP-ANN) framework (adapted from [31]).

235 Nonlinear autoregressive exogenous (NARX) is a dynamic recurrent ANN which can capture
 236 inherent intricate relationships between inputs in its memory and effectively predict the outputs.

237 Especially for nonlinear discrete time series, NARX ANN can serve as a dynamic modeling tool
 238 that encloses multiple layers with feedback connections [32]. As shown in Figure 7, two primary
 239 configurations exist: (a) the open-loop or series-parallel mode (NARX-SP) represents a stable
 240 network in which actual target values from previous tests are fed back during training process, and
 241 (b) the closed-loop or parallel mode (NARX-P) represents a network where predicted outputs are
 242 fed back as inputs for the feedforward neural network and incorporated in the output regressor due
 243 to the absence of true outputs for new data. Thus, the NARX-P mode is an FFBP network with a
 244 feedback connection from output to input. As such, it can generate final predictions using the
 245 training and test data from the NARX-SP mode [31].

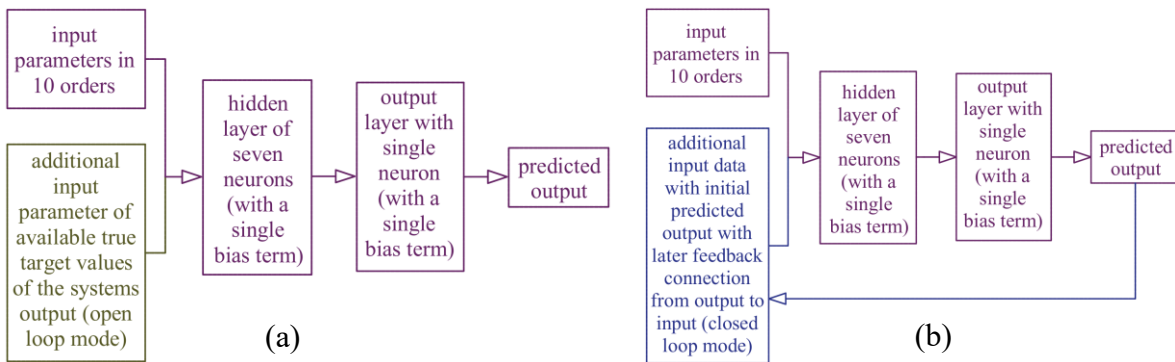


Figure 7. Nonlinear autoregressive exogenous-artificial neural networks (NARX-ANN) frameworks: (a) NARX-SP; (b) NARX-P (adapted from [31]).

246 Long short-term memory recurrent neural network (LSTM-RNNs) is a variant of the recurrent
 247 neural network (RNNs), and its basic modeling pattern is the same as that of ANNs. However,
 248 LSTM-RNNs consist of several decisive hidden layers apart from the input and output layers, as
 249 well as a group of LSTM cells with four interrelated units, i.e., an internal cell, an input gate, a
 250 forget gate, and an output gate (Figure 8). By utilizing a self-recurrent connection, the internal cell
 251 remembers the cell state at the former time step, while the input gate regulates the input activation
 252 flow into the internal cell state. The forget gate allows the LSTM cell to forget or reset the cell

253 memory, as necessary. The tangent gate or tanh (hyperbolic tangent) function transforms values
 254 (compressing between -1 and 1) before values are read from cell state. The output gate normalizes
 255 the flow of output activation into the LSTM cell output [33].

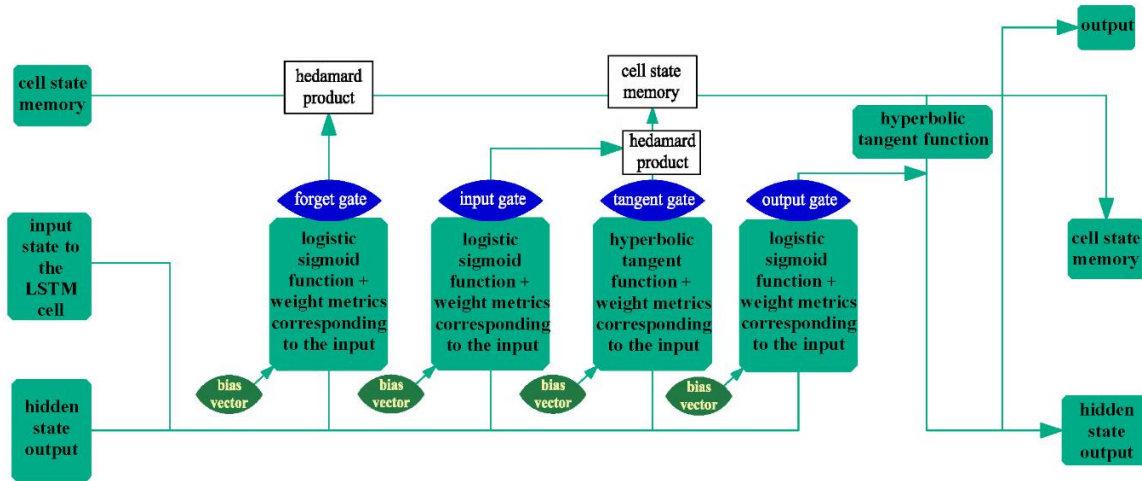


Figure 8. Long short-term memory (LSTM) cell diagram (adapted from [33]).

256 2.3 Machine Learning (ML) and Deep Learning (DL) Algorithms

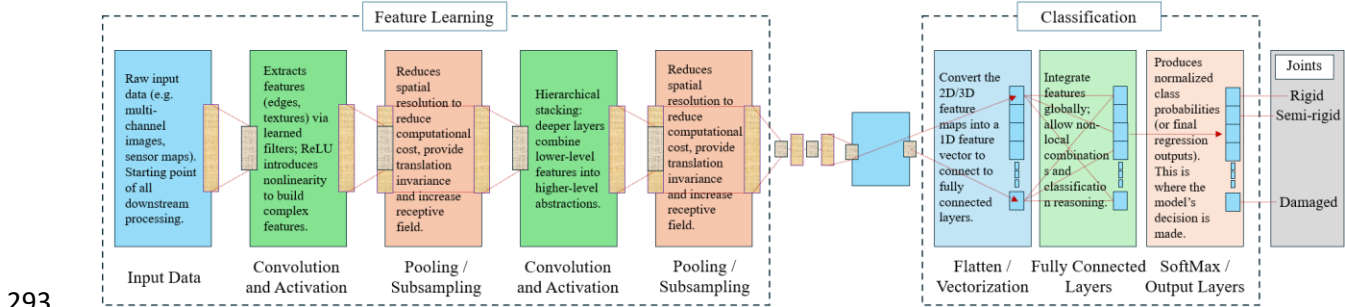
257 ML encompasses four types of learning methods, i.e., supervised, unsupervised, semi-supervised
 258 and reinforcement learnings [7]. In supervised learning that accounts for approximately 70% of
 259 ML applications, the algorithm is trained on an experimental dataset containing both inputs and
 260 outputs. The model predictions are compared with the true outputs to identify the errors, and the
 261 learning process is refined accordingly. Patterns are assessed to predict labeled information for
 262 additional unlabeled data. In contrast, unsupervised learning involves exploration of data for
 263 pattern identification in the absence of historical labels. This approach is well-suited for
 264 transactional data. Popular unsupervised learning algorithms (e.g., self-organizing maps, nearest-
 265 neighbor mapping, k-means clustering, and single-value decomposition) have been used to
 266 segment textual topics, recommend items, and identify data outliers. Semi-supervised learning
 267 follows a pattern similar to, but its amount of unlabeled information is much higher than, the

268 supervised learning. Classification, regression, and prediction models are trained using this
269 learning method. Reinforcement learning aims to learn the best options available by adapting a
270 trial-and-error process involving three primary mechanisms: the learner or decision maker,
271 environmental components, and actions. The goal of the learner is to adopt the best actions
272 available to produce the expected result within a pre-scheduled time, following the most suitable
273 pattern [7].

274 DL is a branch of ML that employs unsupervised networks to learn from unstructured or unlabeled
275 data [34]. It starts with the input layers that are connected to a series of hidden layers through
276 nonlinear activation functions. The activation functions generate approximation forms that allow
277 gradient-based optimization. Results from the optimization process are displayed as final output.
278 The main objective of DL architecture is to learn the feature illustration of input data and achieve
279 implicit representation that best generates an output $Y = f(\sum_{i=1}^n l_n w_{ij} + b_j)$, where f is the
280 activation function, l_n represents i th input signal, b_j represents bias value of j th neuron, w_{ij}
281 represents connecting weights between l_n and b_j [35].

282 Multiple hidden layers create deep neural networks (DNN) and more hidden layers result in deeper
283 networks [34]. A variation of DNN is convolutional neural networks (CNN) which is specialized
284 for image recognition. CNNs mimic the visual cortex to distinguish and classify images. The
285 architecture consists of two main sections: feature learning and classification (Figure 9). Initially,
286 input images pass through the feature extraction network, where convolutional layers transform
287 the images and pooling layers reduce dimensionality. The resulting feature maps are then fed into
288 classification layers to generate predictions. In classification layers, flatten layer converts the 2D
289 feature maps into a 1D vector allowing fully connected layers to process them as input. Soft-max
290 layer produces probabilities for each class such as no visible cracks (connections), micro-cracks

291 (partial degradation) and significant cracks (full separation) are processed as rigid, semi-rigid and
 292 damaged joints, respectively. [36].



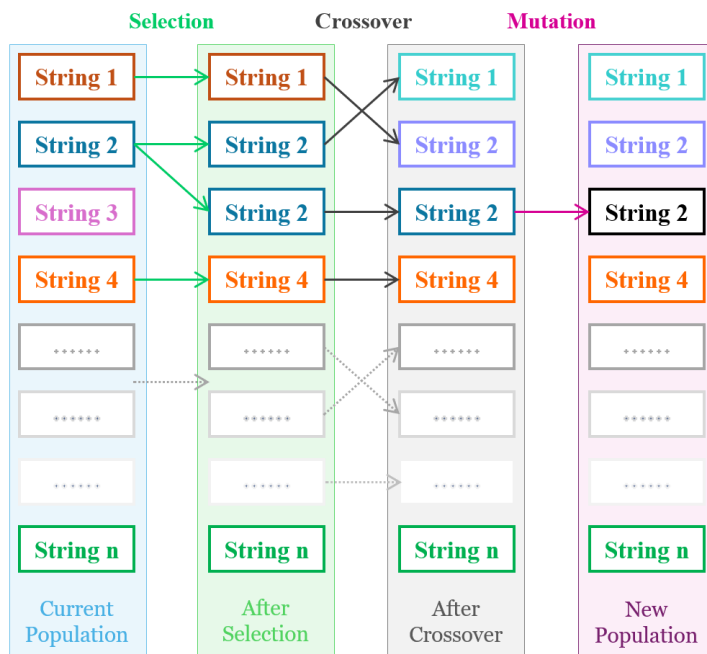
294 **Figure 9.** Basic convolutional neural networks (CNN) model architecture (adapted from [36]).

295 **2.4 Naïve Bayes (NB) and K-nearest Neighbors (KNN)**

296 NB is a simple multiclass linear classification algorithm that is based on Bayes' theorem [32]. Its
 297 learning process can be simplified using generative assumptions and parameter estimations. By
 298 using Bayes optimal classifier, the required number of equations of NB increases exponentially
 299 with an increase in the number of features. Hence, by simplifying Bayes classifier through
 300 appropriate assumptions in equations, the number of features can be significantly reduced.
 301 However, modifying one feature does not alter other features, as this method neglects possible
 302 correlations between features [26]. In contrast, KNN is a nonparametric ML algorithm that is used
 303 for both classification and regression, and it does not incorporate assumptions regarding the
 304 decision on boundaries [37]. For each test instance, the algorithm identifies the K most relevant
 305 data points (nearest neighbors) within the training dataset and predicts outcomes based on the most
 306 frequently occurring class among these neighbors. This approach, often referred to as the majority
 307 rule, is conceptually similar to the probabilistic reasoning used in Bayesian methods [38].

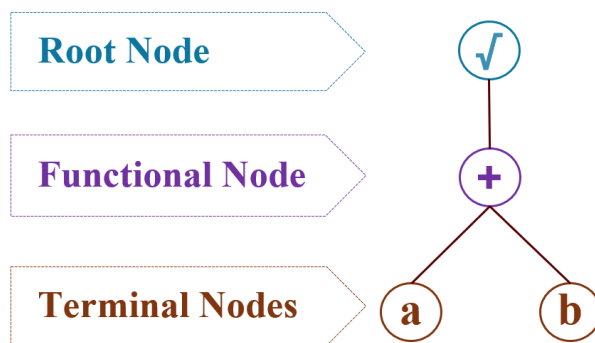
308 **2.5 Genetic Algorithm (GA) and Particle Swarm Optimization (PSO)**

309 GA and PSO are another type of AI methods that are broadly used for optimization and searching.
310 GA is a strategic model based on the principles of genetic evolution [39], focusing on the principles
311 of survival of the fittest and adaptation. GA continuously produces new groups of genes
312 (populations of chromosomes or strings) to perform a task by formulating old groups of genes. A
313 GA contains three parts: (i) coding and decoding of variables into strings, (ii) evaluating the fitness
314 of each solution string, and (iii) applying genetic operators (crossover, mutation) to generate the
315 generations of next solution strings [40]. To derive accurate solutions (Figure 10), an appropriate
316 number of chromosomes (strings) must be selected, which are obtained in multiple phases. First,
317 the necessity of reproducing a string is assessed based on its fitness function. If the optimal solution
318 is not reached, a crossover operation creates modified offspring by combining parent genes, and
319 mutation introduces additional variability. This process is repeated until an optimal solution is
320 obtained [41].



321 **Figure 10.** Operational structure of genetic algorithm (GA) (adapted from [42])
322

323 Genetic programming (GP) is an extension of GA in which solutions are represented as computer
324 programs, whereas GA typically produces numeric strings as solutions. The classical version,
325 known as tree-based GP, constructs models as trees consisting of functions and terminals with a
326 root node (Figure 11). After generating an initial set of random models, successive generations are
327 created using mutation, crossover, and reproduction, and the best program across all generations
328 is selected as the output [43]. Gene expression programming (GEP) is a developed version of GP
329 first invented by Ferreira [44] where new generations of models created by GP are represented as
330 linear strings that are decoded and expressed as nonlinear entities (trees) [45]. Multi-expression
331 programming (MEP) is a more advanced linear GP approach, where a single chromosome can
332 encode multiple programs. Fitness values are evaluated across these programs to identify the
333 optimal solution [46].



334
335 **Figure 11.** A tree-structured genetic programming (GP) model (adapted from [43]).

336 PSO resembles GA and is inspired by communal behavior of animals with five main features [41]:
337 (i) Proximity: Simple calculations are performed in definite time and space; (ii) Stability: The
338 system does not react to every environmental change; (iii) Quality: Significant changes in the
339 environment are detected to ensure solution quality; (iv) Diverse response: No singular limitation
340 exists in system response to environmental changes; (v) Adaptability: Changes in the environment
341 are considered during optimization.

342 2.6 Gaussian Process Regression (GPR) and Multivariate Adaptive Regression Spline 343 (MARS)

344 GPR is a nonparametric model that systematically quantifies the prediction uncertainty of
345 nonlinear high-dimensional problems with small simplistic samples. It has a simple training
346 process by selecting appropriate functions according to the pattern in the training data. By setting
347 the initial values and optimizing the hyperparameters using the input training data, prior
348 distributions are determined, and prior model is transformed into posterior model, respectively.
349 Thus, GPR offers adaptability in hyperparameter selection with flexible nonparametric inference.
350 Finally, it performs its prediction using the regression prediction model [19]. Another method,
351 MARS, is suitable for generating solutions to problems with continuous numerical outcomes and
352 high input dimensions. Similar to GPR, it can perform nonparametric and nonlinear regression. It
353 partitions the input space into subgroups and fits piecewise regression models within each
354 subgroup using basic functions. This process enables MARS to capture complex data structures
355 and identify potential interactions among input variables across all degrees [19].

356 2.7 Tree Algorithm-based Models and Boosting Methods

357 Decision trees (DT), also referred to as regression trees (RT), are nonparametric models that solve
358 classification and regression problems by recursively splitting data into a hierarchy of simple
359 decisions based on one or more input features. A typical DT structure is shown in Figure 12 and
360 involves two key steps: (1) *tree-building*: training dataset is partitioned into non-overlapping
361 regions, and (2) *tree-pruning*: reduces overfitting by trimming unnecessary branches of the tree
362 [37]. Random forest (RF), also called an ensemble of decision trees, consists of multiple DTs
363 operating together (Figure 12).

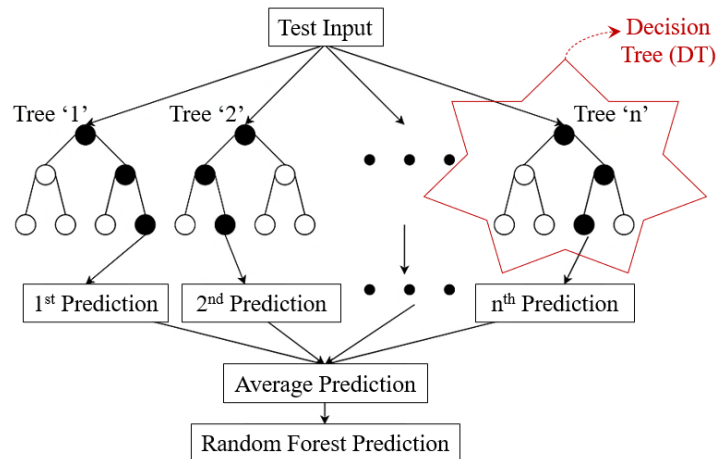


Figure 12. Tree pattern of random forest (RF) model (adapted from [47]).

364

365

366

367

368

369

370

371

372

373

374

375

376

377

378

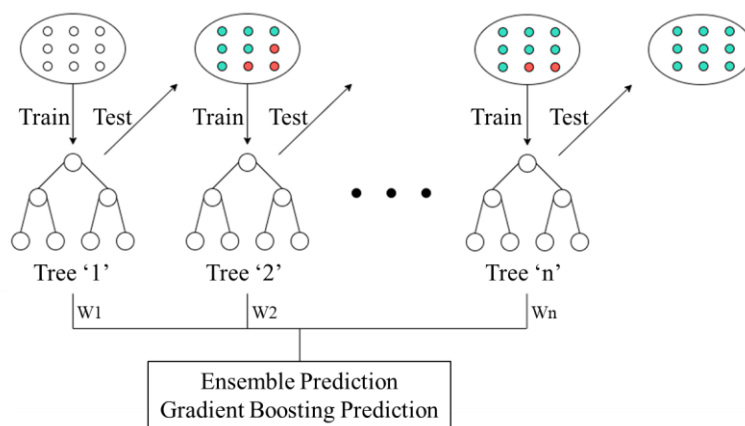
379

380

Each tree generates predictions on new data, and the final output is obtained via majority voting for classification or averaging for regression. Overfitting in individual trees is mitigated because multiple trees contribute to the final result [47]. The performance and robustness of DTs and other single predictive models can be significantly enhanced using ensemble ML methods. One such method is the bagging regressor (BR), which primarily relies on bootstrap aggregating. In this process, multiple copies of the original dataset are generated through resampling (bagging) [48]. Data points are randomly selected from the original dataset with replacement to create bootstrap samples, suggesting some original data may not appear in certain samples. Finally, base models (e.g., DTs) are then trained on these samples, and predictions on new data are combined, typically using majority voting for classification or averaging for regression [49]. Bagging reduces variance, variability and noise in predicted output by training multiple models in slightly different data [50].

Apart from BR, some boosting techniques can enhance the performance of DT by merging a set of weak classifiers to form a strong classifier. Among them are adaptive boosting (AdaBoost), extreme gradient boosting (XGBoost), light gradient boosting method (LGBost), natural gradient boosting (NGBoost), gradient boosting regressor (GBR), categorized boosting (CatBoost), and

381 histogram gradient boosting (HGB) [51]. In AdaBoost, all observations are weighted equally,
 382 and the model is retained by correctly classifying the incorrectly classified observations with
 383 higher weights than usual. In this manner, the learners are trained using the weighted classification
 384 accuracy of the previous learners [52]. In contrast, the remaining methods mentioned above are
 385 variants of gradient boosting (GB) framework which performs gradient optimization on the
 386 contribution of each weak learner to reduce the overall error of the strong learner (Figure 13) [53].
 387 XGBoost leverages the misclassification error of the prior model, although the need for successive
 388 model training leads to slow processing. LGBBoost operates leaf-wise rather than depth-wise, thus
 389 providing more precise but complex trees aiming at computational efficiency. It poses enhanced
 390 training speed, greater efficiency, improved precision, lower memory consumption and
 391 competence to process large datasets [54]. NGBBoost generalizes GB to estimate the parameters of
 392 a conditional probability distribution as target for a multiparameter boosting algorithm [55] and
 393 GBR deals with regression problems [56]. CatBoost can control the categorical features of the
 394 input parameters during the training phase by operating in the preprocessing stage [37]. HGBBoost
 395 employs histogram based methods interpreted by DT to handle efficient bulk dataset [51].



396

397

Figure 13. Gradient boosting (GB) pattern (adapted from [47]).

398 **2.8 Support Vector Machine (SVM)**

399 SVM was developed by Vapnik [57] that uses optimal separating hyperplane to separate positive
400 and negative classes of datapoints with the farthest possible two marginal boundary lines (Figure
401 14). Support vectors are derived from datapoints representing the separating hyperplanes in a
402 transformed space [26]. Figure 14(a) shows several possible classifiers separating the datapoints,
403 while one optimal separating hyperplane separates the data with maximum margin as further
404 shown in Figure 14(b). SVM can also be operated through regression applications as support vector
405 regressor (SVR) [56]. As an extension of SVM, SVR aims to find a hyperplane with a specific
406 number of dimensional space (input parameters) that classifies the training datasets in different
407 classes. It differs from SVM as it targets a flat type of hyperplane that accepts the data points
408 within or on the margins and rejects data points outside the margins [58].

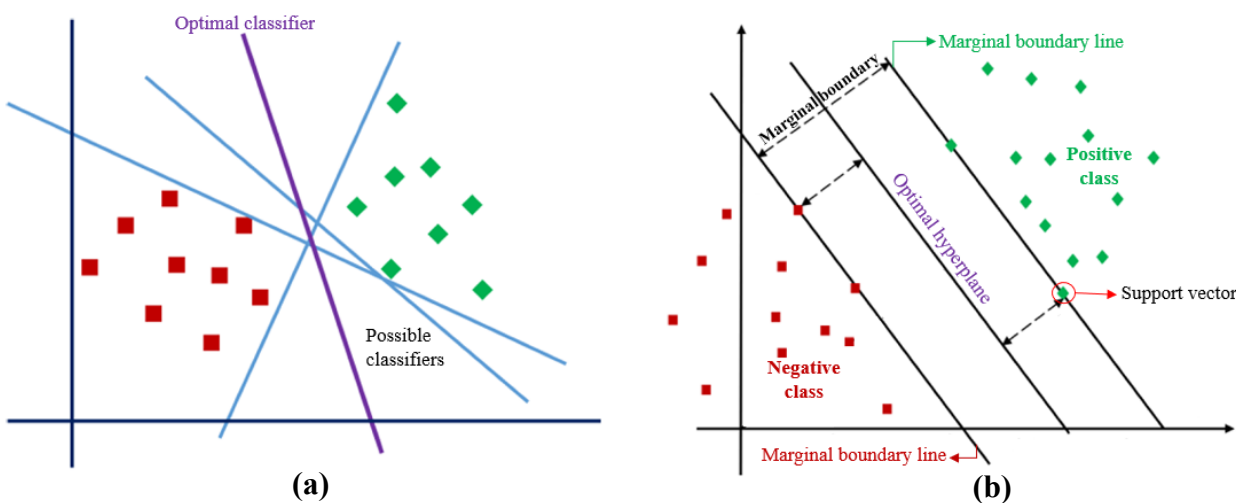


Figure 14. Decision boundary from support vector machine (SVM) (adapted from [59]).

409 **2.9 Key Performance Metrics and Model Validation Techniques**

410 **2.9.1 Performance Evaluation**

411 There is no predefined method for determining the optimal architecture of a model. However, the
412 accuracy of a model layout can be evaluated using several performance criteria, such as root-mean-

413 square error (RMSE), mean absolute error (MAE), mean absolute percentage error (MAPE), and
 414 coefficient of determination (R^2). RMSE quantifies the magnitude of errors and is sensitive to
 415 outliers. MAE utilizes a scale similar to that of the data to compute the variance between predicted
 416 and target values. MAPE measures the range of errors in percentages. R^2 represents the proportion
 417 of the difference in predicted values that can be explained by the model. These metrics can be
 418 mathematically expressed as follows:

$$\text{RMSE} = \sqrt{\frac{1}{m} \sum_{n=1}^m (e_n - \hat{e}_n)^2} \quad \text{Eq. (1)}$$

$$\text{MAE} = \frac{1}{m} \sum_{n=1}^m |e_n - \hat{e}_n| \quad \text{Eq. (2)}$$

$$\text{MAPE} = \frac{1}{m} \sum_{n=1}^m \left| \frac{e_n - \hat{e}_n}{e_n} \right| \quad \text{Eq. (3)}$$

$$R^2 = 1 - \frac{\sum_{n=1}^m (e_n - \bar{e}_n)^2}{\sum_{n=1}^m (e_n - \bar{e}_n)^2} \bar{e} = \frac{1}{m} \sum_{n=1}^m e_n \quad \text{Eq. (4)}$$

419 where m , n , $\bar{e} - \bar{e}_n$, e_n , and \hat{e}_n denote the number of data points, the data sample index (runs from
 420 1 to m), the difference in mean of observed values, the target value, and the predicted value,
 421 respectively. Although various evaluation metrics have been identified [189], RMSE, MAE,
 422 MAPE, and R^2 remain the most widely used for AI-predicted results in engineering applications
 423 [190,191]. However, these metrics have limitations. For example, RMSE is not always appropriate
 424 for comparing accuracy across time series [192], while MAPE can be unreliable and misleading
 425 [193]. R^2 is dimensionless, allowing comparison across heterogeneous target variables (e.g., MPa,
 426 mm/m, %) and enabling cross-dataset benchmarking. Nevertheless, earlier surveys reported that,
 427 although R^2 is the most commonly used metric in engineering, it can sometimes be biased,
 428 insufficient, and misleading; meanwhile, other metrics also present challenges [194]. In fact, no
 429 single metric can be considered universally superior [195]. In this study, most structural

430 engineering papers published between 2020 and 2024 consistently reported R^2 as the primary
431 benchmark for evaluating predictive accuracy, typically alongside complementary metrics such as
432 RMSE, MAE, and MAPE. R^2 is unitless, with values ranging from 0.0 to 1.0 [196]. For RMSE,
433 the normalized values below about 5% are generally regarded as excellent predictive accuracy and
434 for MAE, lower values (e.g., < 0.1 for displacement prediction) demonstrate strong alignment with
435 engineering tolerances [227]. For general cases, MAPE values under 10–15% are frequently
436 considered acceptable, while errors above 20–25% indicate weaker model performance [228].

437 **2.9.2 Model Robustness and Accuracy**

438 Although R^2 is a popular and intuitive measure of accuracy in AI-based structural engineering
439 models, it is important to recognize its limitations to ensure proper interpretation. First, R^2 values
440 are scale-dependent, meaning that the same R^2 can correspond to very different levels of absolute
441 error across datasets, which limits cross-study comparisons [208]. Second, it naturally increases
442 with model complexity, even when added predictors are not meaningful, making it sensitive to
443 overfitting unless paired with adjusted R^2 or error-based metrics [209]. Third, it is insensitive to
444 systematic bias: a model can consistently underpredict or overpredict and still yield a high R^2 if
445 variance trends are well captured [210]. Fourth, it does not provide information about the
446 distribution of errors, meaning outliers may be masked, while metrics like RMSE penalize such
447 deviations more strongly [210]. Finally, because R^2 is bounded above by 1 but unbounded below
448 ($-\infty$), negative values do not clearly quantify the degree of model inadequacy [208]. To address
449 these issues, structural engineering studies often report heterogeneous metrics such as RMSE,
450 MAE, and MAPE to complement R^2 ; for example, Yang and Liu [211] demonstrated that their
451 model's high R^2 was further substantiated by substantially reduced RMSE and MAE compared to
452 code predictions. Similarly, normalized or relative error measures help standardize error

453 magnitudes across studies (e.g., RMSE or errors normalized by mean or range) so that results are
454 more comparable across datasets with different scales [212]. Thus, while R^2 remains a valuable
455 benchmark for variance explanation, pairing it with error- and scale-sensitive metrics provides a
456 more holistic and trustworthy evaluation framework for AI applications in structural engineering.

457 Monte Carlo simulations (MCS) provide a robust method for evaluating model performance and
458 reliability. This sampling-based methodology involves performing many simulations of the same
459 process to converge the average of large samples to an anticipated value for infinite samples. This
460 approach is suitable for randomizing the sampling method of training and testing dataset for the
461 selected models. Subsequently, a specific number of simulations are performed with different
462 dataset splits for training and testing. By employing MCS, random sampling helps enhance model
463 accuracy by reducing errors in AI predictions. For example, if 10 samples are selected from among
464 100 samples that contain 50% each of two different types of data, the correct proportion of the two
465 types of data may not be achieved. Therefore, certain variations may appear as sampling errors in
466 the predictions. The random sampling process can eliminate bias in parameter selection, thereby
467 maximizing accuracy [60].

468 **2.9.3 Data Minimization**

469 The availability of input parameters generally improves the accuracy of model predictions.
470 However, unnecessary data, with no influence on the final prediction, can introduce system noise,
471 mislead the training programs, and compromise the model's performance. The influence of such
472 input parameters can be regulated through a sensitivity analysis. The most widely used methods
473 for sensitivity analysis include the cosine amplitude method, Milne method, and generalized cross-
474 validation (GCV) method, as discussed in the following sections [19]:

475 **2.9.3.1 Cosine Amplitude Method**

476 This method quantifies sensitivity by computing the correlation between the input and output data.

477 The correlation factor (R_i) is calculated as:

$$R_i = (\sum_{k=1}^m x_{ik}y_k) / \sqrt{\sum_{k=1}^m x_{ik}^2 \sum_{k=1}^m y_k^2} \quad \text{Eq. (5)}$$

478 where x_{ik} is the value of the i -th input parameter corresponding to the k -th output, y_k is the value
479 of the k -th output, and m is the total number of samples. A higher value of R_i represents a stronger
480 correlation between the input and output parameters [19].

481 **2.9.3.2 Milne Method**

482 This method analyzes the effects of inputs on outputs based on the weights of the connections
483 between nodes, represented by a static weight matrix:

$$\text{Influence of input parameter} = \frac{\sum_{m=1}^{N_h} \frac{w_{ml} w_{pm}}{\sum_{l=1}^{N_i} |w_{ml}|}}{\sum_{k=1}^{N_i} (\sum_{m=1}^{N_h} \frac{|w_{jk}|}{\sum_{l=1}^{N_i} |w_{ml}|})}, \quad \text{Eq. (6)}$$

484 where N_i represents the number of input parameters (i), N_h represents the number of hidden
485 neurons, w_{ml} represents the weight of the connection between the input neuron l and the hidden
486 neuron m , w_{jk} represents the weight of the connections between node j and node k , and w_{pm}
487 represents the weight of the connection between hidden neuron m and output neuron p [19].

488 **2.9.3.3 GCV method**

489 The significance of an input parameter can be defined as the square root of the GCV of the model
490 with all basic functions containing the eliminated parameter, minus the square root of the GCV of
491 the full model. The GCV can be defined as follows:

$$GCV = MSE_{train} / (1 - enp/n)^2 \quad \text{Eq. (7)}$$

492 Based on this equation, GCV depends on the mean square error of the training data (MSE_{train}),
493 number of samples in the training data (n), and effective number of parameters/variables (enp)
494 [19].

495 **2.9.4 Data Interpretability**

496 As mentioned in Section 2.9.1, RMSE, MAE, MAPE, and R^2 are commonly used in regression
497 problems to evaluate model performance. Beyond accuracy, SHapley Additive exPlanations
498 (SHAP) is an interpretability method that provides insights into feature contributions in regression
499 tasks. For example, SHAP values quantify the influence of each feature on the predicted
500 continuous outcome. SHAP is employed to interpret the decision-making process of complex AI
501 models by providing post-hoc explanations of model predictions [61]. Similar to parametric
502 analysis, SHAP isolates the individual contribution of each input parameter to the model's output.
503 This facilitates a clear understanding of the inherent reasoning behind predictions and allows the
504 relative influence of each parameter on the predicted results to be distinguished [51]. **Feature**
505 **importance** refers to analytical techniques that quantify the relative contribution of each input
506 **variable to the predictive performance of a machine learning model, typically through model-based**
507 **or permutation-based measures. Recent engineering studies show that such methods enable**
508 **researchers to identify which design or material parameters most strongly influence target**
509 **responses, offering insights that align with established physical or experimental understanding.**
510 **For example, Nguyen et al. [222] used SHAP on a boosting model for concrete-filled steel tube**
511 **columns and found that the most important features were exactly the expected mechanical loads**
512 **(bending moment and axial force). In other words, SHAP highlighted that these domain-critical**
513 **forces drive the model's predictions, validating the AI with known structural physics. Similarly, a**
514 **RF-based framework for multi-distress prediction in continuously reinforced concrete pavements**

515 highlighted the dominance of structural and environmental variables, further emphasizing the
516 interpretability of feature importance in linking AI outcomes to engineering behavior [223].

517 However, SHAP and related interpretability methods should be applied with caution, as correlated
518 features may distribute importance scores misleadingly. Additionally, issues such as data leakage
519 during preprocessing or feature engineering can inflate interpretability results, limiting their
520 generalizability. On the other hand, precision and recall are frequently employed evaluation
521 metrics for classification problems due to their ability to capture the trade-off between false
522 positives and false negatives [62]. Precision represents the percentile of successful predictions for
523 each predicted result, while recall measures the fraction of relevant instances. Both metrics are
524 considered more effective when their values approach 1 [37]. Generally, regression metrics
525 (RMSE, MAE, MAPE, and R^2) are considered separately from classification metrics (precision,
526 recall, and F1), with precision and recall applied only when the prediction target is categorical.

527 Only a small proportion of published machine-learning models undergo true external validation –
528 testing on wholly independent data – despite its recognized importance for unbiased performance
529 assessment [224,225]. This gap often reflects practical constraints, but it means many models are
530 evaluated only on internally held-out or cross-validated samples. Dataset sizes are frequently
531 inadequate [226], and most ML studies fail to justify sample-size calculations [226]. Proper
532 validation protocols (e.g. k-fold or nested CV) are therefore essential to mitigate overfitting and
533 bias [224,225]. In addition, performance reports should include measures of variability – such as
534 the standard deviation (SD) or coefficient of variation (CoV) of repeated runs, and 95% confidence
535 intervals (CI) for key metrics – rather than only point estimates [225]. Advanced techniques like
536 Bayesian hyperparameter optimization can help tune models efficiently, and explicit uncertainty
537 quantification (via bootstrapped CIs or Bayesian credible intervals) provide critical insight into

538 model robustness. Finally, assessment should follow established external-validation criteria and
539 report overall performance indices (e.g., accuracy and calibration metrics) with their uncertainties
540 to fully characterize model generalizability [225].

541 **3 Application of AI in Structural Engineering**

542 AI is increasingly being applied to predict the mechanical properties, environmental impacts,
543 durability, life cycle, and service life of structural materials such as concrete, reinforced concrete
544 (RC), composites, and structural steel. Large-scale laboratory experiments can be complemented
545 with AI-based predictions to minimize testing costs and time. The following sections provide an
546 overview of recent studies that have employed AI models in structural engineering.

547 **3.1 Materials Performance Prediction**

548 **3.1.1 AI in Concrete Mix Design and Mechanical Properties**

549 Recent studies have applied various AI and ML methods—such as KNN, ANN, BR, GPR, SVM,
550 DT, RF, MLP, GEP, boosting, and stacking techniques—to optimize concrete mix design and
551 predict its mechanical properties. These approaches have primarily focused on forecasting the
552 compressive strength of concrete incorporating recycled aggregates and supplementary
553 cementitious materials (e.g., slag, silica fume (SF), fly ash, and ground granulated blast-furnace
554 slag (GGBFS)), using datasets ranging from 1,000 to 3,600 samples. Among these, XGBoost
555 [63,64] and stacking methods (an ensemble technique combining multiple models) [65] achieved
556 the highest accuracy, with an R^2 value exceeding 0.950. The most influential parameters were
557 concrete testing age, cement content, and the replacement ratio of recycled coarse aggregates (CA).
558 Similarly, high R^2 values of 0.960 and 0.970 were reported using GEP for SF-concrete [66] and
559 BR for geopolymers concrete [67], respectively. Generic CV (not specified) was applied to reduce
560 overfitting, but no CI or SD values were reported. The influencing parameters were cement and

561 water, identified via sensitivity analysis over a dataset of 283 compressive and 149 tensile samples.
562 The use of multiple ML models and CV improved reliability, but the absence of explicit k-fold
563 details and external datasets limits generalization [66]. Onyelowe et al. [68] examined the mix
564 design of fly ash–incorporated concrete using statistical analysis, linear regression, and AI
565 algorithms, where ANN achieved the best performance ($R^2 = 0.92$) in predicting 28-d compressive
566 strength. The study used 112 mix samples with binder ratios as inputs, and models were validated
567 by statistical comparisons, with uncertainty of 15–20 MPa (SD for compressive strength models)
568 and 2–3 points (environmental impact models). The governing parameters were the fly ash-to-
569 binder ratio and aggregate-to-binder ratio and all methods. The study demonstrated the capability
570 of ANN to develop a robust mix design tool for sustainable concrete with comprehensive
571 parametric considerations considering.

572 GB and XGBoost also outperformed other methods in a study by Kang et al. [69], where the water–
573 cement ratio and SF content were identified as the most critical parameters affecting the
574 compressive and flexural strength of steel fiber–reinforced concrete, based on a dataset of 220
575 samples. Similarly, GB was shown to be more accurate and robust in determining the flexural
576 strength of fiber-reinforced concrete beams, achieving a higher slope validation ratio (0.83/1). The
577 depth of the beam was the most influential factor, followed by the flexural reinforcement area [70].
578 In contrast, Khan et al. [71] reported ANN to be superior to RF, reaching an R^2 of 0.990, while
579 using ~120 FRP beam samples with geometric, reinforcement, and material inputs. For validation,
580 dataset was split into training/test sets with error indices RMSE of 7.37 kN-m. This result was
581 further validated by Zhang et al. [72] over 134 data points, where ANN ($R^2 = 0.979$) outperformed
582 GEP and existing ACI 440.11-22 [188] equations. Li et al. [73] recommended XGBoost ($R^2 =$
583 0.93) for predicting the flexural strength of concrete with cementitious materials. Using SHAP

584 analysis, the water–cement ratio and curing age were identified as the key factors. Khan et al. [46]
585 used GEP and MEP to determine the flexural capacity in FRP-strengthened beams using 200
586 samples. Validation was based on holdout sets, not k-fold CV. No uncertainty intervals were
587 provided, though strong R^2 values (0.96–0.98) and low MAE demonstrated accuracy. SHAP
588 analysis identified beam width, depth, and reinforcement ratio as key predictors. Overfitting was
589 managed with evolutionary learning techniques, but the study was limited to smaller dataset size
590 and lack of external validation.

591 The prediction of split tensile strength for concrete containing different cementitious materials
592 (e.g., GGBFS and Portland slag), sand replacements, and recycled aggregates was examined using
593 up to twelve AI methods on 168, 310, 381 dataset points. The peak R^2 values achieved were 0.98
594 (XGBoost) [74], 0.892 (extra tree regressor) [75], and 0.842 (XGBoost) [76], respectively. The
595 common influencing factors were water-cement ratio, curing age and ratio cementitious materials.
596 Nguyen et al. [56] implemented four ML methods, i.e., SVR, MLP, GBR, and XGBoost, to
597 determine the strength characteristics of high-performance concrete. Among these, SVR and
598 XGBoost offered the most accurate results (R^2 of 0.96–0.98) with reduced computational effort
599 via random-search-tuned train/test validation. Key governing factors were cement contents, blast
600 furnace slag, fly ash, water–cement ratio, superplasticizer, coarse and fine aggregates (FA), and
601 curing period. Overfitting was reduced by efficient parameter tuning and data imputation
602 strategies, though the absence of k-fold CV or external test sets limits robustness.

603 Earlier, Gholampour et al. [77] developed empirical models using GEP to predict the 28-d
604 compressive strength, elastic modulus, flexural strength, and splitting tensile strength of recycled
605 aggregate concrete (RAC). A comprehensive database with 650 compressive strength values, 421
606 elastic modulus values, 346 splitting tensile strength values, and 152 flexural strength values from

607 previous reports was compiled to compare the performance of 34 mechanical-property models for
608 RAC, developed in 21 other studies. The proposed GEP model provided more accurate results than
609 other models on large datasets and exhibited consistency with existing code expressions. Similarly,
610 a hybrid GP model was developed in a study to predict the triaxial compression loading based on
611 330 tests on concrete samples: comparisons with earlier studies across several statistical criteria
612 confirmed the model's accuracy and reliability. The GEP-based approach using only the mix-
613 design properties as predictors achieved $R^2 = 0.81$ [17]. In another study [47], four models (RF,
614 NN, GB, and AdaBoost) were applied to predict the fatigue life of concrete under uniaxial
615 compression. The dataset, containing 1300 sets of experimental data, was split 90:10 for training
616 and testing. **Instead of CV, the authors focused on dataset cleaning and feature analysis.** Six key
617 input variables, related to the material and dimensional properties (compressive strength of
618 concrete, height-to-width ratio, and shape of test specimen) and the loading conditions (maximum
619 stress level, minimum stress-to-maximum stress ratio, and loading frequency), were adopted.
620 Maximum stress level and frequency were the most influential features. The GB model yielded
621 the lowest error and high predictive accuracy ($R^2 \approx 0.915$) across the three datasets. Overfitting
622 risk was reduced by outlier filtering, though the absence of CV and uncertainty measures limits
623 confidence in generalization. **Cascardi et al. [78] proposed an ANN-based analytical model to**
624 **predict the compressive strength of circular concrete columns wrapped with fiber-reinforced**
625 **polymer (FRP). The compressive strength of the FRP-confined concrete was influenced by the**
626 **column diameter, compressive strength and Young's modulus of the unconfined concrete, and**
627 **thickness of the FRP jacket. A total of 465 samples were included in the database and key**
628 **parameters were column diameter, unconfined concretes' compressive strength, thickness and**
629 **Young's modulus of FRP jacket.** The model achieved high consistency and accuracy (R^2 of 0.83)

630 when compared with results from laboratory tests and equations derived from international codes
631 and scientific literature.

632 Few researchers have used ML to assess the self-healing ability of cementitious materials. Using
633 results from 12 experimental studies, [Rajczakowska et al. \[20\]](#) compiled a detailed database with
634 197 records to predict the compressive strength recovery of concrete using four interpretable ML
635 methods: SVM, RT, ANN, and ensemble of RT. The 12 input variables were water-cement ratio,
636 concrete age, cement content, fine and CA, peak loading temperature and its duration, cooling
637 regime and duration, curing regime and duration, and volume of samples. The stability of the
638 models was verified through Monte Carlo analysis. The Ensembled RT achieved the highest
639 accuracy ($R^2 > 0.900$) and robustness. The most influential parameters were temperature, curing
640 regime, curing time, and aggregate amounts. In terms of self-healing ability, [Huang et al. \[79\]](#)
641 [assessed 797 bacterial self-healing concrete test results with 22 features. ML models including](#)
642 [GBR, SVR, RF, and DNN were compared, with GBR performing best \(\$R^2 = 0.956\$ \). 10-fold CV](#)
643 [and grid search optimization were applied to reduce overfitting. No CI was reported, but RMSE](#)
644 [was used for error estimation. Key parameters were bacteria type, healing time, crack width, and](#)
645 [environment. Overfitting risk was explicitly addressed with CV and sensitivity analysis, improving](#)
646 [robustness.](#) Some other studies also reported promising accuracy such as GEP with an R^2 of 0.938
647 for admixture-based concrete [using 619 data points \[80\]](#), and BR with an R^2 of 0.974 for engineered
648 cementitious composite based concrete [using 617 crack data samples \[81\]](#). [Most of the contributing](#)
649 [variables were associated with FA, cementitious materials \(e.g., fly ash, SF, and limestone](#)
650 [powder\), water–binder ratio, and crack width before self-healing.](#)

651 3.1.2 Durability and Fire Resistance of Materials

652 Predicting the long-term serviceability of structural materials is crucial for effective structural
653 design. Several studies have explored optimal performing methods for examining key durability
654 factors (DF). For example, ANN achieved an R^2 exceeding 0.950 in predicting moisture exposure
655 using 429 observations. Regression models were tuned via Bayesian optimisation and evaluated
656 on a held-out test set; classification used stratified 10-fold CV. The study does not report SD/CI
657 for model outputs; it reports standard predictive metrics (R, MSE, RMSE, MAE). Important
658 influential variables include exposure duration and environmental factors (relative humidity,
659 temperature) alongside geometrical and material properties. The use of stratified CV and Bayesian
660 hyperparameter tuning reduces overfitting risk but the study provides limited formal uncertainty
661 quantification [82]. In similar manner, Multi Expression Programming achieved R^2 of 0.921 and
662 0.977 in modeling concrete corrosion using 256 experimental records (chemical and biological
663 tests). Models were trained on a 50/50 split and performance reported using MSE and R^2 (MEP
664 performed best). Inputs were very small (time \pm pH), so influential parameters are essentially
665 exposure time and pH; because feature dimensionality is low the models are simpler, but the study
666 does not report formal uncertainty bounds (SD/CI) nor use an external test set — this limits
667 quantified generalization/overfitting analysis beyond train/test errors [83]. SVM (88–89%
668 accuracy; 204 datasets) and back propagation NN (85% accuracy; 159 specimens) were used to
669 predict chloride resistance [26,84]. In a study of Khan et al. [50], BR achieved an R^2 of 0.999 in
670 predicting depth of wear with 216 datapoints, and SHAP analysis identified testing time and
671 specimen age as the dominant features. The study addressed overfitting by using ensembles,
672 objective function minimization, and external validation metrics — although the paper did not
673 present formal SD/CI intervals for predictions. External validation criteria and performance index

674 were used to support model generalization claims. Similarly, peak accuracies were observed for
675 RF ($R^2 = 0.950$) to estimate frost resistance using 100 groups of orthogonal-experimental data
676 samples. and for optimized ANN ($R^2 = 0.926$) to evaluate impermeability using 417 sets of
677 experimental data from published literature [85,86]. In another study, hybrid ANN achieved an R^2
678 exceeding 0.990 in modeling carbonation penetration with 532 data records, and the models were
679 trained with a 70/15/15 split and ten-fold CV. Uncertainty is presented via SD and fold-by-fold
680 MAE/RMSE (no classical CI). The top influential parameters were exposure time ($\approx 27\%$), CO_2
681 concentration ($\approx 22\%$), and water-binder ratio ($\approx 18\%$). CV and validation partition were used to
682 limit overfitting; the hybrid ANN consistently reduced errors in comparison to plain ANN across
683 training, validation, test and CV folds, but the authors still recommended enlarging the database
684 to further lower overfitting risk [87]. Across these studies, the key parameters included duration
685 of exposure, volume fraction of CA, cement content, water-binder ratios, FA, supplementary
686 cementitious materials (SCM) content, thickness of protective layer, and ratio of environmental to
687 relative humidity. Liu et al. [19] predicted the frost durability of RAC based on the DF using three
688 soft computing models: ANN, GPR, and MARS. The database contained experimentally measured
689 DF values of 142 samples from 23 published studies. The ANN model (with 19 neurons) achieved
690 the highest accuracy ($R^2 = 0.951$) followed by GPR, with the lowest RMSE and MAPE. Sensitivity
691 analysis identified air-entrainment as the most critical factor influencing frost durability.
692 Parametric analysis further showed that frost resistance improved with reduced recycled aggregate
693 replacement, higher air-entrainment, lower water-cement ratio, and an optimized sand-RAC ratio.
694 At elevated temperatures due to fire exposure, structural materials often lose strength and
695 durability. Because full-scale fire tests on structural prototypes are difficult to conduct, there is a
696 growing demand for numerical and AI-based predictive models. Numerous studies have explored

697 AI for predicting fire-induced effects on structural components. Concrete is widely used by fire
698 engineers, but all concrete types may fail under extreme fire exposure [88]. Liu et al. [89] examined
699 the thermal spalling of steel and polypropylene fiber-reinforced concrete. Among six tested AI
700 models, XGBoost achieved the highest accuracy ($R^2 = 0.972$), with polypropylene fiber content
701 identified as the key parameter for preventing spalling. Habib et al. [90] evaluated six classification
702 models on fire-exposed fiber-reinforced concrete beams using 50 experimental tests, with
703 AdaBoost demonstrating reasonable accuracy ($R^2 = 0.90$), followed by GB. In another study, SVR,
704 RF, and DNN were employed using a compiled database to predict the fire resistance of FRP-
705 strengthened RC beams. DNN performed best ($R^2 = 0.910$), with critical parameters including
706 geometrical features of the beam section, applied loading, and thermal properties of fire insulation
707 [29]. Similarly, ensemble models (XGBoost, CatBoost, LGBost, HGBost, GB, and RF)
708 achieved accuracy exceeding 0.90, outperforming traditional ML models (ANN, DT, PR, and
709 SVM) when trained on 21,000 data points from numerical simulations. SHAP analysis revealed
710 the most significant negative factors as loading ratio, FRP area, and total applied load, while the
711 positive factors were total area of steel reinforcement, thickness of insulation on beam sides, and
712 steel reinforcement cover depth [51].

713 Composite structures are widely used in industrial buildings and commercial spaces. Because steel
714 is more prone to failure than concrete in fire exposure, construction with composite structures is
715 often preferred, and related AI-based research has received significant interest. Moradi et al. [91]
716 implemented an ANN model using 300 experimental data points to evaluate the fire resistance and
717 strength behavior of concrete-filled steel tubes. The model achieved R^2 values of 0.967 and 0.970,
718 a more accurate model than the existing empirical relationships. However, these tubes require
719 protective fire coatings, making concrete encased steel columns superior in fire resistance. Naser

720 [92,21] studied the fire behavior of RC columns using a combination of AI methods, including
721 intelligent PR, GP, DL, and traditional multi-linear regression. The study analyzed 112 test
722 observations under standard fire conditions for exposure durations of up to 5 h. The governing
723 factors associated with concrete performance were concrete mix proportion, components
724 (aggregate type and water–cement ratio), and supplementary additives (e.g., superplasticizers,
725 fibers, and SF). In predicting fire-induced spalling, GP achieved the highest precision ($R^2 = 0.940$),
726 followed by DL. Moreover, DL also performed better in predicting the relationship between the
727 governing factors and the fire resistance of concrete columns. Li et al. [93] developed ANN and
728 analytical models to predict the buckling resistance of axially loaded concrete-encased steel
729 columns exposed to fire conditions, considering 15200 specimens. The ANN and analytical
730 models achieved R^2 values of 0.990 and 0.950, respectively, and showed lower dispersion (smaller
731 SD) than the analytical equations. Validation was conducted by an 80/20–train/test–split and by
732 comparison with experimental fire tests. The temperature of concrete and steel sections were
733 affected by concrete grade, heating time, section factor and thickness of concrete cover. The very
734 large synthetic dataset and direct comparison to experimental tests reduce overfitting risk, though
735 explicit regularization or nested-CV details were not found in the examined parts of the study.
736 Naser and Kodur [35] used a dataset including 494 observations, incorporating a wide range of
737 geometric characteristics and material properties, to develop a systematic ML (combining
738 ensemble of RF, XGBoost and DL) approach to enable explainable and rapid assessment of fire
739 resistance and fire-induced spalling of normal- and high-strength RC columns. This ensemble
740 could analyze 5000 reinforced columns within 60 s, achieving an R^2 of 0.86. Although tunnel fires
741 are relatively infrequent [94], the growing number of tunnels has resulted in catastrophic incidents
742 worldwide [95]. Wu et al. [96,97] investigated fire source behavior, hazards, and critical

743 temperature fields in tunnels using LSTM-RNN and Transpose-CNN under 100 simulated tunnel
744 fire scenarios. The LSTM-RNN model achieved an accuracy of 0.90 with recommended 20 m
745 sensor spacing, while the Transpose-CNN model achieved ~0.97 accuracy with 32 sensors placed
746 at 5 m intervals. Both models effectively identified critical temperature fields, providing valuable
747 insights for safe evacuation, emergency response, and firefighting strategies.

748 Globally, the structural frames of most tall buildings, older buildings, and large-span warehouses
749 are either composed of or supported by steel components. Fire remains a critical hazard with
750 potentially catastrophic consequences for steel and steel–concrete interfaces. Engineers must
751 therefore accurately assess design parameters to ensure fire safety, a process increasingly
752 supported by AI-based predictive models. [Fu \[60\]](#) developed an ML framework incorporating DT,
753 KNN, and NN to rapidly predict the failure patterns of simple steel-framed buildings subjected to
754 fire and to assess the potential for subsequent progressive collapse. Failure patterns were defined
755 using the critical temperature method, and MCS and random sampling were performed to develop
756 a sufficiently large dataset for training and testing. The KNN and NN models provided satisfactory
757 predictions of the failure pattern and collapse potential of a two-story, two-bay steel-framed
758 building. Data driven ML models such as ANN, RF, GB and KNN have also been used to explore
759 the performance of the concrete-steel bond under high temperatures. [Al Hamd and Warren \[98\]](#)
760 analyzed 316 data points from previous laboratory-based studies and found GB to be the most
761 accurate model ($R^2 = 0.970$), with the other models also yielding consistent results. [The key input
762 features were concrete compressive strength, testing age, concrete surface temperature at failure,
763 thermal saturation ratio, bond length-to-diameter ratio, cover-to-diameter ratio, and fiber volume.
764 The dataset was validated with train-test split, and uncertainty was reported with RMSE of 1.08–
765 2.62 MPa and CoVs ranging from 18 to 74%.](#)

766 3.2 Structural Behavior Analysis

767 3.2.1 AI in Reinforced Concrete and Steel Structural Elements

768 A recent extension in GP, a GEP-based nonlinear model, was developed by [Gandomi et al. \[99\]](#) to
769 assess the shear resistance of RC beams with shear steel. The database comprised 466 experimental
770 measurements for both high- and normal-strength concrete beams. The proposed model
771 outperformed existing design-code models, achieving an R^2 value approximately 0.89. Sensitivity
772 analysis revealed that concrete compressive strength, web width, and effective depth were the key
773 factors controlling the variations in the shear resistance of RC beams with stirrups. [Cascardi \[100\]](#)
774 developed an analytical ANN model to predict the in-plane shear strength of masonry panels
775 retrofitted with fiber-reinforced mortar. The study considered different varieties of masonry types
776 (by material and texture) and reinforcement, in terms of both the fiber (glass, carbon, steel, basalt,
777 phenylene-benzobisoxazole) and matrices (cement, lime, and hydraulic mortars). Despite the large
778 diversity in the input parameters, the model demonstrated high precision and accuracy ($R^2 = 0.91$),
779 demonstrating robustness and sensitivity, with predictions consistent with results obtained using
780 international design codes. To assess rapid damage and seismic risks, and determine appropriate
781 retrofitting strategies, [Mangalathu et al. \[37\]](#) developed a comprehensive database of 393 one-
782 story, one-bay RC shear walls with both rectangular and non-rectangular sections. The dataset
783 included 152 flexural failure, 96 flexure–shear failure, 122 shear failure, and 23 sliding failure
784 samples. The model performances were evaluated using three metrics: global accuracy, precision,
785 and recall. Among the eight ML algorithms, RF achieved the highest accuracy (0.86), with a recall
786 of 70% and precision of 84% in identifying the flexure–shear failure mode on the test set. The
787 aspect ratio of the shear wall, boundary element reinforcement indices, and wall length–to–
788 thickness ratio were the critical factors governing the failure mode. Retaining walls provide

789 permanent lateral support for vertical soil slopes in infrastructure such as roads and bridges. In one
790 study, a modified SVM model outperformed alternatives in determining the safety criteria of
791 cantilever-type retaining walls [101]. Key parameters, including cohesion, angle of shearing
792 resistance, angle of wall friction, and reliability index, were computed using the first-order–
793 second-moment method. The modified SVM predictions deviated from synthetic reference values
794 by less than 2%.

795 An ANN model was developed to predict the ultimate compressive load of rectangular concrete
796 filled steel tube columns in both concentric and eccentric loading. The dataset included 1,224 test
797 results for both long and short specimens. The model showed improved accuracy compared with
798 available design codes (50% reduction in RMSE), and the most influencing parameters were steel
799 tube dimensions, thickness, and material strength [102]. For a similar case, Asteris et al. [103]
800 developed three alternative models using optimized ANN with a hybrid database of 1,857
801 specimens. These models outperformed code-based methodologies, with reduced RMSE by 34%.
802 Lemonis et al. [104] developed an ANN model to predict the ultimate axial compressive capacity
803 of square and rectangular concrete filled tubes. The database included experimental results of
804 1,193 long, thin-walled and high-strength specimens. The model offered satisfactory results, with
805 a 20% error margin for 92% of the specimens. Sensitivity analysis revealed that the influencing
806 factors were the tube dimensions and steel yield limit. Ferreira et al. [105] built a finite element
807 (FE)-based database and trained five ML models to predict global shear capacity of a steel-concrete
808 composite down-stand cellular beams with precast hollow-core units. Among the models, the
809 Catboost regressor algorithm showed optimal performance (R^2 of 0.982), followed by GEP (R^2 of
810 0.953), using more than 6 geometrical features (e.g., opening diameter, web opening spacing, tee-
811 section height, concrete topping thickness, interaction degree, and number of shear studs above

812 web opening). The FE-based database and the reliability analysis were used to quantify prediction
813 uncertainty at the design level, but per-prediction SD/CI numbers were not presented in the
814 examined portions of the study.

815 Lateral torsional buckling resistance, including web-post buckling and web distortional buckling
816 of slender cellular beam were accurately predicted (R^2 of 0.99) by developing ANN formula on
817 768 training models [106], validated with a 70/15/15 (training/validation/testing) hold-out split. A
818 7-neuron model was chosen for stability and practicality as overfitting risk increased with more
819 neurons. The key input parameters were beam dimensions, eccentricity from shear center and
820 moment gradient factor, and uncertainty was quantified via RMSE(1.2-2.2)/MAE(0.6-1.5)/SD.
821 Degtyarev [54] proposed an interactive notebook to predict elastic buckling (3645 FE datasets)
822 and ultimate loads (78390 FE datasets) of steel cellular beams using FE method optimized with
823 seven ML models (DT, KNN, RF, XGBoost, GBR, LGBost, CatBoost). The ML models were in
824 remarkable agreement with the numerical data and surpassed design codes (GBR with an R^2 of
825 0.997). The key influencing factors were beam span length, flange width, and web thickness. The
826 study used 10-fold CV for validation but did not report uncertainty intervals. Overfitting was
827 addressed with CV and model comparisons, though reliance solely on FE-generated data meant
828 external validation was not performed. Shamass et al. [107] implemented a MATLAB-based
829 graphical interface design tool by utilizing ANN with an overall accuracy of 0.932. This tool
830 integrated data generation from FE analysis, web-post buckling resistance predictions, and failure
831 mode classification of perforated steel beams with elliptical web openings. For similar case, Rabi
832 et al. [108] used a total of 10,764 web-post FE models on high strength steel beams. The dataset
833 was further employed to train and validate different ML methods (ANN, SVR, and GEP),
834 achieving R^2 values of 0.998, 0.999, 0.977, respectively. These methods were compared with

835 analytical model ($R^2 = 0.982$), and a novel design model was proposed. The study used 10-fold CV
836 and grid search for tuning, and reported detailed statistics including SD and CoV to quantify
837 uncertainty and compare generalisation. SVR showed the lowest CoV and smallest RMSE in the
838 reported comparisons. Overfitting was explicitly assessed via CV and training/validation splits.
839 Degtyarev et al. [61] applied the NGBoost model to predict the probabilistic load-bearing
840 capacities of laterally restrained cellular beams subjected to uniformly distributed loads,
841 considering all possible failure modes and their interactions. A database with 14,094 numerical
842 simulation results was considered, and the model was further interpreted with SHAP method. The
843 dataset was validated with 10-fold CV (80/20 train–test split) and uncertainty was reported with
844 CoV (≈ 0.014 across test data). The model significantly outperformed the existing design
845 provisions with an R^2 of 0.999 while offering probabilistic predictions.

846 Le et al. [41] investigated the prediction capability of two hybrid AI models, GA and PSO,
847 combination with a modified ANN to determine the buckling loads of 420-MPa high-strength steel
848 Y-section columns with slenderness ratios of 30-80. The dataset included 57 buckling test results
849 from previous studies. The input variables were column length, cross-sectional geometry, and
850 initial geometrical deviation in the x and y directions. Both models performed well, but the PSO
851 combined with the modified ANN model achieved a higher R^2 value of 0.929. Gandomi et al. [17]
852 used GEP to construct an accurate empirical prediction model that could relate the load capacity
853 of castellated steel beams (CSB) to their geometrical and mechanical properties. Considering the
854 nonlinear collapsible characteristics of CSBs, the GEP model and derived equation outperformed
855 a multivariable linear regression and conventional constitutive models based on first-principle
856 investigations (e.g., elasticity and plasticity theories). Because of the repetitive nature of beam–
857 column connections, compact and efficient designs are required to reduce fabrication costs while

858 maintaining quality. However, the vast number of connection types and loading scenarios makes
859 obtaining sufficient experimental data from laboratory setups impractical. Abdollahzadeh and
860 Shabanian [109] addressed this by using both mechanical modeling and an NN-based approach to
861 simulate the complex hysteresis behavior of beam–column connections with flange plates. The
862 combined neural network approach accurately captured the narrowed hysteresis behavior, with
863 $RMSE = 0.712$ and $MAPE = 0.9166$. Paral et al. [36] developed a DL-based nonparametric
864 approach that used continuous wavelet transforms of acceleration signal and 2D CNN for image
865 recognition to facilitate condition assessment of structural connections. Updated FE models were
866 used to train the CNN model, which successfully identified damaged locations and measured the
867 stiffness loss in the damaged beam-column joint. The study considered 80% training and 20%
868 testing data split for hold-out validation method.

869 **3.2.2 Structural Response Under Lateral Loads**

870 Inelastic dynamic analysis based on modern building codes is widely used to accurately determine
871 the seismic response of building frames. However, for large-scale structures, such analysis
872 becomes computationally intensive and difficult to implement. To address this challenge,
873 predictive models can be employed to achieve sufficiently accurate results with significantly
874 reduced computational demand, thereby facilitating seismic analysis and optimization of large
875 structures. Moreover, these models support the design and installation of structural solutions such
876 as retrofitting, BRBs, and dampers. In a recent study, an AI-enhanced computational method was
877 proposed by integrating AI with a shear building model, to determine the nonlinear seismic
878 response of RC frames under displacement controlled quasi-static cyclic loading and dynamic
879 earthquake ground motions. The database included test results of 272 RC columns. Numerical
880 results showed reductions of 60% and 62% in RMSE and MAE, respectively, indicating that the

881 proposed method outperformed existing physics-based and classical fiber-based models. In
882 particular, the AI technique accurately used real-world experimental data to evaluate the lateral
883 stiffness, and the shear model efficiently formulated the structural stiffness matrix [110]. Another
884 study highlighted the capability of wavelet-weighted least squares-SVM and an FFBP-ANN to
885 predict the inelastic force- and displacement-based seismic responses of an 18-story RC frame.
886 The model was trained with design-basis and maximum ground earthquake motions. The study
887 showed how training sample size (75/150/225) and choice of inputs (first three natural period
888 combinations) affect accuracy (assessed by MAPE, NRMSE, R^2). Uncertainty was expressed via
889 these error metrics and performance sensitivity, emphasizing robustness across sample sizes to
890 address overfitting risk. The ANN model achieved slightly higher accuracy ($R^2 = 0.999$ with 225
891 samples) while exhibiting lower sensitivity compared with integrated SVM model [111].
892 Gondaliya et al. [112] applied a probabilistic framework combining classification models (ANN)
893 and regression models (LASSO regression, RF, and GB) to assess the seismic response of a four-
894 story RC building frame under epistemic uncertainty. The models achieved high accuracy, ranging
895 from 0.87 to 0.97. To investigate the ultimate load-bearing capacity of inadequate RC frames, six
896 ML models were developed and validated against experimental and numerical analyses of the
897 load-displacement behavior of a one-story frame. Among these, RF performed best, achieving an
898 R^2 of 0.870. The most influential input parameters were axial load, rebar diameter, and concrete
899 strength [113]. As a solution to such inadequate capacity of columns, additional confining pressure
900 can be provided by utilizing FRP-retrofitting jacketing with internal grouting, which prevents
901 failure under extreme seismic and blast conditions. Shin et al. [114] proposed a rapid decision-
902 making tool for multi-hazard assessment and mitigation using ANN models capable of rapidly
903 generating large datasets. The ANN-based models achieved $R^2 = 0.98$ over 78 samples under

904 seismic loading and $R^2 = 0.99$ over 83 samples under blast loading. In a follow-up study, Shin et
905 al. [115] developed hybrid ML models which could optimize the retrofit details within desired
906 performance by controlling the confinement and stiffness ratios. First, ANN was used to rapidly
907 generate seismic and blast responses, and then GA was employed to optimize the retrofit details
908 within multiple objective functions. The ANN model achieved a high regression value of 0.994
909 using dataset from FE simulation-based ML models. For the model, validation conducted against
910 full-scale dynamic seismic tests and blast tests of RC frames, and reliability reported via small
911 simulation variations (<12% for seismic, <3% for blast) compared to experimental tests.

912 Few studies have incorporated AI methods to determine seismic response of structural steel
913 building frames. In a recent study, a portal frame was analyzed through four machine learning
914 models (RF, GB, XGBoost, and DNN) to determine its top floor displacement under lateral load.
915 RF outperformed others ($R^2 = 0.987$) in predicting displacement, and XGBoost also demonstrated
916 satisfactory performance in determining failure probability. While not explicitly stating CV, the
917 study used a holdout test set to validate models. Uncertainty was not reported via SD or CI; instead,
918 the study presented a battery of performance metrics (e.g., RMSE, MAE, and MAPE) [116]. Later,
919 RF was hybridized into three variants: RF dragonfly optimization algorithm (RF-DOA), RF
920 sparrow search algorithm (RF-SSA), and RF whale optimization algorithm (RF-WOA). RF-WOA
921 outperformed RF-DOA and RF-SSA, offering engineers a valuable tool for designing portal
922 frames with enhanced features. The study adopted a train/test split validation strategy and
923 compared among the hybrid models through rank analysis and regression line performance.
924 Uncertainty was not expressed via SD/CI, but through reliability indices and error/rank metrics.
925 Influential features include structural and loading variables incorporated into the RF models.
926 Overfitting risk was mitigated by comparing multiple hybrid configurations and leveraging

927 reliability analysis, though no explicit CV was declared [117]. Seismic fragility analysis
928 traditionally requires sophisticated numerical models and significant computational resources. By
929 contrast, ML models can efficiently identify high-dimensional input variables and capture complex
930 nonlinear relationships. In line with this, four ML models—RF, AdaBoost, GB regression tree
931 (GBRT), and XGBoost—were employed to construct fragility curves based on nonlinear time-
932 history analyses of 616 steel moment frames subjected to 240 ground motions. The models were
933 trained on 56,479 datapoints, and a graphical user interface was developed using best performing
934 models (GBRT and XGBoost, both achieving $R^2 = 0.999$). The inputs consisted of structural
935 descriptors and the first three natural periods, capturing the essential dynamic properties of the
936 frames. Model training and evaluation used a 70/30 holdout split, with hyperparameter tuning
937 performed (e.g., number of trees, and learning rate) to enhance generalization. The very large
938 dataset helped minimize variance and overfitting risk, and the ensemble models were chosen
939 specifically for their robustness. Feature-importance analysis highlighted the natural periods as
940 particularly influential in predicting fragility parameters. No independent experimental test dataset
941 was used, since all data came from simulation. However, the size and diversity of the generated
942 dataset strengthen external validity. The models were implemented using Scikit-learn v0.22.2 in
943 Python. [118]. Automatic seismic design was explored by Guan et al. [18], who developed a
944 nonlinear structural model to simulate the static–dynamic response of steel moment-resisting
945 frames (SMRF) using a Python-based end-to-end modular platform. Automatic seismic design and
946 analysis (AutoSDA) was implemented as the first module to generate SMRF designs (such as
947 section sizes and detailing) for beams, columns, and beam–column connections. The input design
948 parameters included building characteristics (e.g., number of stories, number of lateral-force-
949 resisting systems, and building dimensions), applicable loads (i.e., dead and live loads on each

950 floor), and site conditions (mapped spectral acceleration). OpenSees was then used to create two-
951 dimensional nonlinear structural models based on these designs. This module performs nonlinear
952 static and dynamic analyses to comprehensively evaluate seismic performance. The model-based
953 framework and object-oriented programming structure made the platform easily adaptable,
954 efficient, reliable, and accurate. Zhang et al. [33] developed an LSTM RNN-based DL approach
955 to model and predict data-driven nonlinear structural seismic responses. Specifically, two schemes
956 were developed: LSTM-f (full sequence-to-sequence mapping) and LSTM-s (stacked sequence-
957 to-sequence mapping), both incorporating multiple LSTM layers and fully connected layers to
958 create time-dependent and causal input–output sequence models. The approach was validated
959 through three case studies: a nonlinear hysteretic system (100 data samples), a six-story
960 instrumented building with field sensing recordings (23 earthquake records) and a three-story
961 nonlinear SMRF (548 datasets generated via incremental dynamic analysis). Among the models,
962 LSTM-s demonstrated superior precision ($R^2 = 0.99$), reliability, computational efficiency,
963 robustness, and scalability compared with LSTM-f and a classical ANN (MLP).

964 In seismic design, BRBs and supplemental dampers (e.g., steel plate, viscous and viscoelastic
965 dampers) are important devices that provide high stiffness, ductility, and energy dissipation to
966 lateral-force-resisting systems. BRBs, with a stable yielding core and an outer restraining member,
967 exhibit symmetrical hysteresis and absorb large inelastic deformations, significantly enhancing a
968 structure’s energy dissipation capacity. Steel dampers likewise provide additional damping by
969 stiffening the frame, absorbing vibration energy, and reducing seismic loads, which enhances
970 overall dynamic response and structural resilience. Moreover, the use of BRBs and dampers
971 together can reduce damage during earthquakes in a synergistic manner. BRBs are focused on
972 yielding in sacrificial braces, while dampers are responsible for dissipating energy and limiting

973 displacement. In a study on BRB frames, four ML methods (RF, ANN, XGBoost, and AdaBoost)
974 were applied across six brace–frame configurations using 79,500 FE-based pushover analyses in
975 OpenSeesPy. Inputs included frame geometry, BRB core area, section properties, and loads. The
976 dataset was divided into 80/20 train-test splits, repeated across different configurations and for
977 combined data. No uncertainty intervals were reported; performance was assessed using R^2 ,
978 RMSE, MAE, and MSE. A graphical interface with the most accurate model (XGBoost, R^2 of
979 0.983-0.993) was developed, and feature importance analysis showed the base-shear to be most
980 significantly governed by number of stories, followed by BRBs core area. While AdaBoost
981 achieved perfect R^2 in training, its testing accuracy dropped, indicating overfitting. XGBoost
982 provided the most balanced performance, reducing overfitting risk [121]. Conventional concentric
983 braces face several limitations, including low ductility, asymmetric behavior under tension and
984 compression, strength deterioration, and stiffness degradation. To address these limitations,
985 AlHamaydeh et al. [31] combined an FFBP with NARX-ANN to predict the nonlinear hysteric
986 behavior of BRBs under cyclic loading with 4 full-scale BRB specimens. Normalized brace forces
987 during load reversals, as a response to normalized time-delayed inputs to the NARX-ANN, were
988 denormalized using the auxiliary FFBP-ANN. Brace deformation was used as the input variable,
989 while brace forces were set as the output variable in the proposed model. The model captured both
990 linear deformations with corresponding linear forces and nonlinear deflections with corresponding
991 nonlinear forces, with predictions closely matching experimental results (accuracy between 0.969
992 to 0.981). The ANN-based model outperformed the traditional FE modeling approach for the
993 following reasons: (i) it established closed-form relationships between the input and response data;
994 (ii) it learned and adapted to different types of data, (iii) it formed a simple structure, which
995 facilitated reconfiguration and ensured significantly faster simulation runs. Sun et al. [213] applied

996 ML methods to perform seismic fragility analysis of large-scale steel BRBs. A database of 9,000
997 nonlinear time-history simulations was created to generate training and testing data. Input features
998 included ground motion intensity measures, BRB design parameters and structural responses.
999 Models were validated with 10-fold CV, achieving good generalization without severe overfitting.
1000 Uncertainty was quantified through fragility curves with confidence bounds, while peak values for
1001 predictive metrics such as R^2 (0.986) and RMSE (0.056) were also reported for XGBoost model.
1002 The large synthetic dataset and CV approach reduced overfitting risk, though no real-world
1003 external testing was performed. Tamimi et al. [214] combined FE modeling, ANN, and Monte
1004 Carlo simulation to evaluate the seismic reliability of BRBs. Experimental tests (5 specimens)
1005 validated the FE model, which was then used to generate simulation data. Sensitivity indices
1006 revealed that gap size, friction coefficient, and steel core thickness were the most influential
1007 parameters. A bias factor distribution (mean = 0.99, SD = 0.038) quantified prediction uncertainty.
1008 Overfitting was mitigated by filtering non-influential variables before ANN training and using
1009 Monte Carlo for robustness. Although k-fold CV was not performed, the study ensured
1010 generalization by integrating ANN with reliability-based simulations. Anand et al. [215] developed
1011 ML models to predict seismic engineering demand parameters (maximum inter story drift, residual
1012 drift, and maximum and cumulative ductility) of BRBs. A database of 16,694 nonlinear time-
1013 history analyses records of BRB frames was generated from OpenSees models. Nine ML
1014 algorithms were tested with hyperparameter tuning via 10-fold CV on the training set, followed
1015 by evaluation on the test set. XGBoost emerged as the best-performing model, with peak R^2 values
1016 of 0.963 (maximum inter story drift), 0.928 (residual drift), 0.968 (maximum ductility), and 0.983
1017 (cumulative ductility). Influential parameters identified by SHAP included spectral accelerations
1018 at 1–5s, Arias intensity, and peak ground velocity. Overfitting was minimized through CV and the

1019 large dataset, but external real-world validation was not performed. Sagheer et al. [216] developed
1020 a deep learning framework that combines ResNet for classifying BRB specimen types and LSTM
1021 for predicting their cyclic hysteretic response. The study used experimental data from six
1022 specimens (threaded, shaved, and notched core bars), expanded into thousands of training
1023 sequences by resampling and segmentation. An 80/20 split was used for validation, supplemented
1024 by dynamic hyperparameter tuning. ResNet classification reached up to 99–100% accuracy with
1025 $R^2 \approx 0.993$, while LSTM achieved force prediction–index of agreement values ranging from 0.979
1026 to 0.999, demonstrating very high fidelity. Overfitting was mitigated using dropout, pooling layers,
1027 and sequence augmentation, though the study lacked external test data beyond the same
1028 experimental campaign. The results showed that deep learning models provided accurate and
1029 efficient alternatives to computationally expensive non-linear FE analyses simulations.
1030 Mohammadi et al. [217] investigated ANN-based models to estimate seismic demands of BRBs
1031 subjected to pulse-like ground motions. Using several hundred nonlinear dynamic analyses, the
1032 study trained ANNs to predict maximum inter-storey and global drift ratios as key seismic demand
1033 parameters. Validation relied on an 80/20 train–test split, with no k-fold CV. The best ANN models
1034 achieved peak R^2 values of 0.96 for maximum inter-storey drift ratio and 0.95 for global drift ratio
1035 in training, with corresponding test values of 0.94 and 0.93. Although no uncertainty intervals
1036 were provided, the performance metrics (R^2 , RMSE, MAE) indicated strong predictive accuracy.
1037 Overfitting was reduced by optimizing ANN architecture and testing on separate holdout datasets,
1038 but lack of external data remained a limitation.

1039 For dampers, a recent study proposed a fast-forward approach to analyze seismic vulnerability
1040 through FE analysis, structural design software, and ANN, with fluid viscous dampers in varied
1041 locations of a building frame [119]. In another study, two crucial properties of a steel plate damper,

1042 stiffness and slenderness factor, were predicted using response surface methodology (RSM), ANN,
1043 and evolutionary polynomial regression (EPR). The study considered elastic-inelastic-plastic
1044 buckling modes and flexural, shear, and flexural–shear failure mechanism of concentrically braced
1045 frames, with 33 geometric property entries. EPR showed the best performance, with R^2 of 0.999
1046 for slenderness and 1.000 for stiffness. Validation was conducted by splitting dataset into training
1047 and validation sets with multiple error metrics, while uncertainty was expressed through
1048 descriptive statistics and error values [120]. Onyelowe et al. [218] presented a hybrid framework
1049 combining response surface methodology and ML models to predict the seismic performance of
1050 steel plate dampers in concentrically braced frames. Input features included geometric and material
1051 properties of dampers. The study used a train–test validation approach, where ANN outperformed
1052 response surface methodology and other ML methods, achieving R^2 values up to 0.99 with low
1053 RMSE and MAE. Although uncertainty intervals were not explicitly reported, results highlighted
1054 ANN’s superior predictive ability. Overfitting was addressed by benchmarking different methods,
1055 though dataset size and lack of broad external testing limited generalization. Chen and Chien [219]
1056 trained MLP and auto-regressive model with exogenous controllers for seismic response control
1057 and validated their performance through both numerical simulations and shake-table experiments
1058 on a single-degree-of-freedom specimen. Validation combined offline train/validation splits from
1059 excitation data and real-time experimental closed-loop tests. The paper reports objective metrics
1060 averaged across records (objective functions, RMSE) but does not report R^2 for accuracy and
1061 SD/CIs for uncertainty. Experimental validation was a strong mitigation against overfitting; auto-
1062 regressive model with exogenous controllers performed faster and with similar accuracy to MLP
1063 in tests. Shao and Andrawes [220] trained ANNs to predict the maximum displacement of a single-
1064 degree-of-freedom reinforced concrete structure with super-elastic dampers using a large

1065 simulated dataset generated in OpenSees, consisting of approximately 109,000 samples derived
1066 from 200 ground motions. The validation method was a hold-out split (70% training, 15%
1067 validation, and 15% testing), and generalization was further tested on separate ground motions
1068 whose parameter values differed from those in the training set. Reported uncertainty was given in
1069 terms of RMSE and average error (best performance: RMSE \approx 0.1012, average error \approx 6.55% for
1070 the 200-ground motion case). The most influential parameters were spectral acceleration and peak
1071 ground acceleration. Hu et al. [220] built an explainable probabilistic buckling-stress predictor by
1072 training ML models (ANN performing best: RMSE \approx 0.0094, $R^2 \approx$ 0.9952) on an FE-generated
1073 database of \sim 32,400 cases. They validated FE against experiments, used Latin hypercube sampling
1074 to propagate input uncertainties, and produced probability densities and global sensitivity analysis
1075 indices which showed yield-stress and initial-imperfection to be the dominant uncertainty drivers.
1076 Validation relied on held-out testing and distributional comparisons; ensembles (RF/XGBoost)
1077 and the large database helped reduce overfitting risk. Bae et al. [122] investigated a double-coke
1078 damper with multiple strips based on a modified radius-cut section. In this configuration,
1079 increasing numbers of plastic hinges on a single strip increased the ductility of the entire damper,
1080 producing a stable hysteresis diagram. Computations based on the proposed equation (for damage
1081 index determination using parameters such as maximum strength and effective stiffness),
1082 experimental results, and ML-derived predictions were found to be in close agreement. The fatigue
1083 performance of the damper was assessed through a constant cyclic loading test on a specimen. The
1084 analyses revealed a stable load–displacement hysteresis graph, a shear resistance exceeding the
1085 theoretical value, and an increase in ductility or fractural strength. A low-cycle fatigue model was
1086 developed using a linear regression algorithm based on ML to estimate the damage index. The
1087 damage point was estimated based on the maximum strain and effective stiffness variation. The

1088 number of periodic failures was found to be in excellent agreement with the experimental results.
1089 The model achieved over 0.90 accuracy and RMSE of 0.1 over 6 different specimens in predicting
1090 damage points compared with test data.

1091 **3.3 Environmental and Economic Impact Analysis**

1092 Conventional LCA and lifecycle cost (LCC) analysis are the two primary approaches for
1093 evaluating the environmental and economic feasibility of building construction. However, these
1094 methods often rely on assumptions—such as a building lifespan of more than 50 years and the
1095 exclusion of maintenance costs—that may result in inaccuracies in practical applications. ML
1096 techniques offer a more reliable alternative by predicting effective lifespans and estimating costs
1097 while accounting for variability in environmental factors (e.g., material manufacturing,
1098 transportation, construction, operation and maintenance, demolition, and waste disposal) and
1099 economic conditions (e.g., operational and maintenance costs). [Ji and Yi \[123\]](#) collected 1,812,700
1100 records related to construction and demolition processes to analyze the lifespan of buildings using
1101 modern prediction models, including linear regression, XGBoost, LGBost, and DNN. For the
1102 study area, the average lifespans of RC-structured and brick-structured buildings were found to be
1103 22.8- and 29.3-y, respectively, significantly lower than the assumed span of 50-y. The DNN model
1104 achieved the highest accuracy ($R^2 = 0.955$). [Onyelowe et al. \[68\]](#) extensively explored the mix
1105 design of fly ash-incorporated concrete using statistical analysis, linear regression, and AI to
1106 predict the environmental impact. The database included 112 concrete samples, with three input
1107 variables: fly ash-to-binder ratio, FA (sand)-to-binder ratio, and CA-to-binder ratio. ANN achieved
1108 the best accuracy ($R^2 = 0.991$), identifying the aggregate-binder ratio as the most influential
1109 parameter. An increase in both the fly ash-to-binder ratio and the aggregate-to-binder ratio was
1110 found to reduce the carbon footprint. [Validation was conducted using a holdout split \(90/22–](#)

1111 training/validation); no k-fold or nested CV was reported. Uncertainty was presented via SDs of
1112 inputs/outputs and residual diagnostics — the study reported residual SD bands and average error
1113 percentages; explicit CIs were not provided. [Koyampambath et al. \[204\]](#) processed 980
1114 datapoints (784 for training) from environmental production declarations data to predict
1115 environmental impacts for construction products with 7 vital information (e.g., name/description,
1116 location, 3 classification levels, functional unit, and values of selected impacts category). The
1117 study employed RF to predict environmental impacts such as photochemical ozone creation
1118 potential ($R^2 = 0.70$), abiotic depletion potential for fossil resources ($R^2 = 0.77$), global warming
1119 potential ($R^2 = 0.81$), and acidification potential ($R^2 = 0.68$). [Sharif et al. \[205\]](#) developed surrogate
1120 models to predict energy consumption using ANN with 463 renovation scenarios (325 training and
1121 138 testing datasets) generated from simulation-based multi-objective optimization. The models
1122 achieved strong predictive accuracy with lower error rates (MSE from 0.016 to 0.124), confirming
1123 their reliability in forecasting total energy consumption, LCC, and LCA. Another recent study
1124 from [Baehr et al. \[206\]](#) predicted life cycle environmental impacts filtering 5251 datasets (60% for
1125 training, 20% for validation, and 20% for testing) integrating ML methods (ANN, residual GPR,
1126 and ANN-residual GPR). ANN-GPR hybrid models produced most accurate results ($R^2 = 0.95$)
1127 with input parameters (e.g., environmental production declarations' attributes, product class,
1128 functional unit/reference flow, embodied fossil/renewable energy, and recycled contents).
1129 [Askarinejad and Behnia \[207\]](#) implemented ML algorithms (DT, polynomial regression, SVR, and
1130 elastic-net) as early design tools using several high-rise buildings (varying heights up to 100
1131 floors), four different types of construction materials (concrete, steel, hybrid and timber) and
1132 concrete with varied strength (32 to 90 MPa). DT outperformed other models with an accuracy of

1133 0.99 (MAE of 13 and MSE of 452). In this study, validation was carried out via hold-out splits,
1134 and uncertainty was not quantified beyond overfitting concerns.

1135 **3.4 Summary on Comparative Structural Analysis with AI models**

1136 AI techniques, such as ANN, GEP, XGBoost, GB, RF, BR, CNN, and emerging methods like
1137 MEP, SVR, and LGBost have demonstrated high efficiency and robustness in predicting concrete
1138 mix design–driven mechanical properties, durability, structural seismic response, and fire-induced
1139 effects. As shown in [Table 1](#), NN and their optimized variants are among the most widely applied
1140 models across these domains because they can capture highly complex nonlinear structural
1141 behavior, predict strength and durability properties with high accuracy, and enable rapid post-
1142 earthquake assessments that improve structural safety [[124](#)]. They also learn directly from
1143 experimental data, offer computational efficiency by generalizing new fire scenarios and structural
1144 configurations with diverse training datasets [[125](#)], and, in their optimized versions, provide
1145 quantifiable and transparent insights that improve the reliability of predictions [[126](#)]. In addition
1146 to NNs, boosting methods are also widely adopted because of their ability to sequentially correct
1147 errors from weaker models. These methods effectively capture complex relationships between
1148 seismic parameters and structural response, efficiently handle data variability, reduce errors in
1149 predicting damage states compared to standalone models, avoid bias to generate more stable and
1150 generalizable predictions, and improve precision and recall in classification tasks [[127](#)]. For
1151 durability-related studies, tree-based algorithms have been particularly effective. In the context of
1152 seismic response, they can manage complex nonlinear interactions among structural parameters,
1153 provide interpretable results through visualizations, and process large input datasets with relatively
1154 low computational demand [[128](#)]. For durability analyses, they can capture interactions between
1155 environmental conditions and material properties, identify the most critical factors contributing to

1156 concrete deterioration, and handle diverse datasets with limited sensitivity to outliers [129].
1157 However, they remain underutilized for evaluating the mechanical properties of structural
1158 members. GA and its extensions (GP and GEP) have been more commonly applied to predicting
1159 the strength properties of concrete. GA offers a simple yet robust encoding process, GP improves
1160 interpretability through flexible expression trees, and GEP combines the strengths of both by
1161 capturing complex nonlinear relationships while maintaining interpretable formulations that
1162 closely align with experimental data [130]. Among the AI methods in Table 1, deep learning–
1163 based algorithms remain less explored across most areas of structural engineering, although they
1164 show considerable promise in applications such as carbon footprint estimation and economic
1165 assessment. SVM and its variants (e.g., SVR) have also demonstrated consistent robustness and
1166 accuracy across different applications. Table 2 presents the comparative performance of these AI
1167 techniques along with their field-specific advantages and limitations. On average, accuracy values
1168 of about 0.80 were observed for NN, GA, tree-based and boosting algorithms, while optimized or
1169 hybridized versions of AI algorithms achieved notably higher prediction accuracy, averaging
1170 around 0.90.

1171 As a continuation of Tables 1 and 2, Table 3 presents comparative metadata with an overview of
1172 dataset size, features, validation methods, metrics, and external test indications for each AI
1173 integrated field. From the reviewed studies, the most used feature sets included material
1174 composition and mix proportions (cement, water, aggregates, admixtures, and age) for concrete
1175 strength and durability, extended by geometric and loading parameters in fire-induced and
1176 mechanical property analyses, while seismic response models predominantly relied on natural
1177 periods and structural descriptors. In terms of validation methods, the dominant approaches were
1178 holdout splits (typically training/testing of 70/30, 75/25, or 80/20) and 10-fold CV. The most

1179 frequently reported metrics were R^2 , RMSE, and MAE, with occasional use of MAPE, and
1180 classification indices (basic introduction in Section 2.9.1). For external test indication, most studies
1181 validated models only on internal datasets, with comparatively fewer works employing
1182 independent experimental databases or literature-based test comparisons for external validation.
1183 According to field-based data shown in Table 3, Table 4 further presents commonly used software
1184 packages and libraries in the reviewed AI integrated fields. Across the reviewed studies,
1185 MATLAB, Python, and Scikit-learn are found to be the most frequently used tools, often serving
1186 as core environments for model development and data analysis. TensorFlow/Keras, XGBoost, and
1187 SHAP are also common for deep learning, boosting, and explainability tasks, while specialized
1188 tools like OpenSees, GeneXproTools, and EPR Toolkits appear in domain-specific applications.

Table 1. Accuracy of prominently used AI-algorithms in structural engineering based on the coefficient of determination (R^2).

AI Applications in the determination of Properties		Section 2.2	Section 2.3	Section 2.5	Section 2.7		Section 2.8	References
		NN: ANN, RNN, KNN	DL: DNN, CNN	GA: GP, GEP, MEP	Tree-based Algorithms	Boosting Methods	SVM, SVR	
Section 3.1.1 Concrete Strength Properties	Mix Design-Compressive Strength	0.92	0.89	0.96	0.97	0.95		[63,66-68,131]
	Tensile Strength	0.95				0.84-0.98	0.98	[56,74-76]
	Flexural Strength	0.98		0.81-0.98	0.99			[71,72,132,133]
	Uniaxial-Triaxial Compression			0.99		0.92-0.97		[17,47,134]
	Self-healing Ability			0.94	0.9-0.97	0.96		[20,79-81]
Section 3.1.2 Durability of Concrete	Moisture Exposure	0.95						[82]
	Corrosion of Concrete			0.98				[83]
	Chloride Resistance	0.85			0.94*	0.96	0.89	[26,84,135,136]
	Depth of Wear	0.99		0.97-0.99	0.99			[50,137-139]
	Frost Durability/Resistance	0.96			0.95	0.96	0.98	[19,85,140,141,142]
	Impermeability	0.93*			0.95	0.97-0.99*	0.97	[86,143,144]
	Carbonation Penetration	0.98-0.99*		0.88		0.98		[87,145-147]
Section 3.1.2 Fire-Induced Effect	Thermal Spalling of FRP-based Concrete	1.00	0.91		0.90	0.90-0.97		[29,51,89,90]
	Fire-induced Spalling of Reinforced Concrete Member	0.99	0.86	0.94		0.96		[21,52,148-150]
	Buckling & Thermal Spalling of Composite Member	0.97-0.99		0.82		0.91-0.99		[91,93,97,151,152]
	Buckling & Progressive Collapse of Steel Frame	1.00	0.96	0.90			0.99	[58,60,153,154]
	Concrete-Steel Bond Strength				0.95	0.92-97		[98,155,156]
Section 3.2.1 Mechanical Properties of Sections	Shear Resistance of RC Member	0.89		0.89	0.95		0.95*	[99,157-159]
	Capacity of Masonry and RC Wall	0.95-0.99			0.8-0.94	0.97		[37,100,160-164]
	Safety Criteria of Retaining Wall	0.97				0.99	1.00	[101,165,166]
	Compression on Composite Column	0.80-0.99				0.98-0.99*		[103,104,167-169]
	Shear Capacity of Composite Beam	0.93-0.99		0.95				[105,170]
	Shear Capacity of Composite Slab	0.89				0.96-0.99	0.96	[172-175]
	Buckling of Steel Beam	0.93-0.99		0.97			0.99	[106-108,176]
	Buckling of Steel Column	0.93*-0.99						[41,177,178]
Section 3.2.2 Seismic Response	Behavior of Column-Beam Joint	0.99	1.00		0.87	0.91		[36,62,179,180]
	Load-Deflection Response of RC Frame	0.87-0.99	0.92		0.8-0.97	0.98	0.98	[111-113,181,182]
	Deformation-based Fragility of Steel Frame	0.96-0.98			0.99	0.96-0.99	0.96-0.98*	[116,118,178,183-185]
	Nonlinear Hysteretic Behavior of Retrofitting Systems	0.94-0.95			0.96	0.99		[27,120,186,187]
Section 3.3 Analysis		0.97	0.96					[68,123]

*Optimized or hybridized versions of an AI method.

Note: Peak accuracy values are considered screening R^2 values between 0.80 to 1.00 from Section 3. Optimized/hybrid models offering such peak accuracies are also added in this table.

Table 2. Summary of different AI methods across operations comparing performances, advantages, and limitations.

Sections	Reviewed AI Techniques	Performance based on the coefficient of determination (R^2)	Advantages	Limitations
2.2	NN: ANN, RNN, KNN	Accuracy > 0.80 across all study fields	<ul style="list-style-type: none"> • Models highly complex nonlinear structural behavior • Learns directly from experimental data. • Computationally efficient in predicting new fire scenarios and structural configurations using diverse datasets • Optimized ANN provides quantifiable and transparent insights, improving reliability 	<ul style="list-style-type: none"> • Struggles to generalize across varied conditions, particularly for concrete durability and seismic response
2.3	DL: DNN, CNN	Accuracy > 0.85 for mix design, fire-induced effects, beam-column joints, seismic response of RC frames, and lifecycle analysis	<ul style="list-style-type: none"> • Captures complex nonlinear relationships, enabling accurate prediction of fire-induced effects, seismic response, and beam-column joint behavior • Supports life-cycle analysis by identifying hidden patterns in RC frame performance and durability. 	<ul style="list-style-type: none"> • Sensitive to noise and computationally intensive, limiting practical deployment in structural assessment
2.5	GA: GP, GEP, MEP	$R^2 = 0.81-0.99$ (concrete strength), $0.97-0.992$ (durability), $0.823-0.94$ (fire-induced effects), $0.89-0.97$ (shear resistance and buckling of RC members)	<ul style="list-style-type: none"> • Widely used for predicting strength properties of concrete. • GA offers a simple yet robust encoding process • GP improves GA with interpretable, flexible expression trees • GEP combines GA and GP, capturing nonlinear relationships with interpretable formulas closely matching experimental data 	<ul style="list-style-type: none"> • Less commonly applied to seismic response and concrete durability
2.7	Tree-based Algorithms	$R^2 > 0.90$ for concrete strength; > 0.94 for durability; $0.87-0.99$ for seismic response	<ul style="list-style-type: none"> • Manages intricate non-linear interactions, provides transparent visualization, and processes wide input data influencing seismic performance. • Handles large and diverse input datasets for seismic performance, identifies key factors influencing concrete durability while remaining robust to outliers 	<ul style="list-style-type: none"> • Underexplored for evaluating the mechanical properties of structural members
	Boosting Methods	Accuracy > 0.91 across most domains	<ul style="list-style-type: none"> • Sequentially corrects errors from weaker models. • Captures complex relationships between seismic parameters and structural response. • Handles variability efficiently while reducing errors in damage prediction • Avoids bias, improving generalization and stability • Enhances precision and recall in classification tasks 	<ul style="list-style-type: none"> • High computational cost and sensitivity to input features, particularly for predicting mechanical, fire-induced, and durability-related concrete responses
2.8	SVM, SVR	Specifically, better results in determining concrete tensile strength: $R^2 = 0.98$ (concrete tensile strength), $0.89-0.98$ (durability), $0.95-0.96$ (RC shear resistance), 0.99 (steel beam buckling), 0.98 (RC seismic response), $0.96-0.98$ (steel seismic response)	<ul style="list-style-type: none"> • Demonstrates high accuracy and robustness across multiple areas 	<ul style="list-style-type: none"> • Limited application to concrete properties, fire effects, and lifecycle analysis due to challenges in handling complex nonlinearities and interpretability issues

Table 3. Comparative metadata (field-based tasks, data size, features, validation methods, metrics, external test validation) across reviewed AI integrated fields

Fields	Tasks	Data set Size	Features	Validation Methods	Metrics	External Test Indication	References
Section 3.1.1 Concrete Strength Properties	Mix Design-Compressive Strength	432	6 (cement, FA, CA, water, superplasticizer, SF)	<i>NS</i>	MAE, RMSE, R^2	No external dataset	Nafees et al. [66]
	Tensile Strength	<i>NS</i>	8–9 (cement, slag, fly ash, water, superplasticizer, CA, FA, age)	Hyperparameter tuning (random search), no explicit CV	RMSE, R^2	No external dataset	Nguyen et al. [56]
	Flexural Strength	200	~5–7 (beam width, depth, reinforcement ratio, FRP parameters)	Holdout (train/validation split)	R^2 , MAE	No external dataset	Khan et al. [46]
	Uniaxial-Triaxial Compression	1298	6 (crushing strength, height–width ratio, shape, Pearson correlation coefficient, stress ratio, loading frequency)	Data cleaning/averaging, no explicit CV	R^2 (0.75–0.915)	No external dataset (literature-based)	Son & Yang [47]
	Self-healing Ability	797	22 (e.g., bacteria type, healing environment, cement type, crack width, healing time)	10-fold CV + grid search	R^2 (0.956), RMSE	No external dataset	Huang et al. [79]
Section 3.1.2 Durability of Concrete	Moisture Exposure	429	8–10 inputs (Geometric, mechanical, and environmental)	Train/test split (regression), Stratified 10-fold CV (classification)	R^2 , MSE, RMSE, MAE; classification metrics	Yes – held-out test set (no independent external dataset)	Baghaei and Hadigheh [82]
	Corrosion of Concrete	256	Chemical: time, pH; Biological: time	50/50 split (train/test)	MSE, R^2	No external dataset (internal only)	Sabour et al. [83]
	Chloride Resistance	30+/study	Water/cement, thickness, aggregate fraction, temperature/humidity ratios, exposure time ratio	Train/validation; scikit-learn DT defaults; k-fold mentioned	Accuracy %, RMSE, errors	Yes – compared with external test results from literature	XuanRui et al. [84]
	Depth of Wear	216	Cement, fly ash, water, aggregates, plasticizer, age/time, curing/test	Train/validation split + external validation framework	R^2 , MAE, RMSE	Yes – external validation criteria applied	Khan et al. [50]
	Frost Durability/Resistance	94	10 inputs (cement, water, sand, natural and recycled CA, fly ash, recycled CA replacement ratio, water absorption, RCA treatment method, air-entraining type)	75/25 train/test split	R^2 , RMSE, MAE	No (train/test only)	Esmacili & Sarkhani [141]
	Impermeability	417	≈10 (water, water–cement ratio, cement, aggregates, rubber size, cycles)	347 train / 70 test split	R^2 , RMSE, MAE	No independent dataset (literature split only)	Huang et al. [86]
Carbonation Penetration	532	6 inputs (cement, FA, water–binder ratio, CO ₂ %, relative humidity, exposure time)	70/15/15 split + 10-fold CV	MAE, RMSE, R^2	Yes – held-out test set and CV folds	Kazemi [87]	

Section 3.1.2 Fire-Induced Effect	Thermal Spalling of FRP-based Concrete	531	17 inputs (e.g., mix proportions, moisture, specimen size, temperature, heating rate, fibers, silica fume)	K-fold CV + supplementary test	Accuracy, F1, precision/recall	Yes – 36 experimental tests + expanded dataset	Liu et al. [89]
	Fire-induced Spalling of Reinforced Concrete Member	100+	Concrete material and mix proportions, geometric and configuration/size features, and those relating to applied loading, intensity, heating rate, and exposure duration	Database validation vs test series (not k-fold)	Comparisons with experimental outcomes	Yes – multiple independent fire test campaigns	Naser & Seitllari [21]
	Buckling & Thermal Spalling of Composite Member	15,200	7 inputs (cross-sectional dimensions, thicknesses of concrete cover for steel section and rebars, steel area ratio, effective length, concrete grade, steel grade, and heating time)	80/20 train-test split	R^2 , MAE, SD vs. analytical eqns	15,200 specimens (synthetic FD model)	Li et al. [93]
	Buckling & Progressive Collapse of Steel Frame	NS	Thermal/mechanical variables (fire temperature, maximum steel temperature, load Ratio, critical temperature based on the Eurocode)	80/20 train-test split	Accuracy, classifier comparison	Monte Carlo + random sampling (case study 2×2 building)	Fu [60]
	Concrete-Steel Bond Strength	316	7 inputs (compressive strength under elevated temperature, testing age, surface temperature at failure, thermal saturation ratio Δ , length–diameter ratio, cover–diameter ratio, total volume of fiber if used)	Train-test split (no explicit k-fold)	MAE, RMSE, R^2 , CoV	316 experimental tests	Al Hamd & Warren [98]
Section 3.2.1 Mechanical Properties of Sections	Shear Resistance of RC Member	466	Geometrical and mechanical variables (beam/stirrup properties)	Train/validation within dataset, sensitivity analysis	Error metrics vs. codes	Validated against experimental database	Gandomi et al. [99]
	Capacity of Masonry and RC Wall	NS	Masonry & FRM mechanical/geometrical variables	Trained on lab results (no CV specified)	Accuracy/precision qualitatively	Yes – calibrated vs lab tests	Cascardi et al. [100]
	Safety Criteria of Retaining Wall	NS	Cohesion, angle of shearing resistance, angle of wall friction, and unit weight	10-fold CV	Reliability index (first-order second moment method)	Compared to reference reliability values	Mishra et al. [101]
	Compression on Composite Column	NS	Geometrical and material properties	ANN training/validation (no CV info in snippet)	Comparative performance (R^2 , RMSE likely)	Yes – experimental DB	Lemonis et al. [104]
	Shear Capacity of Composite Beam	NS	6+ geometrical/interaction vars (e.g., opening diameter, web opening spacing, tee-section height, concrete topping thickness, interaction degree, number of shear studs above web opening)	Comparative training, reliability analysis	Performance metrics, safety factors (1.25–1.26)	FE-based, compared with literature	Ferreira et al. [105]
	Shear Capacity of Composite Slab	273	≈8–10 (e.g., slab depth, slab side length, flexural reinforcement ratio, FRP type/properties, concrete compressive strength, loading type)	10-fold CV	R^2 , RMSE, MAE	External: dataset compiled from multiple independent experiments	Shen and Liang [172]

	Buckling of Steel Beam	9744	≈10 geometric features (e.g., height, web thickness, opening height/width/radius)	Holdout (train/validation/test splits)	R^2 , RMSE, MAE, SD/Variation, a20-index	No external experiments (FE model vs ANN)	Shamass et al. [177]
	Buckling of Steel Column	10,764	Multiple geometric & material grades (e.g., web thickness, web-post width, opening height, steel grade)	10-fold CV and train/validation/test splits	R^2 , RMSE, MAE, SD, CoV	FE model vs Euro-Code 3 (no experimental set)	Rabi et al. [108]
	Behavior of Column-Beam Joint	387	11 (cross-section dimensions (top/bottom flange widths & thicknesses, max/min section heights, web thickness), elastic modulus, column height and corrosion time for corroded cases)	Holdout (train/validation/test)	R^2 , RMSE	No external experiments (analytical dataset)	Nguyen et al. [179]
Section 3.2.2 Seismic Response	Load-Deflection Response of RC Frame	300	First three natural periods (T1-T3) and combinations thereof; natural periods derived from generated frames	Holdout (varying train/test sizes)	MAPE, NRMSE, R^2	Synthetic (OpenSees) – no external experiments	Gharehbaghi et al. [111]
	Deformation-based Fragility of Steel Frame	56,479	First three natural periods and other structural descriptors; inputs chosen to build Probabilistic Seismic Demand Models (PSDMs)	Holdout 70/30	R^2 , RMSE, MAPE	Large synthetic dataset built from extensive nonlinear analyses (616 frames × 240 motions)	Nguyen et al. [118]
	Nonlinear Hysteretic Behavior of Retrofitting Systems	33	4 geometric properties of damper (e.g., plate thickness, plate dimensions, and the number of plates used.)	Holdout (train/val splits)	R^2 , RMSE	No external validation	Onyelowe et al. [120]
Section 3.3 Life Cycle Carbon Assessment	NS	Encoded text/categorical environmental production declaration features	Holdout (80/20)	R^2	20% environmental production declaration as external holdout	Koyamparam bath et al. [204]	

Note: *NS* refers to *not specified value* in a certain study. Similar studies in certain fields may include such values which are not significant for this table.

1191

Table 4. Software packages and libraries commonly used in the reviewed studies

AI Integrated Reviewed Study Fields	Software Packages / Libraries Mentioned
Section 3.1.1 Concrete Strength Properties	MATLAB [66, 46], Python [66, 46, 47], sci-kit learn [56, 47, 79], XGBoost [56], SHAP for explainability [46], ML ensemble methods [47], DNN frameworks (TensorFlow/Keras/Pytorch) [79], Grid Search Algorithm (GSA) [79]
Section 3.1.2 Durability of Concrete	MATLAB [82], Python [82], sci-kit learn [50,84], SHAP for explainability [50], Bayesian Optimisation [82], custom C++ for GP/MEP [83], decision tree defaults [84], custom SVR with metaheuristic implementations [86,141], Alyuda NeuroIntelligence [87], hybrid ANN [87]
Section 3.1.2 Fire-Induced Effect	MATLAB [93], Python [60,89], sci-kit learn [89, 98], XGBoost [89], TensorFlow [60, 98], Keras [60]
Section 3.2.1 Mechanical Properties of Sections	MATLAB [172, 177], Python, sci-kit learn [108], GeneXproTools [108]
Section 3.2.2 Seismic Response	Scikit-learn [118], FE Modeling [111], OpenSees [111], EPR Toolkits [120]
Section 3.3 Life Cycle Carbon Assessment	Python (Selenium, SQLite) [204]

1192

1193 **4 Challenges and Future Directions in AI methods**

1194 Building on the future opportunities for industrial integration of AI, the prediction accuracy of AI
1195 models at the laboratory scale can be observed from the previous section and the demonstrations
1196 in [Tables 1 and 2](#). Extensive research has applied AI methods to evaluate the properties of concrete
1197 specimens as well as RC, composite, and steel structural members and frames. However, only
1198 limited studies have addressed areas such as self-healing ability and concrete–steel bonding under
1199 severe fire conditions. Similarly, seismic response analysis of steel frames with bracings, shear
1200 capacity of RC members, and failure modes of column–beam connections have received
1201 comparatively less attention than other AI applications. Fire-induced effects on BRBs, column–
1202 beam connections, and LCA also remain underexplored. Nevertheless, significant potential exists
1203 for optimized and hybridized variants of widely used algorithms, such as NN and GA-based, tree-
1204 based models, and boosting techniques. [Sections 4.1, 4.2, and 4.3 discuss the industrial](#)
1205 [applications of AI, the limitations observed in laboratory scale studies, and future](#)
1206 [recommendations for AI integration in structural engineering.](#)

1207 **4.1 Industrial Implications, Barriers to Adoption and Potential for Implementations**

1208 [For construction projects that rely on accurately evaluating environmental factors \(e.g., seismic](#)
1209 [events\), risks, and costs, AI offers significant practical advantages \[197\]. ML is increasingly](#)
1210 [applied in big data analytics for risk detection and assessment, and ML models are also used in](#)
1211 [robotics and automation. For instance, aerial drones and robotic vehicles are frequently deployed](#)
1212 [on survey sites to generate 3D models of building structures. AI algorithms further support on-site](#)
1213 [problem identification and provide strategic solutions that enhance efficiency. In construction](#)
1214 [automation, AI is also applied to improve workers safety through smart wearable technologies that](#)
1215 [monitor movement, activities, and posture, helping to prevent collisions between workers and](#)

1216 heavy equipment [198]. Despite these benefits, several barriers hinder AI adoption in the
1217 construction industry. These include the fragmented nature of the industry, challenging
1218 environmental conditions on-site, and non-standardized building designs, all of which complicate
1219 data collection, integration, and standardization [199]. Additional constraints include limited
1220 technical skills, inappropriate business processes, and insufficient knowledge, making AI adoption
1221 time-consuming, costly, and prone to errors [200,201]. Moreover, many large firms continue to
1222 rely on traditional processes rather than automation, and subcontractors often follow the same
1223 outdated practices [203]. On a positive side, the construction industry has been investing heavily
1224 in AI, with an estimated USD 8 billion allocated in the five years leading up to 2019 [202]. This
1225 investment paves the way for AI-enabled technologies such as digital twins and 3D printing, which
1226 can significantly reduce repetitive and labor-intensive tasks. Looking ahead, future AI integration
1227 should also target innovative fields such as fire-induced effects, seismic impact analysis, and LCA.
1228 This study has reviewed AI-based findings in these areas using laboratory scale experimental and
1229 numerical databases; the associated limitations and prospects are discussed in the following
1230 sections.

1231 **4.2 Limitations in AI applications in structural engineering**

1232 Limited access to diverse and representative datasets, high costs of data collection, and data
1233 scarcity due to legal restrictions often result in inadequate data availability. Missing data, model
1234 bias, data drift, and errors further affect the reliability of AI predictions. These challenges, arising
1235 from limited datasets, difficulties in maintaining data quality, and **research gaps**, can be
1236 summarized as follows:

- 1237 1. In studies on the mix design of sustainable concrete, only limited scale experimental
1238 datasets have been used in recent research. The generalization performance of AI models

1239 for sustainable concrete preparation can only be suggested from these limited studies, and
1240 future work should involve extensive tests on various SCMs used in concrete.
1241 Additionally, some studies have reported missing information (e.g., inappropriate or
1242 incomplete input variables) from experimental data which lessens the prediction accuracy
1243 and reliability.

1244 2. For predicting the strength and durability of concrete materials, variations are observed in
1245 the optimal algorithms, such as XGBoost, GEP, BR, ANN, GB, MEP, SVM, and RF. The
1246 selection of a specific AI method is often subjective and depends on researcher's expertise.
1247 In some cases, even the most preferred methods fail to outperform the existing design
1248 codes. Apart from reliance of quality datasets, another issue is the time-consuming process
1249 of parameter tuning.

1250 3. AI-based predictions generally require large volumes of experimental data to ensure
1251 accuracy and precision. However, data availability for specific problems is often limited
1252 owing to laboratory constraints (e.g., fire testing facilities for fire resistance analysis). In
1253 such cases, AI models may suffer from numerical complexities, including overfitting
1254 training data without comparable practical test data for validation.

1255 4. Notably, most reviewed studies compiled their datasets from prior works conducted in
1256 different regions. However, these prior studies often differ significantly in environmental
1257 conditions, material characteristics, and experimental setups, which may limit the
1258 reliability and generalizability of AI models.

1259 A few studies have incorporated random sampling and SHAP analysis, which are important
1260 for selecting appropriate data and providing detailed explanations of model accuracy. Some
1261 researchers have also resorted to using synthetic data to train and validate ML models due to

1262 the lack of real-world data. However, this approach can yield unrealistic results. Emerging
1263 structural concepts, such as carbon-neutral and easy-to-dismantle beam–column joints, offer
1264 promising solutions to reduce the carbon footprint across the structural lifecycle. Yet, no AI
1265 methods have been developed to evaluate their fatigue performance, load-carrying capacity, or
1266 associated carbon footprint.

1267 **4.3 Recommendations for Future Research in Structural Engineering**

1268 This section addresses the previously discussed limitations related to data availability and quality,
1269 while also providing insights into potential solutions and highlighting new research opportunities:

- 1270 1. Extensive research has been conducted on AI-based sustainable concrete mix design using
1271 SCMs, byproducts, and waste materials. However, further studies are needed to assess the
1272 applicability of single AI-based mix design approaches across different concrete types.
1273 The use of locally available experimental data is recommended to obtain more accurate
1274 predictions for optimum mix proportions of concrete materials. ML approaches combined
1275 with heuristic methods, such as PSO, can further enhance prediction accuracy in mix
1276 design.
- 1277 2. The inertia in selecting AI techniques for similar problems can be reduced through
1278 collaboration among researchers to identify the most suitable methods for specific,
1279 concrete-related challenges. Issues related to parameter tuning can be addressed by
1280 incorporating optimization algorithms such as GA, which can streamline the tuning
1281 process.
- 1282 3. To address numerical complexities caused by limited real-world data, AI models should
1283 be regularly updated, supported by open-access databases that facilitate information
1284 sharing. More diverse data points and comprehensive experimental datasets are required

1285 to capture a wide range of scenarios. Training models with homogeneous data obtained
1286 under specific environmental and material conditions can improve prediction accuracy.
1287 Additionally, random sampling can be employed to refine results after training. Raw
1288 experimental data should be prioritized over synthetic data to ensure practical relevance.
1289 Normalization of input variables into uniform ranges can also minimize dataset bias and
1290 enhance model performance.

1291 4. Existing models for fiber-reinforced concrete elements should be extended to account for
1292 the confinement effects of different fiber-reinforced polymer configurations. For instance,
1293 incorporating input variables such as the placement and orientation of polymer wrappings
1294 could improve the evaluation of structural integrity and failure potential under fire
1295 exposure.

1296 In this study, adaptive explainable AI methods (e.g., SHAP and local explainable model-agnostic
1297 explanations), are not discussed broadly due to limited existing research. Future studies should
1298 explore more of these techniques. Some studies have used a single AI technique for multiple test
1299 specimens with different criteria. Further studies can compare different AI methods to identify the
1300 simplest and most accurate models for a specific problem. At present, most construction projects
1301 utilize structural steel components, and future studies should focus on AI-based analysis of the
1302 LCA and LCC of steel structures. Additionally, a promising innovative research direction can be
1303 represented with AI-based predictions for evaluating the self-healing property, post-fire conditions
1304 and fire-induced effects of concrete structures, and seismic response analyses of steel building
1305 frames. Easy-to-dismantle beam-column multiple connections are crucial for reducing
1306 construction time and labor costs, as they can minimize the requirement of bolts and rivets at
1307 working sites. These prefabricated joints also contribute to lower carbon emissions in the lifecycle

1308 of structures. AI-based research can be suggested for such connections. Moreover, experimental,
1309 theoretical, numerical, and prediction-based analysis must be conducted, and the results should be
1310 compared to determine effective and efficient designs. Moreover, different AI methods can be
1311 used to determine the fire effects, shear capacity, and failure modes of steel beam-column
1312 connections and BRBs.

1313 **5 Conclusions**

1314 AI has demonstrated exceptional accuracy in structural engineering research, producing
1315 predictions that are comparable to, and in many cases superior to, experimental tests, numerical
1316 simulations, and design codes. In recent years (2020-2024), ANN, boosting methods, tree-based
1317 algorithms and SVM models have been widely adopted for their strong predictive capabilities,
1318 while MEP, SVR, BR, LGBost, and deep learning models have also proven robust and reliable
1319 for capturing complex structural behavior. For instance, NN and boosting methods in particular
1320 exhibit high predictive accuracy ($R^2 > 0.80$ and $R^2 > 0.90$, respectively) across diverse applications,
1321 making them the most widely applied approaches. Deep learning methods are particularly effective
1322 in mix design, strength prediction, fire-induced effects, beam-column joints, seismic response of
1323 RC frames, and LCA, achieving accuracy levels above 0.85. Meanwhile, GA, SVM, SVR, and
1324 tree-based models have shown strong performance in specialized tasks, including concrete
1325 durability, fire resistance, shear behavior, and seismic buckling, with reported accuracy ranging
1326 from 0.80 to 0.99. Based on studies published between 2020 and 2024, the main findings can be
1327 summarized as follows:

- 1328 1. **Concrete mix design and strength prediction:** Tree-based algorithms are prominent,
1329 with XGBoost, ANN, GEP, GB, BR, ensemble DT, and stacking methods achieving R^2
1330 values between 0.91 and 0.99. Key influencing parameters include curing age, cement

1331 content, recycled aggregate replacement ratio, SCM-to-binder ratio, aggregate-to-binder
1332 ratio, and specimen dimensions. Integration of AI is highly significant for accurately
1333 predicting mixing parameters that influence the strength properties of concrete.

1334 2. **Durability prediction:** ANN demonstrates strong accuracy ($R^2 = 0.85\text{--}0.99$) for most
1335 durability aspects. Specific properties such as corrosion resistance, chloride permeability,
1336 depth of wear, frost resistance, impermeability, and carbonation depth are best predicted
1337 by MEP, XGBoost, BR, SVR, and optimized ANN models. Governing parameters include
1338 exposure duration, aggregate fractions, cement–SCM ratios, water–binder ratios, FA,
1339 protective layer thickness, and environmental conditions. According to these findings, AI
1340 prediction provides reliable insights into concretes durability while highlighting the
1341 critical role of mix parameters for long-term performance.

1342 3. **Fire-induced effects:** Neural networks and boosting algorithms accurately predict
1343 spalling in RC, composite, and steel structures ($R^2 = 0.90\text{--}1.00$), as well as concrete–steel
1344 bond strength (accuracy of 0.97). Critical parameters include member geometry, applied
1345 load and load ratios, thermal properties, fire insulation depth, and reinforcement area.
1346 These findings show that AI-based approaches have the capacity to effectively capture the
1347 critical factors that influence fire-induced spalling, providing a strong framework for
1348 predictive assessment and design.

1349 4. **Structural behavior and failure modes:** In determining mechanical properties of steel
1350 structural beam-column joints, only a few studies have implemented CNN. Apart from
1351 this, different algorithms show peak accuracy across different fields such as GEP, SVR
1352 and tree algorithms for shear resistance of RC members, ANN and RF for shear strength
1353 of masonry and RC walls, SVM and boosting methods for safety criteria of retaining walls,

1354 optimized ANN and boosting methods for ultimate load capacity of composite beams and
1355 columns, and ANN-SVR for buckling failure modes of steel beam-column. Across these
1356 applications, the most influential parameters include strength properties, section
1357 geometry, and member aspect ratios.

1358 5. **Seismic response:** These have been accurately predicted using classification-based,
1359 hybrid, and optimized ANN variants for RC frames (with accuracy above 0.87), and
1360 hybridized boosting methods for steel frames (with accuracy above 0.96). Key factors
1361 include axial load, concrete strength, reinforcement dimensions, building characteristics,
1362 applied loads, and site conditions. AI integration in seismic response analysis is
1363 particularly significant, as it supports the development of innovative designs incorporating
1364 BRBs, viscoelastic dampers, beam–column joints, and advanced retrofitting technologies.

1365 6. **LCA and economic analysis:** LCA of carbon emissions and lifecycle cost analysis for
1366 optimized building construction solutions can be further enhanced using high-performing
1367 AI methods such as ANN (accuracy above 0.97) and DNN (accuracy above 0.96). By
1368 integrating AI into LCA, it becomes possible to identify complex interdependencies
1369 among materials, energy use, and costs, enabling more precise and strategic sustainability
1370 decisions in construction.

1371 With continued advancements, AI-based predictions have a strong potential to be integrated into
1372 updated structural design codes, provided results are rigorously validated through experimental
1373 and real-world applications.

1374 **Acknowledgments**

1375 This research was supported by the National Research Foundation of Korea (NRF) grant funded
1376 by the Korean Government (MSIT) [grant number 2022R1C1C1003594], and by the Chonnam

1377 National University Smart Plant Reliability Center grant funded by the Ministry of Education
1378 [grant number RS-2020-NF000321].

1379 **Data availability statement**

1380 The data that support the findings of this study are available from the corresponding author,
1381 [Jaehoon Bae], upon reasonable request.

1382 **Credit Author Statement**

1383 **Md. Tarif Aziz:** Writing – original draft. **Dave Montellano Osabel:** Writing – review & editing.
1384 **Youngju Kim:** Writing – review & editing. **Sanghoon Kim:** Validation, Supervision. **Jaehoon**
1385 **Bae:** Funding acquisition, Supervision, Writing – review & editing. **Konstantinos Daniel**
1386 **Tsavidaridis:** Supervision, Writing – review & editing.

1387 **Abbreviations**

AI, artificial intelligence; **CV, cross-validation;** ANN, artificial neural network; PR, pattern recognition; ML, machine learning; DL, deep learning; **NN, neural networks;** **SHM, structural health monitoring;** **BRBs, buckling restrained braces;** LCA, lifecycle assessment; MLP, multi-layer perceptron; FFBP, feedforward backpropagation; NARX, nonlinear autoregressive exogenous; **NARX-SP, NARX series parallel;** **NARX-P, NARX parallel;** **LSTM, long short term memory;** **RNN, recurrent neural network;** DNN, deep neural network; CNN, convolutional neural network; NB, naïve Bayes; KNN, K-nearest neighbors; GA, genetic algorithm; PSO, particle swarm optimization; GP, genetic programming; GEP, gene expression programming; **MEP, multi expression programming;** GPR, Gaussian process regression; MARS, multivariate adaptive regression spline; DT, decision tree; RT, regression tree; RF, random forest; BR, bagging regressor; AdaBoost, adaptive boosting; XGBoost, extreme gradient boosting; LGBost, light

gradient boosting; NGBoost, natural gradient boosting; GBR, gradient boosting regressor; CatBoost, categorized boosting; HGBoost, histogram gradient boosting; GB, gradient boosting; SVR, support vector regressor; SVM, support vector machine; RMSE, root-mean-square error; MAE, mean absolute error; MAPE, mean absolute percentage error; R^2 , coefficient of determination; MCS, Monte Carlo simulation; GCV, generalized cross-validation; SHAP, shapley additive explanations; SD, standard deviation; CoV, coefficient of variation; CI, confidence intervals; RC, reinforced concrete; FE, finite element; FA, fine aggregates; CA, coarse aggregates; SF, silica fume; GGBS, ground granulated blast furnace slag; RAC, recycled aggregate concrete; FRP, fiber-reinforced polymer; DF, durability factor; CSB, castellated steel beam; SMRF, steel moment-resisting frame; EPR, evolutionary polynomial regression; LCC, lifecycle cost; MPa, megapascal.

1388 **References**

- 1389 [1] Russell, S.J. and Norvig, P., 2003. *Instructor's solution manual for artificial intelligence:*
1390 *a modern approach*. Pearson.
- 1391 [2] Warwick, K., 2013. *Artificial intelligence: the basics*. Routledge.
- 1392 [3] Fouse, S., Cross, S. and Lapin, Z., 2020. DARPA's impact on artificial intelligence. *AI*
1393 *Magazine*, 41(2), pp.3–8.
- 1394 [4] Agar, J.O.N., 2020. What is science for? The Lighthill report on artificial intelligence
1395 reinterpreted. *The British Journal for the History of Science*, 53(3), pp.289–310.
- 1396 [5] Menzies, T., 2003. 21st-century AI: proud, not smug. *IEEE Intelligent Systems*, 18(3),
1397 pp.18–24.

- 1398 [6] Groumpos, P.P., 2023. A critical historic overview of artificial intelligence: issues,
1399 challenges, opportunities, and threats. In: *Artificial Intelligence and Applications*, 1(4),
1400 pp.197–213.
- 1401 [7] Ongsulee, P., 2017. Artificial intelligence, machine learning and deep learning. In: *2017*
1402 *15th International Conference on ICT and Knowledge Engineering (ICT&KE)*, pp.1–6.
1403 IEEE.
- 1404 [8] Sarker, I.H., 2022. AI-based modeling: techniques, applications and research issues
1405 towards automation, intelligent and smart systems. *SN Computer Science*, 3(2), p.158.
- 1406 [9] Wang, Y., et al., 2020. Brain-inspired systems: a transdisciplinary exploration on
1407 cognitive cybernetics, humanity, and systems science toward autonomous artificial
1408 intelligence. *IEEE Systems, Man, and Cybernetics Magazine*, 6(1), pp.6–13.
1409 <https://doi.org/10.1109/MSMC.2018.2889502>
- 1410 [10] Flasiński, M., 2016. *Introduction to artificial intelligence*. Springer.
- 1411 [11] Xu, Y., Qian, W., Li, N. and Li, H., 2022. Typical advances of artificial
1412 intelligence in civil engineering. *Advances in Structural Engineering*, 25(16), pp.3405–
1413 3424.
- 1414 [12] Pan, Y. and Zhang, L., 2021. Roles of artificial intelligence in construction
1415 engineering and management: a critical review and future trends. *Automation in*
1416 *Construction*, 122, p.103517.
- 1417 [13] Manzoor, B., Othman, I., Durdyev, S., Ismail, S. and Wahab, M.H., 2021.
1418 Influence of artificial intelligence in civil engineering toward sustainable development—
1419 a systematic literature review. *Applied System Innovation*, 4(3), p.52.

- 1420 [14] Vadyala, S.R., Betgeri, S.N., Matthews, J.C. and Matthews, E., 2022. A review of
1421 physics-based machine learning in civil engineering. *Results in Engineering*, 13,
1422 p.100316.
- 1423 [15] Rezania, J., Hamian, M. and Rasekhi, A., 2023. Investigating the application of
1424 artificial intelligence in civil engineering and progressive collapse. *Civil and Project*,
1425 5(9), pp.11–22.
- 1426 [16] Harle, S.M., 2024. Advancements and challenges in the application of artificial
1427 intelligence in civil engineering: a comprehensive review. *Asian Journal of Civil*
1428 *Engineering*, 25(1), pp.1061–1078.
- 1429 [17] Gandomi, A.H., Alavi, A.H., Mousavi, M. and Tabatabaei, S.M., 2011. A hybrid
1430 computational approach to derive new ground-motion prediction equations. *Engineering*
1431 *Applications of Artificial Intelligence*, 24, pp.717–732.
1432 <https://doi.org/10.1016/j.engappai.2011.01.005>
- 1433 [18] Guan, X., Burton, H. and Sabol, T., 2020. Python-based computational platform
1434 to automate seismic design, nonlinear structural model construction and analysis of steel
1435 moment resisting frames. *Engineering Structures*, 224, p.111199.
- 1436 [19] Liu, K., Zou, C., Zhang, X. and Yan, J., 2021. Innovative prediction models for
1437 the frost durability of recycled aggregate concrete using soft computing methods. *Journal*
1438 *of Building Engineering*, 34, p.101822.
- 1439 [20] Rajczakowska, M., Szelağ, M., Habermehl-Cwirzen, K., Hedlund, H. and
1440 Cwirzen, A., 2023. Interpretable machine learning for prediction of post-fire self-healing
1441 of concrete. *Materials*, 16(3), p.1273.

- 1442 [21] Naser, M.Z. and Seitllari, A., 2020. Concrete under fire: an assessment through
1443 intelligent pattern recognition. *Engineering with Computers*, 36(4), pp.1915–1928.
- 1444 [22] Amezquita-Sanchez, J.P., Valtierra-Rodriguez, M. and Adeli, H., 2020. Machine
1445 learning in structural engineering. *Scientia Iranica*, 27(6), pp.2645–2656.
- 1446 [23] Thai, H.T., 2022. Machine learning for structural engineering: a state-of-the-art
1447 review. In: *Structures*, 38, pp.448–491. Elsevier.
- 1448 [24] Kumar, P. and Kota, S.R., 2024. Machine learning models in structural
1449 engineering research and a secured framework for structural health monitoring.
1450 *Multimedia Tools and Applications*, 83(3), pp.7721–7759.
- 1451 [25] Tapeh, A.T.G. and Naser, M.Z., 2023. Artificial intelligence, machine learning,
1452 and deep learning in structural engineering: a scientometrics review of trends and best
1453 practices. *Archives of Computational Methods in Engineering*, 30(1), pp.115–159.
- 1454 [26] Taffese, W.Z. and Espinosa-Leal, L., 2022. Prediction of chloride resistance level
1455 of concrete using machine learning for durability and service life assessment of building
1456 structures. *Journal of Building Engineering*, 60, p.105146.
- 1457 [27] Mohammadi, A., Karimzadeh, S., Yaghmaei-Sabegh, S., Ranjbari, M. and
1458 Lourenço, P.B., 2023. Utilising artificial neural networks for assessing seismic demands
1459 of buckling restrained braces due to pulse-like motions. *Buildings*, 13(10), p.2542.
- 1460 [28] Kaveh, A., Eskandari, A. and Movasat, M., 2023. Buckling resistance prediction
1461 of high-strength steel columns using metaheuristic-trained artificial neural networks. In:
1462 *Structures*, 56, p.104853. Elsevier.

- 1463 [29] Bhatt, P.P., Sharma, N., Kodur, V.K.R. and Naser, M.Z., 2024. Machine learning
1464 approach for predicting fire resistance of FRP-strengthened concrete beams. *Structural*
1465 *Concrete*.
- 1466 [30] Gardner, M.W. and Dorling, S.R., 1998. Artificial neural networks (the multilayer
1467 perceptron)—a review of applications in the atmospheric sciences. *Atmospheric*
1468 *Environment*, 32(14-15), pp.2627–2636.
- 1469 [31] AlHamaydeh, M., Choudhary, I. and Assaleh, K., 2013. Virtual testing of
1470 buckling-restrained braces via nonlinear autoregressive exogenous neural networks.
1471 *Journal of Computing in Civil Engineering*, 27, pp.755–768.
1472 [https://doi.org/10.1061/\(ASCE\)CP.1943-5487.0000247](https://doi.org/10.1061/(ASCE)CP.1943-5487.0000247)
- 1473 [32] Diaconescu, E., 2008. The use of NARX neural networks to predict chaotic time
1474 series. *WSEAS Transactions on Computer Research*, 3(3), pp.182–191.
- 1475 [33] Zhang, R., Chen, Z., Chen, S., Zheng, J., Büyüköztürk, O. and Sun, H., 2019.
1476 Deep long short-term memory networks for nonlinear structural seismic response
1477 prediction. *Computers & Structures*, 220, pp.55–68.
- 1478 [34] Salehi, H. and Burgueño, R., 2018. Emerging artificial intelligence methods in
1479 structural engineering. *Engineering Structures*, 171, pp.170–189.
- 1480 [35] Naser, M.Z. and Kodur, V.K., 2022. Explainable machine learning using real,
1481 synthetic and augmented fire tests to predict fire resistance and spalling of RC columns.
1482 *Engineering Structures*, 253, p.113824.
- 1483 [36] Paral, A., Roy, D.K.S. and Samanta, A.K., 2021. A deep learning-based approach
1484 for condition assessment of semi-rigid joint of steel frame. *Journal of Building*
1485 *Engineering*, 34, p.101946.

- 1486 [37] Mangalathu, S., Jang, H., Hwang, S.H. and Jeon, J.S., 2020. Data-driven
1487 machine-learning-based seismic failure mode identification of reinforced concrete shear
1488 walls. *Engineering Structures*, 208, p.110331.
- 1489 [38] Zhang, S., 2021. Challenges in KNN classification. *IEEE Transactions on*
1490 *Knowledge and Data Engineering*, 34(10), pp.4663–4675.
- 1491 [39] Holland, J.H., 1992. *Adaptation in natural and artificial systems: an introductory*
1492 *analysis with applications to biology, control, and artificial intelligence*. MIT Press.
- 1493 [40] Camp, C., Pezeshk, S. and Cao, G., 1998. Optimized design of two-dimensional
1494 structures using a genetic algorithm. *Journal of Structural Engineering*, 124(5), pp.551–
1495 559.
- 1496 [41] Le, L.M., Ly, H.B., Pham, B.T., Le, V.M., Pham, T.A., Nguyen, D.H., Tran, X.T.
1497 and Le, T.T., 2019. Hybrid artificial intelligence approaches for predicting buckling
1498 damage of steel columns under axial compression. *Materials*, 12(10), p.1670.
- 1499 [42] Mathew, T.V., 2012. Genetic algorithm. Report submitted at IIT Bombay, 53,
1500 pp.18–19.
- 1501 [43] Mousavi, S.M., Aminian, P., Gandomi, A.H., Alavi, A.H. and Bolandi, H., 2012.
1502 A new predictive model for compressive strength of HPC using gene expression
1503 programming. *Advances in Engineering Software*, 45(1), pp.105–114.
- 1504 [44] Ferreira, C., 2001. Gene expression programming: a new adaptive algorithm for
1505 solving problems. *arXiv preprint cs/0102027*.
- 1506 [45] Oltean, M. and Grosan, C., 2003. A comparison of several linear genetic
1507 programming techniques. *Complex Systems*, 14(4), pp.285–314.

- 1508 [46] Khan, M., Khan, A., Khan, A.U., Shakeel, M., Khan, K., Alabduljabbar, H.,
1509 Najeh, T. and Gamil, Y., 2024. Intelligent prediction modeling for flexural capacity of
1510 FRP-strengthened reinforced concrete beams using machine learning algorithms.
1511 *Heliyon*, 10(1).
- 1512 [47] Son, J. and Yang, S., 2022. A new approach to machine learning model
1513 development for prediction of concrete fatigue life under uniaxial compression. *Applied*
1514 *Sciences*, 12(19), p.9766.
- 1515 [48] Borra, S. and Di Ciaccio, A., 2002. Improving nonparametric regression methods
1516 by bagging and boosting. *Computational Statistics & Data Analysis*, 38(4), pp.407–420.
- 1517 [49] Nafees, A., Khan, S., Javed, M.F., Alrowais, R., Mohamed, A.M., Mohamed, A.
1518 and Vatin, N.I., 2022. Forecasting the mechanical properties of plastic concrete
1519 employing experimental data using machine learning algorithms: DT, MLPNN, SVM,
1520 and RF. *Polymers*, 14(8), p.1583.
- 1521 [50] Khan, M., Khan, A.U., Houda, M., El Hachem, C., Rasheed, M. and Anwar, W.,
1522 2023. Optimizing durability assessment: machine learning models for depth of wear of
1523 environmentally-friendly concrete. *Results in Engineering*, 20, p.101625.
- 1524 [51] Kumarawadu, H., Weerasinghe, P. and Perera, J.S., 2024. Evaluating the
1525 performance of ensemble machine learning algorithms over traditional machine learning
1526 algorithms for predicting fire resistance in FRP-strengthened concrete beams. *Electronic*
1527 *Journal of Structural Engineering*, 24(3), pp.47–53.
- 1528 [52] Ho, T.N.T., Nguyen, T.P. and Truong, G.T., 2024. Concrete spalling
1529 identification and fire resistance prediction for fired RC columns using machine learning-
1530 based approaches. *Fire Technology*, pp.1–44.

- 1531 [53] Friedman, J.H., 2001. Greedy function approximation: a gradient boosting
1532 machine. *Annals of Statistics*, pp.1189–1232.
- 1533 [54] Degtyarev, V.V. and Tsavdaridis, K.D., 2022. Buckling and ultimate load
1534 prediction models for perforated steel beams using machine learning algorithms. *Journal*
1535 *of Building Engineering*, 51, p.104316.
- 1536 [55] Duan, T., Anand, A., Ding, D.Y., Thai, K.K., Basu, S., Ng, A. and Schuler, A.,
1537 2020. NGBoost: Natural gradient boosting for probabilistic prediction. In: *International*
1538 *Conference on Machine Learning*, pp.2690–2700. PMLR.
- 1539 [56] Nguyen, H., Vu, T., Vo, T.P. and Thai, H.T., 2021. Efficient machine learning
1540 models for prediction of concrete strengths. *Construction and Building Materials*, 266,
1541 p.120950.
- 1542 [57] Vapnik, V., 2013. *The nature of statistical learning theory*. Springer Science &
1543 Business Media.
- 1544 [58] Tong, Q., Couto, C. and Gernay, T., 2022. Machine learning models for
1545 predicting the resistance of axially loaded slender steel columns at elevated temperatures.
1546 *Engineering Structures*, 266, p.114620.
- 1547 [59] Roy, A. and Chakraborty, S., 2023. Support vector machine in structural
1548 reliability analysis: A review. *Reliability Engineering & System Safety*, 233, p.109126.
- 1549 [60] Fu, F., 2020. Fire induced progressive collapse potential assessment of steel
1550 framed buildings using machine learning. *Journal of Constructional Steel Research*, 166,
1551 p.105918. <https://doi.org/10.1016/j.jcsr.2019.105918>

- 1552 [61] Degtyarev, V.V., Hicks, S.J., Ferreira, F.P.V. and Tsavdaridis, K.D., 2024.
1553 Probabilistic resistance predictions of laterally restrained cellular steel beams by natural
1554 gradient boosting. *Thin-Walled Structures*, 205, p.112367.
- 1555 [62] Gao, X. and Lin, C., 2021. Prediction model of the failure mode of beam-column
1556 joints using machine learning methods. *Engineering Failure Analysis*, 120, p.105072.
- 1557 [63] Liu, K., Zheng, J., Dong, S., Xie, W. and Zhang, X., 2023. Mixture optimization
1558 of mechanical, economical, and environmental objectives for sustainable recycled
1559 aggregate concrete based on machine learning and metaheuristic algorithms. *Journal of*
1560 *Building Engineering*, 63, p.105570.
- 1561 [64] Zandifaez, P., Shamsabadi, E.A., Nezhad, A.A., Zhou, H. and Dias-da-Costa, D.,
1562 2023. AI-assisted optimisation of green concrete mixes incorporating recycled concrete
1563 aggregates. *Construction and Building Materials*, 391, p.131851.
- 1564 [65] Golafshani, E.M., Kim, T., Behnood, A., Ngo, T. and Kashani, A., 2024.
1565 Sustainable mix design of recycled aggregate concrete using artificial intelligence.
1566 *Journal of Cleaner Production*, 442, p.140994.
- 1567 [66] Nafees, A., Javed, M.F., Khan, S., Nazir, K., Farooq, F., Aslam, F., Musarat,
1568 M.A. and Vatin, N.I., 2021. Predictive modeling of mechanical properties of silica fume-
1569 based green concrete using artificial intelligence approaches: MLPNN, ANFIS, and GEP.
1570 *Materials*, 14(24), p.7531.
- 1571 [67] Zou, Y., Zheng, C., Alzahrani, A.M., Ahmad, W., Ahmad, A., Mohamed, A.M.,
1572 Khallaf, R. and Elattar, S., 2022. Evaluation of artificial intelligence methods to estimate
1573 the compressive strength of geopolymers. *Gels*, 8(5), p.271.

- 1574 [68] Onyelowe, K.C., Ebid, A.M., Mahdi, H.A., Onyelowe, F.K., Shafieyoon, Y.,
1575 Onyia, M.E. and Onah, H.N., 2023. AI mix design of fly ash admixed concrete based on
1576 mechanical and environmental impact considerations. *Civil Engineering Journal*, 9,
1577 pp.27–45.
- 1578 [69] Kang, M.C., Yoo, D.Y. and Gupta, R., 2021. Machine learning-based prediction
1579 for compressive and flexural strengths of steel fiber-reinforced concrete. *Construction
1580 and Building Materials*, 266, p.121117.
- 1581 [70] Amin, M.N., Iqbal, M., Khan, K., Qadir, M.G., Shalabi, F.I. and Jamal, A., 2022.
1582 Ensemble tree-based approach towards flexural strength prediction of FRP-reinforced
1583 concrete beams. *Polymers*, 14(7), p.1303.
- 1584 [71] Khan, K., Iqbal, M., Salami, B.A., Amin, M.N., Ahmad, I., Alabdullah, A.A.,
1585 Arab, A.M.A. and Jalal, F.E., 2022. Estimating flexural strength of FRP reinforced beam
1586 using artificial neural network and random forest prediction models. *Polymers*, 14(11),
1587 p.2270.
- 1588 [72] Zhang, T., Gao, D. and Xue, C., 2024. Flexural strength prediction of concrete
1589 beams reinforced with hybrid FRP and steel bars based on machine learning. In:
1590 *Structures*, 65, p.106652. Elsevier.
- 1591 [73] Li, Y., Liu, Y., Lin, H. and Jin, C., 2023. Study of flexural strength of concrete
1592 containing mineral admixtures based on machine learning. *Scientific Reports*, 13(1),
1593 p.18061.
- 1594 [74] Paswan, R.K., Gogineni, A., Sharma, S. and Kumar, P., 2024. Predicting split
1595 tensile strength in Portland and geopolymers concretes using machine learning algorithms:
1596 a comparative study. *Journal of Building Pathology and Rehabilitation*, 9(2), p.129.

- 1597 [75] Albaijan, I., Mahmoodzadeh, A., Flaih, L.R., Ibrahim, H.H., Alashker, Y. and
1598 Mohammed, A.H., 2023. Evaluating the tensile strength of reinforced concrete using
1599 optimized machine learning techniques. *Engineering Fracture Mechanics*, 292,
1600 p.109677.
- 1601 [76] de-Prado-Gil, J., Palencia, C., Jagadesh, P. and Martínez-García, R., 2022. A
1602 comparison of machine learning tools that model the splitting tensile strength of self-
1603 compacting recycled aggregate concrete. *Materials*, 15(12), p.4164.
- 1604 [77] Gholampour, A., Gandomi, A.H. and Ozbakkaloglu, T., 2017. New formulations
1605 for mechanical properties of recycled aggregate concrete using gene expression
1606 programming. *Construction and Building Materials*, 130, pp.122–145.
- 1607 [78] Cascardi, A., Micelli, F. and Aiello, M.A., 2017. An artificial neural networks
1608 model for the prediction of the compressive strength of FRP-confined concrete circular
1609 columns. *Engineering Structures*, 140, pp.199–208.
1610 <https://doi.org/10.1016/j.engstruct.2017.02.047>
- 1611 [79] Huang, X., Sresakoolchai, J., Qin, X., Ho, Y.F. and Kaewunruen, S., 2022. Self-
1612 healing performance assessment of bacterial-based concrete using machine learning
1613 approaches. *Materials*, 15(13), p.4436.
- 1614 [80] Althoey, F., Amin, M.N., Khan, K., Usman, M.M., Khan, M.A., Javed, M.F.,
1615 Sabri, M.M.S., Alrowais, R. and Maglad, A.M., 2022. Machine learning-based
1616 computational approach for crack width detection of self-healing concrete. *Case Studies*
1617 *in Construction Materials*, 17, p.e01610.
- 1618 [81] Alabduljabbar, H., Khan, K., Awan, H.H., Alyousef, R., Mohamed, A.M. and
1619 Eldin, S.M., 2023. Modeling the capacity of engineered cementitious composites for self-

- 1620 healing using AI-based ensemble techniques. *Case Studies in Construction Materials*, 18,
1621 p.e01805.
- 1622 [82] Baghaei, K.A. and Hadigheh, S.A., 2021. Durability assessment of FRP-to-
1623 concrete bonded connections under moisture condition using data-driven machine
1624 learning-based approaches. *Composite Structures*, p.114576.
- 1625 [83] Sabour, M.R., Dezvareh, G.A. and Niavol, K.P., 2021. Application of artificial
1626 intelligence methods in modeling corrosion of cement and sulfur concrete in sewer
1627 systems. *Environmental Processes*, 8, pp.1601–1618.
- 1628 [84] XuanRui, Y., 2022. Developing an artificial neural network model to predict the
1629 durability of the RC beam by machine learning approaches. *Case Studies in Construction
1630 Materials*, 17, p.e01382.
- 1631 [85] Chen, H., Cao, Y., Liu, Y., Qin, Y. and Xia, L., 2023. Enhancing the durability of
1632 concrete in severely cold regions: Mix proportion optimization based on machine
1633 learning. *Construction and Building Materials*, 371, p.130644.
- 1634 [86] Huang, X., Wang, S., Lu, T., Wu, K., Li, H., Deng, W. and Shi, J., 2024. Frost
1635 durability prediction of rubber concrete based on improved machine learning models.
1636 *Construction and Building Materials*, 429, p.136201.
- 1637 [87] Kazemi, R., 2024. A hybrid artificial intelligence approach for modeling the
1638 carbonation depth of sustainable concrete containing fly ash. *Scientific Reports*, 14(1),
1639 p.11948.
- 1640 [88] Jansson, R. and Boström, L., 2013. Factors influencing fire spalling of self-
1641 compacting concrete. *Materials and Structures*, 46, pp.1683–1694.

- 1642 [89] Liu, J.C., Huang, L., Chen, Z. and Ye, H., 2022. A comparative study of artificial
1643 intelligent methods for explosive spalling diagnosis of hybrid fiber-reinforced ultra-high-
1644 performance concrete. *International Journal of Civil Engineering*, 20(6), pp.639–660.
- 1645 [90] Habib, A., Barakat, S., Al-Toubat, S., Junaid, M.T. and Maalej, M., 2024.
1646 Developing machine learning models for identifying the failure potential of fire-exposed
1647 FRP-strengthened concrete beams. *Arabian Journal for Science and Engineering*, pp.1–
1648 16.
- 1649 [91] Moradi, M.J., Daneshvar, K., Ghazi-Nader, D. and Hajiloo, H., 2021. The
1650 prediction of fire performance of concrete-filled steel tubes (CFST) using artificial neural
1651 network. *Thin-Walled Structures*, 161, p.107499.
- 1652 [92] Naser, M.Z., 2019. Heuristic machine cognition to predict fire-induced spalling
1653 and fire resistance of concrete structures. *Automation in Construction*, 106, p.102916.
- 1654 [93] Li, S., Liew, J.R. and Xiong, M.X., 2021. Prediction of fire resistance of concrete
1655 encased steel composite columns using artificial neural network. *Engineering Structures*,
1656 245, p.112877.
- 1657 [94] Carvel, R.O., Beard, A.N. and Jowitt, P.W., 2005. Fire spread between vehicles in
1658 tunnels: effects of tunnel size, longitudinal ventilation and vehicle spacing. *Fire
1659 Technology*, 41, pp.271–304.
- 1660 [95] Li, Y.Z. and Ingason, H., 2018. Overview of research on fire safety in
1661 underground road and railway tunnels. *Tunnelling and Underground Space Technology*,
1662 81, pp.568–589.

- 1663 [96] Wu, X., Park, Y., Li, A., Huang, X., Xiao, F. and Usmani, A., 2021. Smart
1664 detection of fire source in tunnel based on the numerical database and artificial
1665 intelligence. *Fire Technology*, 57, pp.657–682.
- 1666 [97] Wu, X., Zhang, X., Huang, X., Xiao, F. and Usmani, A., 2022. A real-time
1667 forecast of tunnel fire based on numerical database and artificial intelligence. In: *Building*
1668 *Simulation*, pp.1–14. Tsinghua University Press.
- 1669 [98] Al Hamd, R. and Warren, H., 2024. Predicting concrete-steel bond performance at
1670 high temperatures: a data-driven approach using AI modelling. In: *4th International*
1671 *Conference on Structural Safety Under Fire & Blast Loading*, September 2024.
- 1672 [99] Gandomi, A.H., Alavi, A.H., Gandomi, M. and Kazemi, S., 2017. Formulation of
1673 shear strength of slender RC beams using gene expression programming, part II: With
1674 shear reinforcement. *Measurement*, 95, pp.367–376.
- 1675 [100] Cascardi, A., Micelli, F. and Aiello, M.A., 2016. Analytical model based on
1676 artificial neural network for masonry shear walls strengthened with FRM systems.
1677 *Composites Part B: Engineering*, 95, pp.252–263.
- 1678 [101] Mishra, P., Samui, P. and Mahmoudi, E., 2021. Probabilistic design of retaining
1679 wall using machine learning methods. *Applied Sciences*, 11(12), p.5411.
- 1680 [102] Asteris, P.G., Lemonis, M.E., Le, T.T. and Tsavdaridis, K.D., 2021. Evaluation of
1681 the ultimate eccentric load of rectangular CFSTs using advanced neural network
1682 modeling. *Engineering Structures*, 248, p.113297.
- 1683 [103] Asteris, P.G., Tsavdaridis, K.D., Lemonis, M.E., Ferreira, F.P.V., Le, T.T.,
1684 Gantes, C.J. and Formisano, A., 2024. AI-powered GUI for prediction of axial

- 1685 compression capacity in concrete-filled steel tube columns. *Neural Computing and*
1686 *Applications*, 36(35), pp.22429–22459.
- 1687 [104] Lemonis, M., Daramara, A., Georgiadou, A., Siorikis, V., Tsavdaridis, K.D. and
1688 Asteris, P., 2022. Ultimate axial load of rectangular concrete-filled steel tubes using
1689 multiple ANN activation functions. *Steel and Composite Structures: An International*
1690 *Journal*, 42(4), pp.459–475.
- 1691 [105] Ferreira, F.P.V., Jeong, S.H., Mansouri, E., Shamass, R., Tsavdaridis, K., Martins,
1692 C.H. and De Nardin, S., 2024. Five machine learning models predicting the global shear
1693 capacity of composite cellular beams with hollow-core units.
- 1694 [106] Ferreira, F.P.V., Shamass, R., Limbachiya, V., Tsavdaridis, K.D. and Martins,
1695 C.H., 2022. Lateral–torsional buckling resistance prediction model for steel cellular
1696 beams generated by artificial neural networks (ANN). *Thin-Walled Structures*, 170,
1697 p.108592.
- 1698 [107] Shamass, R., Ferreira, F.P.V., Limbachiya, V., Santos, L.F.P. and Tsavdaridis,
1699 K.D., 2022. Web-post buckling prediction resistance of steel beams with elliptically-
1700 based web openings using artificial neural networks (ANN). *Thin-Walled Structures*, 180,
1701 p.109959.
- 1702 [108] Rabi, M., Jweihan, Y.S., Abarkan, I., Ferreira, F.P.V., Shamass, R., Limbachiya,
1703 V., Tsavdaridis, K.D. and Santos, L.F.P., 2024. Machine learning-driven web-post
1704 buckling resistance prediction for high-strength steel beams with elliptically-based web
1705 openings. *Results in Engineering*, 21, p.101749.

- 1706 [109] Abdollahzadeh, G. and Shabaniyan, S.M., 2018. Experimental and numerical
1707 analysis of beam to column joints in steel structures. *Frontiers of Structural and Civil*
1708 *Engineering*, 12, pp.642–661. <https://doi.org/10.1007/s11709-017-0457-z>
- 1709 [110] Luo, H. and Paal, S.G., 2022. Artificial intelligence-enhanced seismic response
1710 prediction of reinforced concrete frames. *Advanced Engineering Informatics*, 52,
1711 p.101568.
- 1712 [111] Gharehbaghi, S., Yazdani, H. and Khatibinia, M., 2020. Estimating inelastic
1713 seismic response of reinforced concrete frame structures using a wavelet support vector
1714 machine and an artificial neural network. *Neural Computing and Applications*, 32(8),
1715 pp.2975–2988.
- 1716 [112] Gondaliya, K.M., Vasanwala, S.A., Desai, A.K., Amin, J.A. and Bhaiya, V.,
1717 2024. Machine learning-based approach for assessing the seismic vulnerability of
1718 reinforced concrete frame buildings. *Journal of Building Engineering*, 97, p.110785.
- 1719 [113] Altıok, T.Y., Üstüner, B., Özyüksel Çiftçioğlu, A. and Demir, A., 2024.
1720 Enhancing structural evaluation: Machine learning approaches for inadequate reinforced
1721 concrete frames. *Iranian Journal of Science and Technology, Transactions of Civil*
1722 *Engineering*, pp.1–21.
- 1723 [114] Shin, J., Scott, D.W., Stewart, L.K. and Jeon, J.S., 2020. Multi-hazard assessment
1724 and mitigation for seismically-deficient RC building frames using artificial neural
1725 network models. *Engineering Structures*, 207, p.110204.
- 1726 [115] Shin, J. and Park, S., 2022. Optimum retrofit strategy of FRP column jacketing
1727 system for non-ductile RC building frames using artificial neural network and genetic
1728 algorithm hybrid approach. *Journal of Building Engineering*, 57, p.104919.

- 1729 [116] Sufyan, M.S., Samui, P. and Mishra, S.S., 2023. Reliability analysis of frame
1730 structures under top-floor lateral load using artificial intelligence. *Asian Journal of Civil*
1731 *Engineering*, 24(8), pp.3653–3665.
- 1732 [117] Sufyan, M.S., Samui, P. and Mishra, S.S., 2024. Reliability analysis of portal
1733 frame subjected to varied lateral loads using machine learning. *Asian Journal of Civil*
1734 *Engineering*, 25(2), pp.2045–2058.
- 1735 [118] Nguyen, H.D., Lee, Y.J., LaFave, J.M. and Shin, M., 2023. Seismic fragility
1736 analysis of steel moment frames using machine learning models. *Engineering*
1737 *Applications of Artificial Intelligence*, 126, p.106976.
- 1738 [119] Kudari, R.J., Geetha, L. and Satyanarayana, A., 2024. Assessing seismic
1739 vulnerability of structures with damper using an ANN-based approach. *Asian Journal of*
1740 *Civil Engineering*, 25(7), pp.5335–5347.
- 1741 [120] Onyelowe, K.C., Yaulema Castañeda, J.L., Adam, A.F.H., Ñacato Estrella, D.R.
1742 and Ganasen, N., 2024. Prediction of steel plate-based damper for improving the behavior
1743 of concentrically braced frames based on RSM and ML approaches for sustainable
1744 structures. *Scientific Reports*, 14(1), p.4065.
- 1745 [121] Al-Ghabawi, H.H.M., Khattab, M.M., Zahid, I.A. and Al-Oubaidi, B., 2024. The
1746 prediction of the ultimate base shear of BRB frames under push-over using ensemble
1747 methods and artificial neural networks. *Asian Journal of Civil Engineering*, 25(2),
1748 pp.1467–1485.
- 1749 [122] Bae, J., Lee, C.-H., Park, M., Alemayehu, R.W., Ryu, J. and Ju, Y.K., 2020.
1750 Modified low-cycle fatigue estimation using machine learning for radius-cut coke-shaped

- 1751 metallic damper subjected to cyclic loading. *International Journal of Steel Structures*, 20,
1752 pp.1849–1858. <https://doi.org/10.1007/s13296-020-00377-7>
- 1753 [123] Ji, S., Lee, B. and Yi, M.Y., 2021. Building life-span prediction for life cycle
1754 assessment and life cycle cost using machine learning: A big data approach. *Building and*
1755 *Environment*, 205, p.108267.
- 1756 [124] Lazaridis, P.C., Kavvadias, I.E., Demertzis, K., Iliadis, L. and Vasiliadis, L.K.,
1757 2022. Structural damage prediction of a reinforced concrete frame under single and
1758 multiple seismic events using machine learning algorithms. *Applied Sciences*, 12(8),
1759 p.3845.
- 1760 [125] Bartsch, H., Voelkel, J. and Feldmann, M. Developing artificial neural networks
1761 to estimate the fatigue strength of structural steel details using the new European
1762 database. *Steel Construction*.
- 1763 [126] Naser, M.Z. and Kodur, V.K., 2022. Explainable machine learning using real,
1764 synthetic and augmented fire tests to predict fire resistance and spalling of RC columns.
1765 *Engineering Structures*, 253, p.113824.
- 1766 [127] Gondaliya, K.M., Vasanwala, S.A., Desai, A.K., Amin, J.A. and Bhaiya, V.,
1767 2024. Machine learning-based approach for assessing the seismic vulnerability of
1768 reinforced concrete frame buildings. *Journal of Building Engineering*, 97, p.110785.
- 1769 [128] Özsoy Özbay, A.E., 2023. A decision tree-based damage estimation approach for
1770 preliminary seismic assessment of reinforced concrete buildings. *Revista de la*
1771 *Construcción*, 22(1), pp.5–15.
- 1772 [129] Taffese, W.Z., 2020. Data-driven method for enhanced corrosion assessment of
1773 reinforced concrete structures. *arXiv preprint arXiv:2007.01164*.

- 1774 [130] Rauf, A., Asif, U., Onyelowe, K., Javed, M.F. and Alabduljabbar, H., 2024.
1775 Experimental analysis and gene expression programming optimization of sustainable
1776 concrete containing mineral fillers. *Scientific Reports*, 14(1), p.29280.
- 1777 [131] Biswas, R., Kumar, M., Kumar, D.R., Samui, P., Rajak, M.K., Armaghani, D.J.
1778 and Singh, S., 2024. Application of novel deep neural network on prediction of
1779 compressive strength of fly ash-based concrete. *Nondestructive Testing and Evaluation*,
1780 pp.1–31.
- 1781 [132] Murad, Y., Tarawneh, A., Arar, F., Al-Zu'bi, A., Al-Ghwairi, A., Al-Jaafreh, A.
1782 and Tarawneh, M., 2021. Flexural strength prediction for concrete beams reinforced with
1783 FRP bars using gene expression programming. In: *Structures*, 33, pp.3163–3172.
1784 Elsevier.
- 1785 [133] Sharma, N., Thakur, M.S., Upadhyaya, A. and Sihag, P., 2023. Assessment of
1786 flexural strength of concrete with marble powder applying soft computing techniques.
1787 *Journal of Building Pathology and Rehabilitation*, 8(1), p.4.
- 1788 [134] Zhu, W., Huang, L., Mao, L. and Esmaceli-Falak, M., 2022. Predicting the
1789 uniaxial compressive strength of oil palm shell lightweight aggregate concrete using
1790 artificial intelligence-based algorithms. *Structural Concrete*, 23(6), pp.3631–3650.
- 1791 [135] Liu, Y., Cao, Y., Wang, L., Chen, Z.S. and Qin, Y., 2022. Prediction of the
1792 durability of high-performance concrete using an integrated RF-LSSVM model.
1793 *Construction and Building Materials*, 356, p.129232.
- 1794 [136] Gao, P., Song, Y., Wang, J., Yang, Z., Wang, K. and Yuan, Y., 2024. Prediction
1795 model for the chloride ion permeability resistance of recycled aggregate concrete based
1796 on machine learning. *Buildings*, 14(11), p.3608.

- 1797 [137] Malazdrewicz, S. and Sadowski, Ł., 2021. Neural modelling of the depth of wear
1798 determined using the rotating-cutter method for concrete with a high volume of high-
1799 calcium fly ash. *Wear*, 477, p.203791.
- 1800 [138] Khan, M.A., Farooq, F., Javed, M.F., Zafar, A., Ostrowski, K.A., Aslam, F.,
1801 Malazdrewicz, S. and Maślak, M., 2021. Simulation of depth of wear of eco-friendly
1802 concrete using machine learning based computational approaches. *Materials*, 15(1), p.58.
- 1803 [139] Khan, A., Khan, M., Ali, M., Khan, M., Khan, A.U., Shakeel, M., Fawad, M.,
1804 Najeh, T. and Gamil, Y., 2024. Predictive modeling for depth of wear of concrete
1805 modified with fly ash: A comparative analysis of genetic programming-based algorithms.
1806 *Case Studies in Construction Materials*, 20, p.e02744.
- 1807 [140] Gao, X., Yang, J., Zhu, H. and Xu, J., 2023. Estimation of rubberized concrete
1808 frost resistance using machine learning techniques. *Construction and Building Materials*,
1809 371, p.130778.
- 1810 [141] Esmacili-Falak, M. and Sarkhani Benemaran, R., 2024. Application of
1811 optimization-based regression analysis for evaluation of frost durability of recycled
1812 aggregate concrete. *Structural Concrete*, 25(1), pp.716–737.
- 1813 [142] Bae, J., Jang, A., Park, M.J., Lee, J. and Ju, Y.K., 2022. Assessment of concrete
1814 macrocrack depth using infrared thermography. *Steel and Composite Structures: An
1815 International Journal*, 43(4), pp.501–509.
- 1816 [143] Lalitha, G. and Reddy, C.R., 2023. Impermeability evaluation of concrete with fly
1817 ash aggregate and prediction with modelling.
- 1818 [144] Alsubai, S., Alqahtani, A., Hashim Muhodir, S., Alanazi, A., Ahmed, M., Jasim,
1819 D.J. and Palani, S., 2024. The remarkable potential of machine learning algorithms in

1820 estimating water permeability of concrete incorporating nano natural pozzolana.
1821 *Scientific Reports*, 14(1), p.12532.

1822 [145] Londhe, S.N., Kulkarni, P.S., Dixit, P.R., Silva, A., Neves, R. and De Brito, J.,
1823 2021. Predicting carbonation coefficient using artificial neural networks and genetic
1824 programming. *Journal of Building Engineering*, 39, p.102258.

1825 [146] Tran, V.Q., Mai, H.V.T., To, Q.T. and Nguyen, M.H., 2023. Machine learning
1826 approach in investigating carbonation depth of concrete containing fly ash. *Structural*
1827 *Concrete*, 24(2), pp.2145–2169.

1828 [147] Huo, Z., Wang, L. and Huang, Y., 2023. Predicting carbonation depth of concrete
1829 using a hybrid ensemble model. *Journal of Building Engineering*, 76, p.107320.

1830 [148] Cai, B., Zhang, B. and Fu, F., 2020. Post-fire reliability analysis of concrete
1831 beams retrofitted with CFRPs: A new approach. *Proceedings of the Institution of Civil*
1832 *Engineers – Structures and Buildings*, 173(11), pp.888–902.

1833 [149] Hisham, M., Hamdy, G.A. and El-Mahdy, O.O., 2021. Prediction of temperature
1834 variation in FRP-wrapped RC columns exposed to fire using artificial neural networks.
1835 *Engineering Structures*, 238, p.112219.

1836 [150] Kang, S.M. and Kim, J.K., 2023. Prediction of the moment capacity of FRP-
1837 strengthened RC beams exposed to fire using ANNs. *KSCE Journal of Civil Engineering*,
1838 27(8), pp.3471–3483.

1839 [151] Vu, Q.V., Truong, V.H. and Thai, H.T., 2021. Machine learning-based prediction
1840 of CFST columns using gradient tree boosting algorithm. *Composite Structures*, 259,
1841 p.113505.

- 1842 [152] Zhao, X.Y., Chen, J.X. and Wu, B., 2022. An interpretable ensemble-learning-
1843 based open source model for evaluating the fire resistance of concrete-filled steel tubular
1844 columns. *Engineering Structures*, 270, p.114886.
- 1845 [153] Zhu, Y.F., Yao, Y., Huang, Y., Chen, C.H., Zhang, H.Y. and Huang, Z., 2022.
1846 Machine learning applications for assessment of dynamic progressive collapse of steel
1847 moment frames. In: *Structures*, 36, pp.927–934. Elsevier.
- 1848 [154] Qiu, J. and Jiang, L., 2023. Development of modular and reusable AI models for
1849 fast predicting fire behaviour of steel columns in structural systems. *Engineering*
1850 *Structures*, 297, p.116994.
- 1851 [155] Mei, Y., Sun, Y., Li, F., Xu, X., Zhang, A. and Shen, J., 2022. Probabilistic
1852 prediction model of steel to concrete bond failure under high temperature by machine
1853 learning. *Engineering Failure Analysis*, 142, p.106786.
- 1854 [156] Reshi, I.A., Shah, A.H., Jan, A., Tariq, Z., Sholla, S., Rashid, S. and Wani, M.U.,
1855 2024. Machine learning enhanced modeling of steel–concrete bond strength under
1856 elevated temperature exposure. *Structural Concrete*, 25(6), pp.4609–4622.
- 1857 [157] Abuodeh, O.R., Abdalla, J.A. and Hawileh, R.A., 2020. Prediction of shear
1858 strength and behavior of RC beams strengthened with externally bonded FRP sheets
1859 using machine learning techniques. *Composite Structures*, 234, p.111698.
- 1860 [158] Zhang, G., Ali, Z.H., Aldlemy, M.S., Mussa, M.H., Salih, S.Q., Hameed, M.M.,
1861 Al-Khafaji, Z.S. and Yaseen, Z.M., 2022. Reinforced concrete deep beam shear strength
1862 capacity modelling using an integrative bio-inspired algorithm with an artificial
1863 intelligence model. *Engineering with Computers*, 38(Suppl 1), pp.15–28.

- 1864 [159] Yu, Y., Zhao, X.Y., Xu, J.J., Wang, S.C. and Xie, T.Y., 2022. Evaluation of shear
1865 capacity of steel fiber reinforced concrete beams without stirrups using artificial
1866 intelligence models. *Materials*, 15(7), p.2407.
- 1867 [160] Nguyen, D.D., Tran, V.L., Ha, D.H., Nguyen, V.Q. and Lee, T.H., 2021. A
1868 machine learning-based formulation for predicting shear capacity of squat flanged RC
1869 walls. In: *Structures*, 29, pp.1734–1747. Elsevier.
- 1870 [161] Khaleghi, M., Salimi, J., Farhangi, V., Moradi, M.J. and Karakouzian, M., 2021.
1871 Application of artificial neural network to predict load bearing capacity and stiffness of
1872 perforated masonry walls. *CivilEng*, 2(1), pp.48–67.
- 1873 [162] Keshtegar, B., Nehdi, M.L., Kolahchi, R., Trung, N.T. and Bagheri, M., 2022.
1874 Novel hybrid machine learning model for predicting shear strength of reinforced concrete
1875 shear walls. *Engineering with Computers*, pp.1–12.
- 1876 [163] Zhang, H., Cheng, X., Li, Y. and Du, X., 2022. Prediction of failure modes,
1877 strength, and deformation capacity of RC shear walls through machine learning. *Journal*
1878 *of Building Engineering*, 50, p.104145.
- 1879 [164] Tabrizikahou, A., Pavić, G., Shahsavani, Y. and Hadzima-Nyarko, M., 2024.
1880 Prediction of reinforced concrete walls shear strength based on soft computing-based
1881 techniques. *Soft Computing*, 28(15), pp.8731–8747.
- 1882 [165] Koopialipoor, M., Murlidhar, B.R., Hedayat, A., Armaghani, D.J., Gordan, B. and
1883 Mohamad, E.T., 2020. The use of new intelligent techniques in designing retaining walls.
1884 *Engineering with Computers*, 36, pp.283–294.

- 1885 [166] Cakiroglu, C., Islam, K., Bekdaş, G. and Nehdi, M.L., 2023. Data-driven
1886 ensemble learning approach for optimal design of cantilever soldier pile retaining walls.
1887 In: *Structures*, 51, pp.1268–1280. Elsevier.
- 1888 [167] Nguyen, H.Q., Ly, H.B., Tran, V.Q., Nguyen, T.A., Le, T.T. and Pham, B.T.,
1889 2020. Optimization of artificial intelligence system by evolutionary algorithm for
1890 prediction of axial capacity of rectangular concrete filled steel tubes under compression.
1891 *Materials*, 13(5), p.1205.
- 1892 [168] Cakiroglu, C., Islam, K., Bekdaş, G., Isikdag, U. and Mangalathu, S., 2022.
1893 Explainable machine learning models for predicting the axial compression capacity of
1894 concrete filled steel tubular columns. *Construction and Building Materials*, 356,
1895 p.129227.
- 1896 [169] Nguyen, T.A. and Ly, H.B., 2024. Predicting axial compression capacity of
1897 CFST columns and design optimization using advanced machine learning techniques.
1898 In: *Structures*, 59, p.105724. Elsevier.
- 1899 [170] Hanoon, A.N., Al Zand, A.W. and Yaseen, Z.M., 2022. Designing new hybrid
1900 artificial intelligence model for CFST beam flexural performance prediction. *Engineering*
1901 *with Computers*, 38(4), pp.3109–3135.
- 1902 [171] Ebid Nguyen, T.A., Ly, H.B., Mai, H.V.T. and Tran, V.Q., 2021. Using ANN to
1903 estimate the critical buckling load of Y-shaped cross-section steel columns. *Scientific*
1904 *Programming*, 2021, p.5530702.
- 1905 [172] Shen, Y., Sun, J. and Liang, S., 2022. Interpretable machine learning models for
1906 punching shear strength estimation of FRP reinforced concrete slabs. *Crystals*, 12(2),
1907 p.259.

- 1908 [173] Doğan, G. and Arslan, M.H., 2022. Determination of punching shear capacity of
1909 concrete slabs reinforced with FRP bars using machine learning. *Arabian Journal for*
1910 *Science and Engineering*, 47(10), pp.13111–13137.
- 1911 [174] Liu, H., Wang, H., Zhang, Y. and Liu, X., 2024. Shear resistance of UHPC
1912 connection for prefabricated reinforced concrete slabs with shear grooves and dowel
1913 rebars. *Construction and Building Materials*, 454, p.139153.
- 1914 [175] Yan, H., Xie, N. and Shen, D., 2024. Hybrid machine learning algorithms for
1915 prediction of failure modes and punching resistance in slab-column connections with
1916 shear reinforcement. *Buildings*, 14(5), p.1247.
- 1917 [176] Hosseinpour, M., Sharifi, Y. and Sharifi, H., 2020. Neural network application for
1918 distortional buckling capacity assessment of castellated steel beams. In: *Structures*, 27,
1919 pp.1174–1183. Elsevier.
- 1920 [177] Shamass, R., Ferreira, F.P.V., Limbachiya, V., Santos, L.F.P. and Tsavdaridis,
1921 K.D., 2022. Web-post buckling prediction resistance of steel beams with elliptically-
1922 based web openings using artificial neural networks (ANN). *Thin-Walled Structures*, 180,
1923 p.109959.
- 1924 [178] Nguyen, H.D., Dao, N.D. and Shin, M., 2021. Prediction of seismic drift
1925 responses of planar steel moment frames using artificial neural network and extreme
1926 gradient boosting. *Engineering Structures*, 242, p.112518.
- 1927 [179] Nguyen, T.H., Phan, V.T. and Nguyen, D.D., 2023. Practical ANN model for
1928 estimating buckling load capacity of corroded web-tapered steel I-section columns.
1929 *International Journal of Steel Structures*, 23(6), pp.1459–1475.

- 1930 [180] Dabiri, H., Rahimzadeh, K. and Kheyroddin, A., 2022. A comparison of machine
1931 learning- and regression-based models for predicting ductility ratio of RC beam-column
1932 joints. In: *Structures*, 37, pp.69–81. Elsevier.
- 1933 [181] Ramavath, S. and Suryawanshi, S.R., 2024. Optimal prediction of shear properties
1934 in beam-column joints using machine learning approach. *International Journal of*
1935 *Engineering*, 37(1), pp.67–82.
- 1936 [182] Wen, W., Zhang, C. and Zhai, C., 2022. Rapid seismic response prediction of RC
1937 frames based on deep learning and limited building information. *Engineering Structures*,
1938 267, p.114638.
- 1939 [183] Kazemi, F. and Jankowski, R., 2023. Machine learning-based prediction of
1940 seismic limit-state capacity of steel moment-resisting frames considering soil-structure
1941 interaction. *Computers & Structures*, 274, p.106886.
- 1942 [184] Hwang, S.H., Mangalathu, S., Shin, J. and Jeon, J.S., 2022. Estimation of
1943 economic seismic loss of steel moment-frame buildings using a machine learning
1944 algorithm. *Engineering Structures*, 254, p.113877.
- 1945 [185] Su, A., Cheng, J., Wang, Y. and Pan, Y., 2025. Machine learning-based processes
1946 with active learning strategies for the automatic rapid assessment of seismic resistance of
1947 steel frames. In: *Structures*, 72, p.108227. Elsevier.
- 1948 [186] Asgarkhani, N., Kazemi, F., Jakubczyk-Gańczyńska, A., Mohebi, B. and
1949 Jankowski, R., 2024. Seismic response and performance prediction of steel buckling-
1950 restrained braced frames using machine-learning methods. *Engineering Applications of*
1951 *Artificial Intelligence*, 128, p.107388.

- 1952 [187] Al-Ghabawi, H.H.M., Khattab, M.M., Zahid, I.A. and Al-Oubaidi, B., 2024. The
 1953 prediction of the ultimate base shear of BRB frames under push-over using ensemble
 1954 methods and artificial neural networks. *Asian Journal of Civil Engineering*, 25(2),
 1955 pp.1467–1485.
- 1956 [188] Murphy, M.L., et al., 2022. *Building Code Requirements for Structural Concrete*
 1957 *Reinforced with Glass Fiber-Reinforced Polymer (GFRP) Bars – Code and Commentary:*
 1958 *An ACI Standard*. American Concrete Institute.
- 1959 [189] Makridakis, S. and Hibon, M., 1995. Evaluating accuracy (or error) measures
 1960 [online].
- 1961 [190] Botchkarev, A., 2019. A new typology design of performance metrics to measure
 1962 errors in machine learning regression algorithms. *Interdisciplinary Journal of*
 1963 *Information, Knowledge, and Management*, 14, pp.45–76.
- 1964 [191] Naser, M.Z. and Alavi, A.H., 2023. Error metrics and performance fitness
 1965 indicators for artificial intelligence and machine learning in engineering and sciences.
 1966 *Architecture, Structures and Construction*, 3(4), pp.499–517.
- 1967 [192] Armstrong, J.S. and Collopy, F., 1992. Error measures for generalizing about
 1968 forecasting methods: Empirical comparisons. *International Journal of Forecasting*, 8(1),
 1969 pp.69–80.
- 1970 [193] Foss, T., Stensrud, E., Kitchenham, B. and Myrtveit, I., 2003. A simulation study
 1971 of the model evaluation criterion MMRE. *IEEE Transactions on Software Engineering*,
 1972 29(11), pp.985–995.
- 1973 [194] Li, J., 2017. Assessing the accuracy of predictive models for numerical data: Not r
 1974 nor r^2 , why not? Then what? *PLOS ONE*, 12(8), p.e0183250.

- 1975 [195] Silver, E.A., Pyke, D.F. and Thomas, D.J., 2016. *Inventory and Production*
1976 *Management in Supply Chains*. CRC Press.
- 1977 [196] Jarantow, S.W., Pisors, E.D. and Chiu, M.L., 2023. Introduction to the use of
1978 linear and nonlinear regression analysis in quantitative biological assays. *Current*
1979 *Protocols*, 3(6), p.e801.
- 1980 [197] Regona, M., Yigitcanlar, T., Xia, B. and Li, R.Y.M., 2022. Opportunities and
1981 adoption challenges of AI in the construction industry: A PRISMA review. *Journal of*
1982 *Open Innovation: Technology, Market, and Complexity*, 8(1), p.45.
- 1983 [198] Naser, M.Z., 2019. AI-based cognitive framework for evaluating response of
1984 concrete structures in extreme conditions. *Engineering Applications of Artificial*
1985 *Intelligence*, 81, pp.437–449.
- 1986 [199] Yigitcanlar, T., 2021. Greening the artificial intelligence for a sustainable planet:
1987 An editorial commentary. *Sustainability*, 13(24), p.13508.
- 1988 [200] Yun, J.J., Lee, D., Ahn, H., Park, K. and Yigitcanlar, T., 2016. Not deep learning
1989 but autonomous learning of open innovation for sustainable artificial intelligence.
1990 *Sustainability*, 8(8), p.797.
- 1991 [201] Na, S., Heo, S., Han, S., Shin, Y. and Roh, Y., 2022. Acceptance model of
1992 artificial intelligence (AI)-based technologies in construction firms: Applying the
1993 Technology Acceptance Model (TAM) in combination with the Technology–
1994 Organisation–Environment (TOE) framework. *Buildings*, 12(2), p.90.
- 1995 [202] Young, D., Panthi, K. and Noor, O., 2021. Challenges involved in adopting BIM
1996 on the construction jobsite. *EPiC Series in Built Environment*, 2(3), pp.302–310.

- 1997 [203] Gondia, A., Siam, A., El-Dakhakhni, W. and Nassar, A.H., 2020. Machine
1998 learning algorithms for construction projects delay risk prediction. *Journal of*
1999 *Construction Engineering and Management*, 146(1), p.04019085.
- 2000 [204] Koyamparambath, A., Adibi, N., Szablewski, C., Adibi, S.A. and Sonnemann, G.,
2001 2022. Implementing artificial intelligence techniques to predict environmental impacts:
2002 case of construction products. *Sustainability*, 14(6), p.3699.
- 2003 [205] Sharif, S.A. and Hammad, A., 2019. Developing surrogate ANN for selecting
2004 near-optimal building energy renovation methods considering energy consumption, LCC
2005 and LCA. *Journal of Building Engineering*, 25, p.100790.
- 2006 [206] Baehr, J., Koyamparambath, A., Dos Reis, E., Weyand, S., Binnig, C., Schebek,
2007 L. and Sonnemann, G., 2024. Predicting product life cycle environmental impacts with
2008 machine learning: Uncertainties and implications for future reporting
2009 requirements. *Sustainable Production and Consumption*, 52, pp.511-526.
- 2010 [207] Askarinejad, P. and Behnia, B., 2024. Decarbonizing Tall Building Structures:
2011 Implementing Machine Learning At The Early-stage Of Design Process.
- 2012 [208] Chicco, D., Warrens, M.J. and Jurman, G., 2021. The coefficient of determination
2013 R-squared is more informative than SMAPE, MAE, MAPE, MSE and RMSE in
2014 regression analysis evaluation. *Peerj computer science*, 7, p.e623.
- 2015 [209] Sami, B.H.Z., Sami, B.F.Z., Kumar, P., Ahmed, A.N., Amieghemen, G.E., Sherif,
2016 M.M. and El-Shafie, A., 2023. Feasibility analysis for predicting the compressive and
2017 tensile strength of concrete using machine learning algorithms. *Case Studies in*
2018 *Construction Materials*, 18, p.e01893.

- 2019 [210] Hodson, T.O., 2022. Root mean square error (RMSE) or mean absolute error
2020 (MAE): When to use them or not. *Geoscientific Model Development Discussions*, 2022,
2021 pp.1-10.
- 2022 [211] Yang, Y. and Liu, G., 2023. Data-driven shear strength prediction of FRP-
2023 reinforced concrete beams without stirrups based on machine learning
2024 methods. *Buildings*, 13(2), p.313.
- 2025 [212] Kalabarige, L.R., Sridhar, J., Subbaram, S., Prasath, P. and Gobinath, R., 2024.
2026 Machine learning modeling integrating experimental analysis for predicting compressive
2027 strength of concrete containing different industrial byproducts. *Advances in Civil
2028 Engineering*, 2024(1), p.7844854.
- 2029 [213] Sun, B., Zhang, Y. and Huang, C., 2020. Machine learning-based seismic fragility
2030 analysis of large-scale steel buckling restrained brace frames. *Computer Modeling in
2031 Engineering & Sciences*, 125(2), pp.755-776.
- 2032 [214] Tamimi, M.F., Alshannaq, A.A. and Mu'ath, I., 2023. Sensitivity and reliability
2033 assessment of buckling restrained braces using machine learning assisted-
2034 simulation. *Journal of Constructional Steel Research*, 211, p.108187.
- 2035 [215] Anand, T.P., Pandikkadavath, M.S., Mangalathu, S. and Sahoo, D.R., 2024.
2036 Machine learning models for seismic analysis of buckling-restrained braced
2037 frames. *Journal of Building Engineering*, 98, p.111398.
- 2038 [216] Sagheer, A.M., Alhamaydeh, M., Fayaz, J. and Al-Sadoon, Z.A., 2024, May.
2039 Deep learning-based modeling of the cyclic behavior of replaceable fuse buckling-
2040 restrained braces (BRBs). In *Structures* (Vol. 63, p. 106484). Elsevier.

- 2041 [217] Mohammadi, A., Karimzadeh, S., Yaghmaei-Sabegh, S., Ranjbari, M. and
2042 Lourenço, P.B., 2023. Utilising artificial neural networks for assessing seismic demands
2043 of buckling restrained braces due to pulse-like motions. *Buildings*, 13(10), p.2542.
- 2044 [218] Onyelowe, K.C., Yaulema Castañeda, J.L., Adam, A.F.H., Ñacato Estrella, D.R.
2045 and Ganasen, N., 2024. Prediction of steel plate-based damper for improving the behavior
2046 of concentrically braced frames based on RSM and ML approaches for sustainable
2047 structures. *Scientific Reports*, 14(1), p.4065.
- 2048 [219] Chen, P.C. and Chien, K.Y., 2020. Machine-learning based optimal seismic
2049 control of structure with active mass damper. *Applied Sciences*, 10(15), p.5342.
- 2050 [220] Shao, T. and Andrawes, B., 2022. Using machine learning to predict the seismic
2051 response of an SDOF RC structure with superelastic dampers. *International Journal of*
2052 *Civil Engineering*, 20(10), pp.1165-1180.
- 2053 [221] Hu, S., Wang, W. and Lu, Y., 2023. Explainable machine learning models for
2054 probabilistic buckling stress prediction of steel shear panel dampers. *Engineering*
2055 *Structures*, 288, p.116235.
- 2056 [222] Nguyen, T.A., Le Nguyen, K. and Ly, H.B., 2024. Universal boosting ML
2057 approaches to predict the ultimate load capacity of CFST columns. *The Structural Design*
2058 *of Tall and Special Buildings*, 33(2), p.e2071.
- 2059 [223] Alnaqbi, A., Al-Khateeb, G.G., Zeiada, W. and Abuzwidah, M., 2025. Random
2060 forest-based frame work for multi-distress prediction in CRCP: a feature importance
2061 approach. *Discover Civil Engineering*, 2(1), p.140.

- 2062 [224] Gallitto, G., Englert, R., Kincses, B., Kotikalapudi, R., Li, J., Hoffschlag, K.,
2063 Bingel, U. and Spisak, T., 2025. External validation of machine learning models—
2064 registered models and adaptive sample splitting. *GigaScience*, *14*, p.giaf036.
- 2065 [225] Varoquaux, G. and Colliot, O., 2023. Evaluating machine learning models and
2066 their diagnostic value. *Machine learning for brain disorders*, pp.601-630.
- 2067 [226] Riley, R.D., Ensor, J., Snell, K.I., Archer, L., Whittle, R., Dhiman, P., Alderman,
2068 J., Liu, X., Kirton, L., Manson-Whitton, J. and van Smeden, M., 2025. Importance of
2069 sample size on the quality and utility of AI-based prediction models for healthcare. *The*
2070 *Lancet Digital Health*.
- 2071 [227] Ghaffari, A., Shahbazi, Y., Mokhtari Kashavar, M., Fotouhi, M. and Pedrammehr,
2072 S., 2024. Advanced predictive structural health monitoring in high-rise buildings using
2073 recurrent neural networks. *Buildings*, *14*(10), p.3261.
- 2074 [228] Panfeng, B., Songlin, Z., Hongyu, C., Caiwei, L., Pengtao, W. and Lichang, Q.,
2075 2024. Structural monitoring data repair based on a long short-term memory neural
2076 network. *Scientific reports*, *14*(1), p.9974.
- 2077